POLYMERIC AND METALLIC CARDIOVASCULAR BIOMATERIALS: PHOSPHOLIPID AND SILICONE SURFACE MODIFICATION BY GAMMA RADIATION SURFACE GRAFT POLYMERIZATION AND ELECTROPOLYMERIZATION

By

LAURI L. JENKINS

A DISSERTATION PRESENTED TO THE GRADUATE SCHOOL OF THE UNIVERSITY OF FLORIDA IN PARTIAL FULLFILLMENT OF THE REQUIREMENTS FOR THE DEGREE OF DOCTOR OF PHILOSOPHY

UNIVERSITY OF FLORIDA

2000

Copyright 2000

by

Lauri L. Jenkins

This dissertation is dedicated to my parents, Ruth and Don Laurene, and my sister Kay Laurene. The three people in my life that loves me unconditionally.

ACKNOWLEDGMENTS

I would first like to thank Dr. E. P. Goldberg for his guidance and patience and to the all the members of the Goldberg Research Group for their support and encouragement. This has been the most helpful research group that I have ever worked with and I will sincerely miss all of them.

Special thanks goes to Dr. Drew Amery for constantly fixing the XPS and always being there to be my "computer and electronics" guy. The electrochemistry project was a continuance of Drew's oral proposal and without his technical expertise, would have taken months longer to initiate.

Dr. Chris Widenhouse also was also involved in the conception of the electropolymerization project with his first few experiments with the MAOP oligomer.

Kaustubh Rau was always there and ready to help me give me advice. Krau has not only been a good research mate but a good friend.

Thanks go to Dan Urbaniak for his work during the initial electrochemistry feasibility study. Thanks to Paul Martin for coating my SEM stubs.

I am indebted to Prof. Kazuhiko Ishihara, Prof. Nobuo Nakabayashi, and Prof. Yasuhiko Iwasaki who not only provided the groundwork for the phospholipid research, but also were very generous in the supply of the MPC monomer for my research. My sincere gratitude is extended to them for their kindness and generosity.

I would also like to thank Dr. Ambrose for lending me the potentiostat and chart recorder used in the electropolymerization studies and for his insight into the electrochemistry of metal surfaces.

Thanks to my committee members for their guidance and time that they have given me over the last few years.

TABLE OF CONTENTS

page

ACKNOWLEDGMENTS iv

LIST OF TABLES ix

LIST OF FIGURES xi

ABSTRACT xviii

CHAPTERS

1 INTRODUCTION 1

2 BACKGROUND 6

Scientific Goals 6
Surface Modifications 6
Phospholipids 6
Silicones 15
Gamma Radiation Surface Graft Polymerization 17
Electropolymerization 18
Applications 22
Synthetic Vascular Grafts 22
Endoluminal Cardiovascular Stents 25

3 MATERIALS AND METHODS 36

Gamma Radiation Surface Modification of Silicone 36
Materials & Reagents 36
Surface Modification Experiments 37
Gamma Initiated MPC/HEMA and MPC/MAA Copolymer Modification of PDMS 39
Gamma MPC Modification of PDMS 41
Two-Stage Gamma Radiation Modification of PDMS 42
Gamma MPC Modification of PDMS 44
Gamma MPC/MMA Copolymer Modification of PDMS 45
Surface Modification by Electropolymerization 45

Substrates & Reagents 45
Electropolymerization Equipment & Cell Design..... 47
Feasibility Study 47
Electrochemical Experimental Design & Surface Modification Experiments 49
Experimental Designs 50
Methacryoloxy-Terminated-Polydimethylsiloxane (MAOP) Oligomer..... 50
Vinylmethoxysiloxane (VMS) Oligomer..... 50
Methacroylphosphorylcholine (MPC) Monomer 51
Copolymerization Studies 52
VMS – MPC Copolymer 52
MAOP – MPC Copolymer 53
Electropolymerization Control Experiments 53
Electropolymerization Characterization Techniques 54
Contact Angle 54
X-Ray Photoelectric Spectroscopy 55
Scanning Electron Microscopy 56
Fourier Transform Infrared Spectroscopy 56

4 RESULTS AND DISCUSSION 59
Gamma Radiation Surface Graft Modification of Silicone 59
MPC/HEMA and MPC/MAA Copolymer Modification of PDMS..... 59
Gamma MPC Modification of PDMS 62
Two-Stage Gamma Graft Modification of PDMS 65
MPC/MMA Copolymer Modification of PDMS 68
Discussion of Gamma Polymerization of Hydrogel Monomers on PDMS..... 68
Electropolymerization of MPC and Silicone Oligomers on Stainless Steel..... 70
Electropolymerization of Methacryoloxy-Terminated-Polydimethylsiloxane (MAOP) Oligomer 70
Electropolymerization of Vinylmethoxysiloxane (VMS) Oligomer..... 79
Electropolymerization of VMS on Electrodes Coated with Coupling Agent 87
Electropolymerization of Methacroylphosphorylcholine (MPC) Monomer 94
Electrochemical Copolymerization of Silicone Oligomers with MPC ..105
VMS – MPC Copolymer 105
MAOP – MPC Copolymer 112
Electrolyte/solvent Control Experiments 121
Monomer Adsorption Study Experiments 121
Electrolyte/Solvent Control Experiments with no Monomer Present 126
Discussion of Electropolymerization Results 138

5 SUMMARY AND CONCLUSIONS 143

6 SUGGESTED FUTURE RESEARCH 145
Gamma Radiation Graft Surface Polymerization Modification of PDMS..... 145
Electropolymerization..... 146

LIST OF REFERENCES 147

BIOGRAPHICAL SKETCH 153

LIST OF TABLES

Table Page

2.1. The percentage of functional groups on SR controls and MPC modified SR surface as determined by deconvoluted high resolution C1s ESCA spectra. 15

2.2. Summary of major stent manufacturers and stent designs as of 1998 32

2.3. Materials studied for use as stent surface modification. 35

3.1. Listing of samples for the first HEMA/MPC and MAA/MPC co-polymer study. 40

3.2. Listing of samples for the second HEMA/MPC and MAA/MPC co-polymer study. 41

3.3. Conditions for MPC surface modification of PDMS by gamma initiation. 42

3.4. Conditions for first stage modifications of PDMS by gamma initiation. 43

3.5. Samples for the stage two MPC modifications of PDMS by gamma initiation. 44

3.6. MPC modification of PDMS/DMSO. 45

3.7 Preliminary experiments for the polymeric electrochemical surface modification of stainless steel. 48

3.8. MAOP experimental design. 50

3.9.VMS Experimental Design. 50

3.10. Coupling agent coated electrodes & VMS, experimental design. 51

3.11. MPC experimental design. 51

3.12. Copolymerization coating experiments with MPC and VMS. 52

3.13 Copolymerization coating experiments with MPC and MAOP. 53

3.14. Absorption study experiments. 53

3.15. Electrolyte/solvent control experiments. 54

4.1. Listing of samples and contact angle results for the first HEMA/MPC and MAA/MPC copolymer study.....60

4.2. Samples and contact angle results for the second HEMA/MPC and MAA/MPC copolymer study.....61

4.3. Conditions and contact angle results for MPC surface modification of PDMS by gamma radiation surface graft polymerization.....63

4.4 MPC modification of PDMS in DMSO.....65

4.5. Samples and contact angle results for first stage modifications of PDMS by GRIP. 66

4.6. Samples and contact angle results for the stage two MPC modifications of PDMS by gamma radiation surface graft polymerization.....67

4.7. Samples and contact angle results for MPC/MMA coppolymer modification of PDMS. 68

4.8. MAOP Experimental Design/Results. 72

4.9. VMS Experimental Design/Results:.....81

4.10. XPS results for VMS on stainless steel.....81

4.11. Coupling agent coated electrodes & VMS, experimental design and results:.....89

4.12. MPC Experimental Design/Results:.....96

4.13: Results of VMS – MPC copolymer experiments.....107

4.14. Copolymerization coating experiments with MPC and MAOP.....113

4.15. Absorption study experiments.....122

4.17. Electrolyte/solvent control experiments. 128

4.18. XPS results for the electrolyte/solvent control experiments.....128

LIST OF FIGURES

Figure Page

1.1 Chemical structure of the MPC monomer. 3

1.2 Structures for the MAOP and VMS silicone oligomers. 5

2.1 Model for the structure of cell membranes.... 7

2.2. Structure of some common biomembrane phospholipids. 8

2.3. Structures of polymerizable phospholipid monomers developed by Kuo. 10

2.4. General synthetic scheme for phospholipid polymers.... 12

2.5. Expression of IL-1β on polymer surfacesas an indicator for platelet activation. 14

2.6. The gamma induced formation of radicals on silicone. 18

2.7. Basic electrochemical cell design. 21

3.1. Sample turret and gamma ^{60}Co source configurations for gamma radiation polymerization. 38

3.2. Depiction of captive bubble contact angle measurement technique showing (a) sample analysis chamber and (b) bubble at interface. 55

3.3. Schematic of ATR-FTIR crystal, sample and propagation path of laser light. 58

4.1. FTIR spectrum of sample 1B: HEMA/MPC GRIP modified PDMS. 60

4.2. Combined contact angle results for silicone modifications.... 62

4.3. Contact angle results for MPC gamma radiation modification of PDMS with MeOH/water solvent.... 64

4.4. SEM micrographs of sample P1b at magnification of 500x. MAOP coated stainless steel (1 vol % MAOP, DMSO/TEAB, plain electrode, -0.65 V, 6 h) 73

4.5. SEM micrographs of sample P2b at magnification of 500x. MAOP coated stainless steel (1 vol % MAOP, DMSO/NH_4HSO_4, CASS electrode, -1.6 V, 6 h) 73

4.6. SEM micrographs of sample P3b at magnifications of 500x and 5000x. MAOP coated stainless steel (1 vol % MAOP, DMSO/TEAB, CASS electrode, -1.3 V, 6 h). 74

4.7. SEM micrographs of sample P4b at magnifications of 500x and 5000x. MAOP coated stainless steel (1 vol % MAOP, DMSO/NH_4HSO_4, plain electrode, -1.5 V, 24 h). 75

4.8. SEM micrographs of sample P5b at magnification of 500x. MAOP coated stainless steel (5 vol % MAOP, DMSO/TEAB, CASS electrode, -1.0 V, 6 h). 76

4.9. SEM micrographs of sample P6b at magnification of 500x. MAOP coated stainless steel (5 vol % MAOP, DMSO/NH_4HSO_4, plain electrode, -1.65 V, 6 h). 76

4.10. SEM micrographs of sample P7 at magnifications of 500x and 5000x. MAOP coated stainless steel (20 vol % MAOP, DMSO/TEAB, plain electrode, -0.7 V, 24 h). 77

4.11. SEM micrographs of sample P7b at magnifications of 500x and 5000x. MAOP coated stainless steel (5 vol % MAOP, DMSO/TEAB, plain electrode, -0.6 V, 24 h). 77

4.12. SEM micrographs of sample P8b at magnifications of 500x and 5000x. MAOP coated stainless steel (5 vol % MAOP, DMSO/NH_4HSO_4, CASS electrode, -1.0 V, 24 h). 78

4.13. SEM micrographs of sample VMS 1 at magnification of 500x. VMS coated stainless steel (5 vol % VMS, DMSO/TEAB, plain electrode, -1.0 V, 6 h)..... 82

4.14. SEM micrographs of sample VMS 2 at magnification of 100x. VMS coated stainless steel (5 vol % VMS, DMSO/NH_4HSO_4, plain electrode, -1.0 V, 6 h).. 82

4.15. SEM micrographs of sample VMS 3 at magnification of 500x. VMS coated stainless steel (5 vol % VMS, MeOH/TEAB, plain electrode, -1.6 V, 24 h)..... 83

4.16. SEM micrographs of sample VMS 4 at magnifications of 500x and 5000x. VMS coated stainless steel (5 vol % VMS, MeOH/NH_4HSO_4, plain electrode, -1.4 V, 24 h).. 83

4.17. SEM micrographs of sample VMS 5 at magnification of 500x. VMS coated stainless steel (20 vol % VMS, MeOH/TEAB, plain electrode, -1.0 V, 6 h)..... 84

4.18. SEM micrographs of sample VMS 7 at magnification of 500x. VMS coated

stainless steel (20 vol % VMS, DMSO/NH_4HSO_4, plain electrode, -1.4 V, 24 h) 84

4.19. SEM micrographs of sample VMS 7b at magnification of 500x. VMS coated stainless steel (20 vol % VMS, DMSO/TEAB, plain electrode, -0.55 V, 24 h).. 85

4.20. SEM micrographs of sample VMS 8 at a magnification of 500x. VMS coated stainless steel (20 vol % VMS, MeOH/NH_4HSO_4, plain electrode, -1.5 V, 24 h).. 85

4.21. SEM micrographs of sample VMS 9 at magnification of 500x. VMS coated stainless steel (20 vol % VMS, MeOH (95 %)/NH_4HSO_4, plain electrode, -1.6 V, 24 h).. 86

4.22. SEM micrographs of sample VMS 10 at magnification of 100x. VMS coated stainless steel (5 vol % VMS, MeOH/TEAB, plain electrode, -1.2 V, 24 h)).. 86

4.23. SEM micrographs of sample CV1, VMS on CASS electrode, at magnification of 500x (5 vol % VMS, DMSO/TEAB, -1.0 V, 6 h).. 90

4.24. SEM micrographs of sample CV2, VMS on CASS electrode, at magnification of 500x (5 vol % VMS, MeOH/NH_4HSO_4, -1.2 V, 6 h)..... 90

4.25. SEM micrographs of sample CV5, VMS on CASS electrode, magnification of 500 (20 vol % VMS, MeOH/TEAB, -1.0 V, 24 h).. 91

4.26. SEM micrographs of sample CV7, VMS on CASS electrode, at magnification of 500x (20 vol % VMS, DMSO/TEAB, -0.65 V, 24 h). 91

4.27. SEM micrographs of sample CV8, VMS on CASS electrode, at magnifications of 500x and 5000x (20 vol % VMS, MeOH/NH_4HSO_4, -1.25 V, 24 h)..... 92

4.28. SEM micrographs of sample CV9, VMS on CASS electrode, at magnifications of 500x and 5000x (5 vol % VMS, DMSO/TEAB, -0.65 V, 24 h).. 93

4.29. SEM micrographs of sample M1, MPC on SS electrode at magnifications of 100x, 500x and 5000x (1g MPC / 50 ml., DMSO/TEAB, -1.4 V, 6h).. 97

4.30. SEM micrographs of sample M2, MPC on SS electrode at magnification of 500x (1g MPC / 50 ml., MeOH/NH_4HSO_4, -1.3 V, 6h)..... 98

4.31. SEM micrographs of sample M2b, MPC on SS electrode at magnification of 500x (1g MPC / 50 ml., MeOH/NH_4HSO_4, -1.3 V, 24h)..... 98

4.32. SEM micrographs of sample M3, MPC on SS electrode magnification of 500x (1g MPC / 50 ml., MeOH/TEAB, -1.4 V, 24h)..... 99

4.33. SEM micrographs of sample M3b, MPC on SS electrode at magnification of 500x (1g MPC / 50 ml., MeOH/TEAB, -1.3 V, 24h)..... 99

4.34. SEM micrographs of sample M3b sweep, MPC on SS electrode magnification of 500x (1g MPC / 50 ml., MeOH/TEAB, 0 to -1.7 V, 24h).. 100

4.35. SEM micrographs of sample M4, MPC on SS electrode at magnification of 500x (1g MPC / 50 ml., DMSO/NH_4HSO_4, -1.4 V, 24h).. 100

4.36. SEM micrographs of sample M5, MPC on SS electrode at at magnification of 500x (2g MPC / 50 ml., MeOH/TEAB, -1.2 V, 24h)..... 101

4.37. SEM micrographs of sample M5b, MPC on SS electrode at magnification of 500x (2g MPC / 50 ml., MeOH/TEAB, -1.2 V, 24h)..... 101

4.38. SEM micrographs of sample M5b sweep, MPC on SS electrode at magnification of 500x (2g MPC / 50 ml., MeOH/TEAB, 0 to -1.6 V, 24h).. 102

4.39. SEM micrographs of sample M6, MPC on SS electrode at magnification of 500x (2g MPC / 50 ml., DMSO/NH_4HSO_4, -1.8 V, 6h).. 102

4.40. SEM micrographs of sample M7, MPC on SS electrode at magnification of 500x (2g MPC / 50 ml., DMSO/TEAB, -1.0 V, 24h).. 103

4.41. SEM micrographs of sample M8, MPC on SS electrode at at magnification of 500x (2g MPC / 50 ml., MeOH/NH_4HSO_4, -1.1 V, 24h)..... 103

4.42. SEM micrographs of sample M8b, MPC on SS electrode magnification of 500x (2g MPC / 50 ml., MeOH/NH_4HSO_4, -1.1 V, 24h)..... 104

4.43. SEM micrographs of sample M8b sweep, MPC on SS electrode at magnification of 500x (2g MPC / 50 mL, MeOH/NH_4HSO_4, 0 to -1.3 V, 24h).. 104

4.44. SEM micrographs of sample VM1, VMS-co-MPC on CASS electrode at magnification of 500x (2g / 2.5 ml MPC/VMS, MeOH/NH_4HSO_4, -1.3 V, 6h).. 108

4.45. SEM micrographs of sample VM2, VMS-co-MPC on CASS electrode at magnification of 500 (2g / 2.5 ml MPC/VMS, MeOH/TEAB, -1.2 V, 6h)..... 108

4.46. SEM micrographs of sample VM2b, VMS-co-MPC on CASS electrode at magnification of 500x (2g / 2.5 ml MPC/VMS, MeOH/TEAB, -1.2 V, 14h)... 109

4.47. SEM micrographs of sample VM2c, VMS-co-MPC on a plain electrode at magnification of 500x (2g / 2.5 ml MPC/VMS, MeOH/TEAB, -1.3 V, 16h)... 109

4.48. SEM micrographs of sample VM3, VMS-co-MPC on SS electrode at magnification of 500 (2g / 0.5 ml MPC/VMS, MeOH/NH_4HSO_4, -1.3 V, 24h)..... 110

4.49. SEM micrographs of sample VM3b, VMS-co-MPC on CASS electrode at magnification of 500x (2g / 0.5 ml MPC/VMS, MeOH/NH_4HSO_4, -1.2 V, 24h).. 110

4.50. SEM micrographs of sample VM4, VMS-co-MPC on CASS electrode at magnification of 500x (2g / 0.5 ml MPC/VMS, MeOH/TEAB, -1.2 V, 24h).... 111

4.51. SEM micrographs of sample VM4b, VMS-co-MPC on CASS electrode at magnification of 500x (2g / 0.5 ml MPC/VMS, MeOH/TEAB, -1.2 V, 24h).... 111

4.52. SEM micrographs of sample MM1, MAOP-co-MPC on CASS electrode at magnifications of 500x and 5000x (2g / 2.5 ml MAOP/VMS, MeOH/NH_4HSO_4, -1.3 V, 6h)..... 114

4.53. SEM micrographs of sample MM1b, MAOP-co-MPC on CASS electrode at magnifications of 500x and 5000x (2g / 2.5 ml MAOP/VMS, MeOH/NH_4HSO_4, -1.3 V, 24h).. 115

4.54. SEM micrographs of sample MM2a, MAOP-co-MPC on CASS electrode at magnifications of 500x and 5000x (2g / 2.5 ml MAOP/VMS, MeOH/TEAB, -1.2 V, 6h)..... 116

4.55. SEM micrographs of sample MM2b, MAOP-co-MPC on CASS electrode at magnifications of 500x and 5000x (2g / 2.5 ml MAOP/VMS, MeOH/TEAB, -1.2 V, 24h)..... 117

4.56. SEM micrographs of sample MM2c, MAOP-co-MPC on CASS electrode at magnification of 500x (2g / 2.5 ml MAOP/VMS, MeOH/TEAB, -1.2 V, 24h)..118

4.57. SEM micrographs of sample MM3, MAOP-co-MPC on CASS electrode at magnification of 500x (2g / 0.5 ml MAOP/VMS, MeOH/NH_4HSO_4, -1.2 V, 24h).. 118

4.58. SEM micrographs of sample MM3b, MAOP-co-MPC on CASS electrode at magnification of 500x (2g / 0.5 ml MAOP/VMS, MeOH/NH_4HSO_4, -1.3 V, 6h).. 119

4.59. SEM micrographs of sample MM4, MAOP-co-MPC on CASS electrode at magnification of 500x (2g / 0.5 ml MAOP/VMS, MeOH/TEAB, -1.2 V, 6h)... 119

4.60. SEM micrographs of sample MM4b, MAOP-co-MPC on CASS electrode at magnifications of 100x and 500x (2g / 0.5 ml MAOP/VMS, MeOH/TEAB, -1.2 V, 24h)..... 120

4.61. SEM micrographs of sample AP3b. Absorption control of MAOP on CASS electrode at magnification of 500x (2.5 ml MAOP / 50 ml, DMSO/TEAB, 6 h).. 122

4.62. SEM micrographs of sample AP8b. Absorption control of MAOP on a CASS electrode at magnification of 500x (2.5 ml MAOP / 50 ml, DMSO/NH_4HSO_4,24h)..... 123

4.63. SEM micrographs of sample AM2. Absorption control of MPC on a plain electrode at magnification of 500x (1 g MPC / 50 ml, MeOH/NH_4HSO_4, 6 h)..... 123

4.64. SEM micrographs of sample AM5. Absorption control of MPC on a plain electrode at magnification of 500x (2 g MPC / 50 ml, MeOH/TEAB, 24 h)..... 124

4.65. SEM micrographs of sample AM8. Absorption control of MPC on a plain electrode at magnification of 500x (2 g MPC / 50 ml, MeOH/NH_4HSO_4, 24 h)..... 124

4.66. SEM micrographs of sample ACV7. Absorption control of VMS on a CASS electrode at magnifications of 500x (20 vol % VMS, DMSO/TEAB, 24 h)..... 125

4.67. SEM micrographs of sample ACV8. Absorption control of VMS on a CASS electrode at magnification of 500x (20 vol % VMS, MeOH/NH_4HSO_4, 24 h).. 125

4.68. SEM micrographs of sample E1, DMSO/TEAB at –0.8 V for 6h on a CASS electrode. Magnifications of 100x, 500x and 5000x... 129

4.69. SEM micrographs of sample E2, DMSO/TEAB at –1.3 V for 6h on a plain electrode. Magnifications of 500x and 5000x. 130

4.70. SEM micrographs of sample E3, DMSO/TEAB at –0.65 V for 24h on a CASS electrode. Magnifications of 500x and 5000x. 130

4.71. SEM micrographs of sample E5, DMSO/NH_4HSO_4 at –0.8V for 24h on a plain electrode. Magnifications of 500x and 5000x. 131

4.72. SEM micrographs of sample E6, MeOH/TEAB at –1.3 V for 24h on a plain electrode. Magnifications of 500x and 5000x. 132

4.73. SEM micrographs of sample E7, MeOH/NH_4HSO_4 at –1.2 V for 6h on a CASS electrode. Magnifications of 100x, 500x and 5000x. 133

4.74. SEM micrographs of sample E8, MeOH/NH_4HSO_4 at –1.3 V for 6h on a plain electrode. Magnifications of 500x. 134

4.75. SEM micrographs of sample E9, MeOH/NH_4HSO_4 at –1.1 V for 24h on a plain electrode. Magnifications of 500x. 134

4.76. SEM micrographs of sample E10, MeOH/NH_4HSO_4 at –1.2 V for 24h on a CASS electrode. Magnifications of 500x and 5000x. 135

4.77. SEM micrograph of CASS control. Magnifications of 500x and 5000x..... 136

4.78. SEM micrograph of SS control. Magnifications of 500x and 5000x. 137

4.79. Graph showing the overall average contact angles for the oligomer/monmer and copolymer electropolymerization samples compared to non-coated stainless steel. 139

Abstract of Dissertation Presented to the Graduate School
of the University of Florida in Partial Fulfillment of the
Requirements for the Degree of Doctor of Philosophy

POLYMERIC AND METALLIC CARDIOVASCULAR BIOMATERIALS: PHOSPHOLIPID AND SILICONE SURFACE MODIFICATION BY GAMMA RADIATION SURFACE GRAFT POLYMERIZATION AND ELECTROPOLYMERIZATION

By

Lauri L. Jenkins

August 2000

Chairman: Dr. Eugene P. Goldberg
Major Department: Materials Science and Engineering

The objectives of this research were to expand the scientific understanding of hydrophilic phospholipid (PL) surface modifications on silicone and metal substrates via two unique processes: gamma radiation surface graft polymerization and electro-polymerization. This work was novel studying these two polymerization techniques to produce phospholipid-modified surfaces using a vinyl functionalized phosphorylcholine-containing monomer.

A number of synthetic functionalized PLs have been reported to produce surfaces which might better mimic the structure of natural cell membranes. Unique polymerization methods for a methacryl-functionalized PL monomer, were investigated here to prepare homopolymer and copolymers with other vinyl monomers.

The 2-methacryloyloxyethylphosphorylcholine (MPC) monomer studied, originally developed b Ishihara *et al.,* has a structure that is more hydrophilic than common PLs with long hydrocarbon tails.

Copolymers of MPC have been reported to be efficacious in reducing cell adhesion and protein deposition in blood environments. To expand our knowledge of polymers and surfaces derived from such vinyl functional PLs, as MPC, the research reported here involved two new techniques for the surface modification of silicone and stainless steel biomaterials of particular interest for vascular grafts and stents. Surface modification methods explored were gamma radiation surface graft polymerization and electropolymerization.

The first technique, gamma radiation initiated surface graft polymerization, was used produce MPC, MPC-HEMA, MPC-MAA, and MPC-NVP copolymer surfaces on silicone elastomer (polydimethyl siloxane – PDMS). Results of these experiments indicated a significant reduction in contact angle (30 to 50 degree) compared to control silicone substrates.

The second technique was the electrochemical surface polymerization of MPC monomer and copolymerization of MPC with silicone oligomers on stainless steel. The goal of copolymerization of MPC and a silicone oligomer is based on our view that such copolymer surfaces might combine the biocompatibility of a phospholipid with the elastomeric properties of silicone to produce a novel biomedical surface coating. Two silicone oligomers, with different chemical structures, were used in this study. Methacryoloxy-terminated-polydimethylsiloxane (MAOP) oligomer that provides the

typical poly(dimethylsiloxane) (PDMS) structure and vinylmethoxysiloxane (VMS) which is more hydrophilic.

The surfaces produced were characterized by contact angle, XPS and SEM analyses. The MPC surface modifications exhibited a large reduction in contact angle (15° - 32° vs. 71°) on stainless steel and (24° – 55° vs. ca. 75°) on PDMS and may provide a more lubricious surface with improved non-thrombogenic properties. The novel surface polymerization techniques examined here may allow more facile coating of metal and polymer devices with complex geometries and provide improved uniformity and adhesion using processes that may also prove to be relatively simple and inexpensive.

CHAPTER 1
INTRODUCTION

Percutaneous transluminal coronary angioplasty (PTCA) has proven to be a viable minimally invasive technique for treating coronary heart disease. However a large number of such procedures suffer from the problem of restenosis or thickening of the artery wall. Metal mesh stents that are left in place to keep arteries open have been shown to address the problem of restenosis in PTCA procedures successfully. Restenosis rates have been reduced from up to 50 % for PTCA to 15-30 % with stenting in the first 6 months after surgery.[1] It is expected that stents will be used in 56 % of all PTCA procedures worldwide by the year 2001.[1] However, these materials induce platelet adhesion and clot formation upon implantation. Literature reports[2,3] and experience from past studies[4] have reveled that silicone polymers and phospholipids have superior blood compatibility compared to other materials. Furthermore silicone, which is a elastomeric polymer, can also be used as a depot to deliver anti-inflammatory drugs to the site of vascular injury.[4] Therefore, it has been hypothesized that stents coated with silicone and/or phospholipid polymers might reduce stent thrombogenicity and also improve long-term healing of arteries.

The overall goal of this research was to explore the use of a vinyl functional phospholipid, the phosphorylcholine containing monomer (MPC), to develop a series of novel surface modifications for cardiovascular implant materials. Silicone and stainless steel substrates were chosen for this study due to their use in vascular graft and stent

implants. The grafting/polymerization techniques chosen for this research were radiation surface graft polymerization and electropolymerization.

The specific aims for this project were:

1. To demonstrate the feasibility and define the experimental parameters for surface grafting MPC and copolymers of MPC and HEMA, MAA and NVP onto a crosslinked silicone elastomer (PDMS) surface.
2. To demonstrate the feasibility and define the experimental parameters for producing uniform and adherent coatings of polyMPC, vinyl-functional silicones and copolymers thereof onto metal substrates via electropolymerization.

The MPC monomer was chosen for this study because of its unique structure. As seen in Figure 1.1, this monomer differs from most PLs in that it does not possess a long hydrocarbon chain. This allows the incorporation of this monomer into copolymers with a higher concentration of phosphorylcholine functionality and thus a higher degree of hydrophilicity per monomer unit, thus a potentially higher unit concentration on the substrate surface. Upon polymerization, MPC monomer produces a polymer with a methacrylate backbone and pendent phosphorylcholine groups. It is believed that these phosphorylcholine groups can associate with naturally occurring PLs in the blood to form bilayers or multi-layers that better mimic cell membrane structures.[1] The unique amphiphilic structure of naturally occurring PLs forms cell membranes that control the transport of nutrients, proteins, hormones and other bio-chemicals in and out of cells. The cell membrane structure also controls the absorption of blood proteins onto the surface of the cell. MPC and copolymers with butyl methacrylate (BMA) were originally

synthesized by Ishihara *et al.*, [2-4] and have been reported to improve the blood compatibility of polymeric cardiovascular materials.

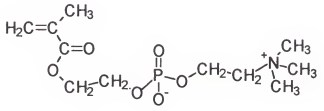

Figure 1.1. Chemical structure of the MPC monomer.

Silicone alone does not possess the mechanical strength to make a viable cardiovascular graft or stent (200-2000 psi tensile strength depending on silica filler concentration). As a coating for vascular grafts and stents it has the advantages of good biocompatibility, elasticity, and is easily loaded with drugs for local delivery. Unfortunately, silicone coatings have been poorly adherent to polymer and metal substrates. The key is to produce a method to prepare more adherent coatings and to surface modify such silicone coated grafts and stents to further improve surface properties; *i.e.* hydrophilicity to enhance lubricity and reduce cell adhesion. The approaches to this problem proposed in this work were to use gamma radiation polymerization to surface modify PDMS elastomer and to use electropolymerization to polymerize silicone PL monomers directly to metal stent surfaces.

Widenhouse *et al.* have developed methods for preparing uniquely adherent silicone coatings on cardiovascular stents and has demonstrated their use for drug delivery.[5] Research reported here may enable a further advantage by gamma radiation

grafting hydrophilic monomers onto such PDMS coatings. This offers an opportunity to improve wettability and lubricity of the PDMS surface, but also to introduce functional groups that can be used to further the incorporate drugs and proteins. Accordingly, studies described here have demonstrated gamma radiation to grafting of NVP, HEMA, MAA, and MPC monomers onto the surface of silicone. The effects of solvent, dose rate, total dose, and monomer concentrations were studied.

The second part of this research was devoted to the investigation of electropolymerization to surface modify stainless steel with silicone, MPC and silicone-MPC copolymers. Such electropolymerization provides a clean and easily controlled method to coat metal surfaces with defect-free, uniform polymer coatings. The goal is to produce a coherent coating that will have the elastic properties of silicone (needed for retention of coating coherence upon stent expansion) and the improved blood compatibility reported for MPC copolymers.[6]

Two vinyl functional silicone oligomers were chosen for this work: methacryoloxy-terminated-polydimethylsiloxane (MAOP) of 33,000 M_n with a viscosity of 1000 cs and vinylmethoxysilicone (VMS) of much lower molecular weight with a viscosity of 8 – 11 cs. The structures for these oligomers are shown in Figure 1.2.

The MAOP oligomer provides a typical hydrophobic PDMS backbone with polymerizable methacryl groups. Bausch and Lomb has patented the use of MAOP for copolymers to improve the oxygen permeability of soft contact lens.[7]

In comparison, the VMS structure provides a large concentration of methoxy groups for enhanced hydrophilicity (and possibly increased compatibility with the MPC monomer) as well as vinyl groups for polymerization, grafting, and crosslinking.

First, an electrochemical feasibility study was conducted to define useful conditions of solvent, electrolyte and monomer. Experiments were then devised to screen monomer concentration, electrolyte, solvent, and time effects. These studies have established that electropolymerization is a viable method for producing thin, coherent, uniform polymeric films of silicones, MPC and their copolymers.

Logical extension of this work will be to coat stents and demonstrate their biological performance in *ex vivo* arterio-venous canine shunt and implant studies.

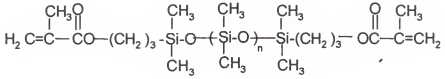

MAOP

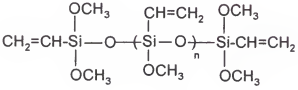

VMS

Figure 1.2. Structures for the MAOP and VMS silicone oligomers.

CHAPTER 2
BACKGROUND

Scientific Goals

Surface Modifications

Phospholipids

Biological Significance. Lipids and proteins are the principal components of cellular membranes. Most cellular membranes are comprised of approximately equal amounts of proteins and lipids. These membranes function to organize cellular matter and create a fluid two-dimensional matrix that controls molecular transport in and out of the cell. The structure of cell membranes is that of a double layer formed by the alignment of phospholipids and glycolipids with the hydrophobic tails of these molecules forming the interior barrier of the membrane. This structure is depicted in Figure 2.1. This lipid bilayer incorporates proteins on the surface and in its interior. Molecules within the membrane are free to move laterally in the membrane plane that often produces domain formation. Phospholipids, neutral lipids, and glycolipids are the three types of lipid found in membranes. Of these, phospholipids are the most abundant. The predominant phospholipids are phosphatidylcholine, phosphatidylethanolamine, phosphatidylserine, and sphingomyelin, some of whose structures are depicted in Figure 2.2.[8]

Synthetic Phospholipid Monomers. Natural phospholipid bilayers are inately mechanically weak and unstable. This makes the synthesis of phospholipid bilayers *in vitro* very difficult. In order to develop stable artifical phospholipid membranes a large number of synthetic phospholipid analouges, most with polymerizable groups, have been studied in the past 25 years.[8] though a variety of other approaches have been explored such as polymers with cholesterol moieties, [9,10] and polymeric glycolipid polymers.[11-14]

In this lab, phospholipid surface modification of biomedical polymers started with the work of Kuo.[16] This research involved the synthesis of two phospholipid monomers, both with a two-tailed structure (Figure 2.3). Kuo successfully modified PMMA with these phospholipids using gamma radiation graft and UV initiated polymerization seperately or coupled with water RF plasma pretreatment. Kuo was able to establish that these surface modifications significantly improved the epithelial cell adhesion and corneal endothelial cell damage characteristics of the PMMA substrates.

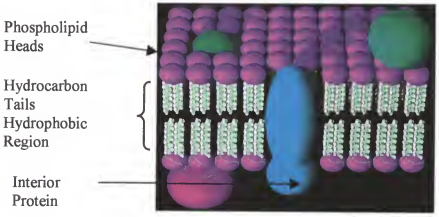

Figure 2.1 Model for the structure of cell membranes.[15]

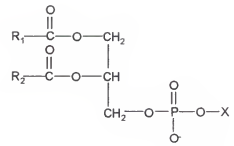

R_1, R_2 = $CH_3(CH_2)_n$-, n=10,12,14,16,18,20
or olenic, linoleic, linolenic group.

X = $CH_2CH_2N^+(CH_3)_3$ Phosphatidylcholine

X = $CH_2CH_2NH_2$ Phosphatidylethanolamine

X = CH_2CHNH_2 (COOH) Phosphatidylserine

X = H Phosphatidic acid

X = Phosphatidylinositol

X = CH_2CHCH_2OH (OH) Phosphatidylglycerol

Figure 2.2. Structure of some common biomembrane phospholipids.[8]

Of the phosphatidylcholine analoges, there are a large variety of both side-chain and main-chain polymers structures in the literature. Since research reported here is focused on the use of 2-(methacryloyloxy)ethyl-2-(trimethylammonium)ethyl phosphate (MPC) monomer, discussion of other systems will be limited to the basic synthetic route to the side-chain monomers and biological property studies specifically involving the MPC monomer. For further discussion on various phospholipid structures and their synthesis, the reader is referred to the review paper by Nakaya *et al.*[8]

The main synthetic route to side and many main-chain phospholipid polymers was first developed in 1974 by Thanh and Chabrier[17] and subsequently by Nakaya and co-workers.[18] This route is shown as Figure 2.4.

The MPC Monomer. Research involving the use of phospholipids for selective binding in the form of liposomes started in the early 1980's.[19] These systems suffered from physical and chemical instability arising from their inability to polymerize. In order to produce stable liposomes and membranes, researchers started synthesizing phospholipids with polymerizable groups in their hydrocarbon tails. One of these systems is 2-methacryloxyethyl phosphorylcholine (MPC), whose chemical structure is shown in Figure 1.1.

The chemical structure of MPC allows it to be co-polymerized with other vinyl monomers via its methacryol group. Polymerization of this monomer produces a PMMA-like backbone with attached flexible chain terminated in a phosphorylcholine (PC) moiety. This allows the resultant polymers to have a rigid backbone with flexible side groups and allows the PC groups to align on the substrate surface at the tissue interface. The MPC monomer is unique in that it does not possess the long hydrocarbon tail groups as in the monomers developed by Kuo. It also differs from Kuo's monomers and the diacetylenic monomers patented by Biocompatibles Limited,[20] due to its single vinyl group. Therefore, the MPC monomer polymerizes to provide a methacrylate backbone chain with pendent phosphoryl choline groups. This monomer is less hydrophobic than the long hydrocarbon chain monomers of Kuo and Yianni that interface. The MPC monomer is unique in that it does not possess the long hydrocarbon tail groups as in the monomers developed by Kuo. It also differs from Kuo's monomers

and the diacetylenic monomers patented by Biocompatibles Limited,[20] due to its single vinyl group. Therefore, the MPC monomer polymerizes to provide a methacrylate backbone chain with pendent phosphoryl choline groups. This monomer is less hydrophobic than the long hydrocarbon chain monomers of Kuo and Yianni that improves solubility in electrolyte systems. MPC will also increase the phosphoryl choline concentration in the polymer relative to the hydrocarbon content.

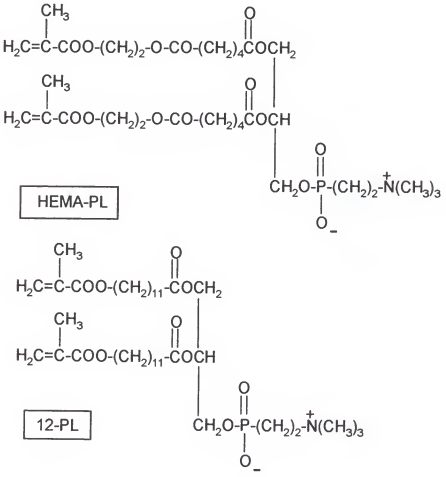

Figure 2.3. Structures of polymerizable phospholipid monomers developed by Kuo.[16]

The Ishihara research group from the Tokyo Medical and Dental Institute have broadly studied MPC and its copolymers for applications in biomedical membranes.[21] The first papers concerned the adsorption of blood phospholipids, blood proteins and platelet activation of MPC-*co*-*n*-butylmethacrylate (BMA) coated acrylic beads[1,22-24] and then *MPC-co-BMA* membranes.[3,25] That work indicated that the MPC-*co*-BMA surfaces adsorbed blood phospholipids to form bilayers which decreased protein adsorption and lowered platelet activation over poly(2-hydroxyethyl methacrylate) (HEMA) coated surfaces and non-coated surfaces.

The next series of papers focused primarily on the effect of copolymer chemical structure and substrates on protein adsorption.[24,26-28] These studies reiterated the importance of phospholipid adsorption onto the modified surface as a mechanism for reduced protein adsorption and platelet activation.

The behavior observed was also inversely proportional to the concentration of MPC in the copolymer, *ie*. the higher the MPC concentration the lower the protein adsorption and platelet activation. The addition of acrylate groups greater than methyl also decreased the blood compatibility,[27] as did ethylene oxide side chain extension greater than n=6.[26] Substrates modified included Cuprophan™ (cellulose haemodialysis membrane)[28], Pellethane™ (an aromatic polyamide), polyethylene, polyBMA[27], and PET[24]. These studies showed that substrate does affect the overall behavior of MPC-*co*-BMA copolymers.

The trend demonstrated in *in vitro* tests show that protein adsorption onto MPC-*co*-BMA coated substrates decreases after the first day. It was suggested that the phosphorylcholine structure allows for desorption of the proteins in preference to

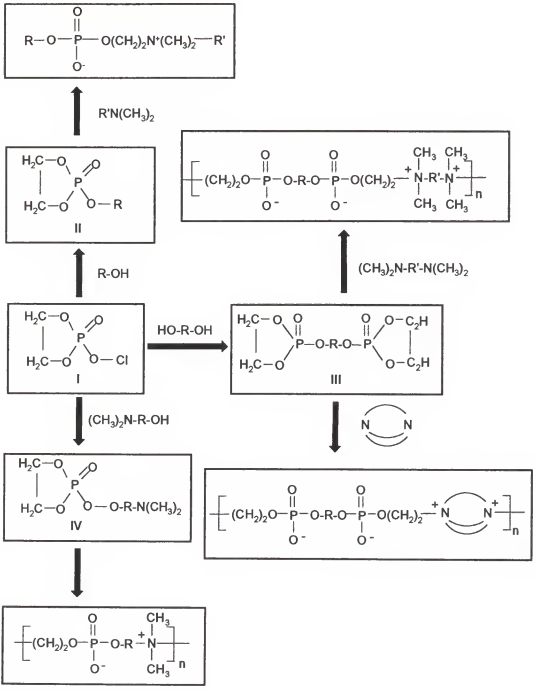

Figure 2.4. General synthetic scheme for phospholipid polymers.[8]

adsorption of phospholipids. Furthermore, MPC was suggested to mediate suppression of fibrinogen and IgG preadsorption which is thought to result in variable modulation of monocyte and macrophage adhesion and activation, possibly through the differential activation of adhesion receptors [27]. Figure 2.5 shows the results of a study comparing the expression of interleukin-1β (IL-1β) when exposed to various polymer surfaces and to three poly(MPC-co-BMA) polymers with different MPC concentrations (5,10, and 30 %).[29] This graph clearly shows reduced activation for poly(MPC-co-BMA) surfaces compared to other polymer surfaces. IL-1β is a multifunctional mediator involved with inflammation and wound healing. IL-1β can stimulate the proliferation and protein synthesis of fibroblasts and endothelial cells. Fibroblast stimulation leads to fibrinogen synthesis and the eventual formation of thrombis. Therefore IL-1β is an indicator of thrombosis activation.

The use of MPC as a surface modification for Dacron and silk fabric has been demonstrated by Yoneyama *et al.*, and Furuzono *et al.*, respectively. Yoneyama *et al.*, used a blend of MPC and segmented poly(etherurethane) (SPU) to dip-coat a 2 mm diameter Dacron vascular graft.

In vivo experiments in rabbits showed patency after five days compared to SPU coated grafts that showed "massive thrombosis" within 90 minutes.[30] Furuzono, *et. al.*, has developed a two-stage surface grafting system for silk fabric using 2-methacryloyloxyethyl isocyanate (MOI) for the stage one modification and then subsequent MPC modification. This system showed significant reduction in platelet adhesion in *in vitro* testing over non-modified controls.[31]

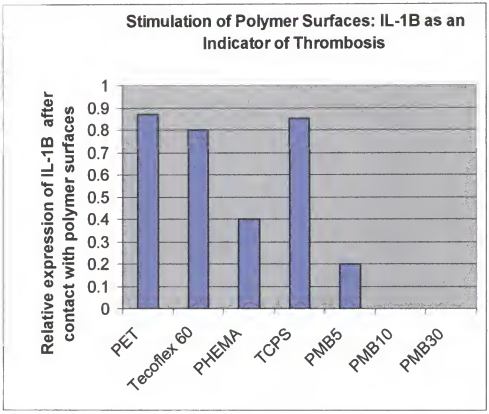

PMB = MPC-co-BMA at 5. 10, and 30 % MPC. TCPS = Tissue culture polystyrene.
N.D. = Non detectable.

Figure 2.5. Expression of IL-1 on polymer surfaces as an indicator for platelet activation (Nakabayashi, *et al.*)[29]

The use of MPC modified silicones as a keratoprosthesis was reported by Chang *et al.* Silicone was surface modified with the MPC polymer via plasma induced graft polymerization.[32] In that work, the modification was characterized by use ATR-FTIR and ESCA. Unfortunately, the phosphorus peak was not observed in the ESCA spectra and concentrations were calculated by deconvolution of the C 1s peak. This data, shown in table 2.3, may not be conclusive and demonstrates the difficulty in analyzing PDMS surfaces. However, personal contact with these researchers revealed that they were able

to prove the presence of phosphorus on the surface of these samples by using labeled ^{31}P monomers and solid state NMR.[33]

Silicones

The process of protein adsorption from the blood to a cardiovascular implant is one of competitive adsorption/desorption as is largely determined by the polarity or hydrophilicity of the implant surface. Silicone has a low surface energy and is hydrophobic with a contact angle of ~ 80°.[34] The low surface energy presumably tends to inhibit the adsorption of polar blood components.

Table 2.1. The percentage of functional groups on SR controls and MPC modified SR surface as determined by deconvoluted high resolution C1s ESCA spectra.[32]

Functional Group:	**C-H**	**C-N**	**C-O**	**O-C=O**
Binding Energy:	**(285.0 eV)**	**(286.4 eV)**	**(287.7 eV)**	**(290.0 eV)**
Control	100	-	-	-
Ar-plasma	77.81	-	15.21	6.89
SR-g-pMPC	60.02	11.2	12.27	16.51

In the competitive absorption of fibrinogen versus albumin, Cooper and Fabrizius-Homan found albumin to have a higher affinity for the silicone surface[35] and generally more favorable adsorption characteristics than polyethylene, polyurethane and Teflon™. This is significant in that surfaces that preferentially adsorb albumin have been regarded as less thrombogenic.

Silicone has also been shown to have significantly lower platelet adhesion than polyethylene in a canine *ex vivo* AV shunt study.[36] This result is not unexpected since silicone tubing has been used to hold samples in *ex vivo* AV shunt studies for years,[37-39] due to excellent blood compatibility. Silicone has been reported to reduce thrombogenicity and inflammatory response for coated Dacron™ cardiovascular grafts. These grafts also showed enhanced endoenthelialization.[40,41] Pure silicone grafts have been tested *in vivo* in canines and exhibited good tissue in-growth and favorable overall patency.[42] This result is supported by endothelial cells cultured onto silicone sheets showing good contractility and mobility, which indicates a healthy environment for cell proliferation.[43] Widenhouse *et al.* showed an inhibition of platelet adhesion on PET surfaces modified with silicone and also produced silicones surface modified with MMA.[34] Previous attempts to surface modify silicone with functionalized alkylsiloxane monolayers via oxygen radio frequency plasma, yielded materials with less favorable characteristics than unmodified silicone.[38]

The performance of silicone in practical implants is limited by poor mechanical strength, especially in the unfilled form. Therefore, it is best used as a surface coating on a stronger substrate. This work explored the use of electropolymerization to coat stainless steel with functionalized silicone oligomers and the feasibility of electro-co-polymerization of these oligomers with MPC. These materials may provide a new type of non-thrombogenic surface for metal stents.

Gamma Radiation Surface Graft Polymerization

Gamma radiation surface graft polymerization provides a clean and easy route to surface modification of polymer surfaces without the use of added chemical initiators, which can lead to compatibility and polymer degradation problems. Gamma radiation ($\lambda = < 0.1$ nm from cobalt 60 (^{60}Co) is a convenient energies of 1.17 and 1.33 MeV.[44]

Gamma initiated modification of polymers proceeds by the simulataneous production of radicals in and on the substrate polymer and radical initiation of the monomer in solution. Radicals formed with silicones are mainly by the reaction shown in Figure 2.6.

This simultaneous creation of reaction sites on substrate and monomer leads to a complex mixture of grafted, crosslinked, and interpenetrating polymer networks. Swelling the substrate in a solvent solution of monomer leads to a surface rich graft region on the substrate. The depth, concentration and profile of this grafted region are largely dependent on the swelling potential of the monomer/solvent system. The solubility of the monomer in the substrate, *i.e.* monomer diffusion, will determine the concentration and depth of the graft. If the monomer/solvent system is not a good solvent for the polymer substrate, then the graft reaction becomes more superficial and diffusion controlled. The efficiency of the graft reaction also depends on the relative stability of the substrate radicals and the monomer radicals. The substrate radicals need to have a significant propensity to react, rather then to recombine or degrade. Graft formation is also increased when radical yields are higher for the substrate than for the monomer.[44]

The radiation-chemical yield of radicals is defined as the number of chemical events occurring per 100 eV of absorbed energy. This quantity is referred to as the

"G-value" of the system and can be used to choose appropriate monomer/polymer systems for co- and graft-polymerization. The G for methylmethacrylate (MMA) is 11.5 and for PDMS is ~7.2. [44] This indicates that radiation induced radical formation will occur at a higher rate in MMA than for PDMS, which is less favorable for surface modification of PDMS. Of course, we cannot directly translate the G value for MMA to that of MPC. Even though they are both methacrylates, they are electronically and structurally very different monomers. Gamma initiation of vinyl monomers has been shown to proceed by a traditional free-radical mechanism, the rate of which is proportional to the monomer concentration and the square root of the dose rate. The reaction rate of a monomer may also be affected by the solvent, pH, and temperature.

Chlorinated solvents have been shown to accelerate the reaction of vinyl monomers upon gamma irradiation, whereas, benzene reduces the rate of reaction, due to formation of relatively stable radicals.[44]

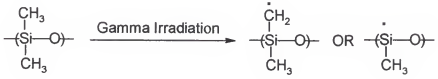

Figure 2.6. The gamma induced formation of radicals on silicone.

Electropolymerization

Electrochemical polymerization on surfaces has been investigated for a variety of monomers and generally for non-medical applications, such as corrosion control. This

research has emphasized the use of PL and silicone vinyl monomers to modify the metal surfaces of implant materials via electropolymerization. To prepare more uniform, adherent, and stable coatings than may be possible by other methods. Electro-polymerization also offers the ability to coat highly complex and sharp edged surfaces uniformly. Uniform, defect-free coatings are inherently likely since electro-polymerization is favored at edges or thin or "pinhole" areas due to lower electrical resistance in these defect areas with respect to coated areas. Electropolymerization also usually can occur under mild conditions of low voltage, room temperature, and low current density.[45]

The investigation of the electropolymerization of vinyl phospholipids reported here is novel. Vinyl phospholipids have been reported in the literature to polymerize by chemical, thermal, photochemical and plasma initiation, but no reference to electro-polymerization of vinyl PLs has been reported.

Electropolymerization involves electronic oxidation or reduction of chemical species that, in turn, initiate the polymerization of monomers in solution. The initiating species can be derived from electrolyte, solvent, or monomer. The polymerization is initiated at the electrode surface, the cathode for reductions and the anode for oxidation. The polymer is formed at the electrode surface and in the bulk of the cell solution, depending on the solubility of the polymer in the solution and the mobility of the initiating species. In order to preferentially coat the electrode surface (the implant or device), and inhibit bulk polymerization, the relative solubility of the polymer and solvent and the rate of initiation must be controlled. Initiation can proceed through an ionic, free radical or mixed mechanism.[45] The initiation of the polymerization can be by

direct reduction or oxidation of the monomer or by reduction or oxidation of an electrochemical initiator. This initiator usually also acts as the electrolyte.

The basic function of the electrochemical cell involves the application of either a set potential (potentiostatic mode) or a set current (galvanostatic mode) in reference to the reference electrode. The working electrode is the surface at which the chemical event takes place. In electropolymerization, the working electrode is the metal to be coated and is usually the cathode (in the electropolymerization of most vinyl monomers). Two common reference electrodes are either a Standard Calomel Electrode (SCE) or a Ag/AgCl electrode. The counter electrode is usually a platinum electrode due to its inert nature and high oxidation potential (so it is not oxidized and plated-out at the cathode). This cell configuration was also used in a potentiometric-scanning mode to run cyclic voltametry that established the reduction/oxidation potentials for the monomers in solution. The system was controlled by a potentiostat. Figure 2.7 shows the basic cell design. Coating experiments can be run in either potentiostatic or galvanostatic mode depending on the specific initiation mechanism of the monomer/electrolyte system. Waveform patterns can also be used in either mode to control the rate and duration of initiation events.

Mengoli, *et. al.*, studied the electropolymerization of methacrylate, methylmethacrylate, t-butyl methacrylate, isoamylmethacrylate and methacrylonitrile polymers. In this study the reduction of acrylic monomers on steel was attributed to an anionic mechanism based on the following experimental observations: [46]

1. The presence of free radical inhibitors did not affect the polymerizaiton.
2. Coating was inhibited by small quantities of water or other protic species.

3. The molecular weight of the polymers in solution was low.
4. The T_g of isobutylmethacrylate polymers matched that of anionically prepared polymer (T_g = 284 °C).

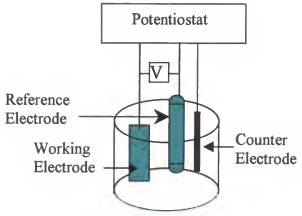

Figure 2.7. Basic electrochemical cell design.

Funt and Williams found that the polymerization mechanism was dependent on the electrolyte species in the co-polymerization of MMA and acrylonitrile.[47] Mengoli, *et. al.*, make two primary points in their conclusions: One is that the polymer formed at the working electrode surface must be insoluble in the solvent/electrolyte system, at least on the time scale of the experiment. Second, the polymer chain length must be low. Otherwise the overall polymerization reaction will not be confined to the surface of the electrode and bulk polymerization will result. One can imagine that coating requires a short-lived initiating species and fast polymerization. The "throwing power" of the reaction is related to the ability of the system to coat both sides of the electrode uniformly. This parameter is also dependent on the solubility of the growing polymer, the

solvent system, monomer concentration and current density. Important parameters that affect the electropolymerization system include:

1. The difference in solubility parameter between the monomer/electrolyte/solvent and the polymer.
2. The current density.
3. The solvent/electrolyte system.
4. Monomer concentration.
5. The pH, in some systems such as 2-vinylpyridine.[48]

The experiments conducted in this research used a basic electrochemical cell as shown in Figure 2.7. All experiments were run in potentiostatic mode or as a potential sweep to insure mainly cathodic initiation. The potentials were determined by cyclic voltamograms (CVs) run prior to the coating experiment. The effects of solvent/electrolyte system, time and monomer concentration were studied in order to establish favorable conditions for coating. Solvents and electrolytes were chosen with the characteristics of biocompatibility, solubility parameter, and likely feasibility from the literature.

Applications

Synthetic Cardiovascular Grafts

Vascular Grafts. Atherosclerosis is a disease caused by the progressive deposition of plaque in the arteries that results in reduced blood flow and is responsible for 50 % of the deaths in the United States.[49] This reduction in blood flow can lead to ischemic heart disease. Treatment for atherosclerosis involves balloon angioplasty, endarterecty or bypass of the affected artery with a vascular prosthesis, a "graft."

Balloon angioplasty is the insertion of a balloon-tipped catheter into the vessel and subsequent inflation of the balloon in the stenosed area to enlarge the narrowed lumen by fracture of the plaque and stretching of the lesser diseased wall at the site. One of the drawbacks of this procedure is that dislodged plaque can act as emboli that can clog arteries and cause stroke, or limb loss. The other problem is injury imposed on the vessel during the procedure, can lead to the formation of thrombus, restenosis, or weakening of the vessel wall.

Before the recent advent of stented angioplasty, by-pass surgery has been the preferred route of treatment for patients with healthy saphenous veins. In this procedure, the saphenous vein is harvested from the patient and used as an autograph (transplants within the same individual) to bypass the occluded vessel(s). Other sources of autograph or homograft (from same species) veins are the mammary and umbilical arteries Veins are used instead of arteries due to the body's ability to re-route blood flow in venous systems. Many patients who undergo bypass surgery suffer from co-morbidities, such as diabetes, which prevents the harvesting of healthy autograph venous tissue. In these individuals, the only alternative is to rely on synthetic vascular prostheses.

Currently available grafts are primarily made from Dacron® or Gore-Tex®. The Dacron® grafts are woven from polyethylene terephthalate (PET) fibers in non-velour or reinforced velour woven manner. The Gore-Tex® grafts are made by high-temperature extrusion of polytetrafluoroethylene (PTFE) to form a foam structure with controllable pore size. Unfortunately, for small diameter graft (<6 mm) these materials suffer from poor patency rates (43 to 57 %).[50] More than 50 % of small diameter grafts occlude within three years.[51] This lack of long-term patency is primarily due to early clotting

and progressive anastomotic intimal hyperplasia. Factors linked to intimal hyperplasia include surface thrombogenicity and compliance mismatch at the anastomosis.[52-55]

Recently, polyurethane vascular grafts have become available and have been shown to exhibit less neointimal proliferation over PTFE vascular grafts. [50,52,56]

Current Research. PET and PTFE vascular grafts have been fairly successful in large diameter (>7mm) applications.[57,58] In small diameter applications (<6mm), these materials suffer from poor long-term patency rates. The effort to improve the surface thrombogenicity and compliance mismatch problems of existing grafts has mainly focused on the surface modification of current synthetic grafts with more biocompatible polymeric coatings. This approach has been combined with drug release and tissue engineering strategies that include endothelial cell seeding and gene therapy. Some researchers have taken this concept further in attempting a more natural vessel-like structure by use of a PGA or PFLA scaffold for cellular seeding.[58]

Some of the polymeric surface coatings that have been studies for this application are:

-Polydimethylsiloxane (PDMS)[34,38]

-Polymethyl methacrylate (PMMA)[34]

-Polysulfoethyl methacrylate (PSEMA)[34]

-Polyurethanes (PUR)[53]

-PDMS-polyurea-urethanes[59]

-PUR, HEMA/styrene block co-polymer[60]

-Phospholipid-PUR copolymers on Dacron,[30] phospholipid modified silk.[31]

A general trend for these coatings is to enhance the surface properties of existing grafts with polymers for better blood compatibility. Silicone coatings also provide a matrix for drug delivery. The copolymerization of phospholipid polymers with PURs reportedly enhances the physical stability on the substrate surface,[30] or the extent of grafting onto the substrate.[31] These studies used 2-methacryloyl-ethylphosphorylcholine (MPC) as the phospholipid containing monomer.

In the MPC studies of Ishihara *et al.*, Dacron vascular grafts (2 mm) were dip-coated with a blend of poly(etherurethane) and polyMPC and showed patency through a 5-day *in vivo* study in rabbit carotid arteries.[30] The silk fabric was chemically grafted with 2-methacryloylethoxy isocyanate (MOI) and then the MPC grafted as a second step. This system was tested for platelet adhesion *in vitro* by measuring the lactic dehydrogenase released by attached/activated platelets.[31] Even though this system is being used to develop modified silk sutures, the same system could be used to modify vascular graft materials with carboxylic acid, amine, or hydroxyl groups.

The research presented here was aimed at combing the characteristics of PDMS with the less thrombogenic and hydrophilic properties of a phospholipid to create a gamma radiation polymerized surface modification for cardiovascular materials such as Dacron.

Endoluminal Cardiovascular Stents (CV Stents)

History. Charles Dotter initially proposed the use of prostheses to maintain endoluminal integrity in 1964. Dotter proposed the use of a silastic supportive material and coined the use of the word "stent" to describe coiled-wire vascular implants. These

early stents were the same size as the vessel and were placed using a guidewire and "pusher" and suffered from displacement and occlusion.[61]

After this initial work, the field was dormant until the early eighties, when the feasibility of transcatheter arterial grafting was shown to be feasible. This was when the use of nitinol (a titanium and nickel alloy) came into use. Nitinol has the ability to be compressed or straightened at room temperature and return to its original form upon heating to body temperatures or higher. Soon after the introduction of the nitinol stent, stainless steel coil stents were introduced by Maass and colleagues.[61] Palmaz introduced balloon-mounted stents for simultaneous dilatation and stent delivery in 1985. These stents were made of continuously woven stainless steel wire with soldered cross-points.

The early animal study results on these stents foretold the main problems that have hindered the use of CV Stents to date: thrombus occlusion and restnosis.[61] The first human implantation of a self-expanding stent was done by Jacques Puel (Toulouse, France) in 1986 and was shortly followed by Ulrich Sigwart (Lausanne, Switzerland). As a result of a landmark study by Sigwart, the US Food and Drug Administration (FDA) gave approval for phase I trials in the United States. These initial trials involved the Gianturco-Roubin™ and Palmaz-Schatz™ balloon-expandable intracoronary stents.[61]

The results of these and other early trials indicated that subacute stent thrombosis was clearly a problem even when aggressive anticoagulation regimens were used. The ideal characteristics for stents were defined as:[61]

1. Trackable
2. Low, unconstrained profile
3. Radio-opaque

4. Thromboresistant
5. Biocompatible
6. Reliably expandable
7. High radial strength
8. Circumferential coverage
9. Low surface area
10. Hydrodynamic compatibility

The next development in stent implantation came from ultrasound imaging that revealed that most stent insertions were far from optimal. Incomplete stent apposition, incomplete or asymmetrical stent expansion, and persistent disease were reduced if the distal and proximal vessel could be seen by this technique. Colombo and colleagues were able to end the requirement of post-intervention anticoagulation therapy by using high-pressure non-compliant balloon catheters deployed with ultrasound guidance.[61] Neumann and colleagues furthered these advances by noting that platelet markers and not coagulation factors indicated thrombosis risk. This has led to the use of antiplatelet therapy that has greatly reduced the incidence of haemorrphagic and vascular complications.[61] These developments have decreased bu tnot eleiminated the risk of sub-acute thrombosis.

Today, ultrasound guidance and antiplatelet therapy are standard procedure. Restenosis and intimal hyperplasia remain significant problems with restenosis rates remaining at 10 to 30 %, depending on the vessel. Approaches being used to reduce these problems include the coating of metallic stents, polymeric and bio-degradable stents, drug-release polymeric coatings, and radioactive stent materials.[62-64]

Current State of Art. Stent availability in the United States is limited due to strict FDA regulation. Europe and Japan enjoy a greater variety of designs. Current stent designs fall into several categories: [65]

- Balloon-expandable versus self-expanding.
- Slotted tubular versus coil stent.
- Premounted versus unmounted stents.
- Covered stents.
- Coated stents.
- Bifurcated stents.

FDA approved coronary stents include the Johnson & Johnson (J&J) Palmaz-Schatz stent, the FlexStent and GRII by Cook, Inc., Guidant's ACS Multilink, and the Wiktor stent by Medtronic.

A primary problem with these types of stents is incorrect sizing to the vessel that can lead to complications in vessel healing. Balloon-expandable stents are sized to the minimum diameter of the vessel, whereas the self-expanding stent is sized to the maximum reference diameter. Both types of stents usually require secondary balloon expansion after deployment. Self-expanding stents often undergo foreshortening during deployment that complicates placement.[65]

Coiled stents were developed to provide flexibility and are still preferred in the case of complex bifurcation lesions. This is due to their flexibility, greater side-branch access and the ability to overlap the proximal ends. Tubular stents are generally more rigid and do not allow for proximal overlap. Tubular stent design has advanced and the flexibility of tubular stents has been improved. Tubular stents have the advantages of

providing greater surface area coverage of the stented lesion and improved radial strength.[65]

Unmounted stents are not available in the United States. Outside the United States, unmounted stents are widely used since it enables the surgeon to mount the stent onto the balloon catheter of their choice. Pre-mounted stents are less likely to be dislodged during the procedure and are reliably crimped onto the balloon catheter. The major disadvantage of pre-mounted stents is that most are delivered on larger-profile balloons that can not withstand high-pressure inflation. This usually leads to the use of a post-deployment balloon for high-pressure complete expansion.[65]

Table 2.1 lists the major manufacturers of cardiovascular stents, their major available stent designs and characteristics thereof.

Complications and Problems. The two major complications of intravascular stenting are thrombosis and restenosis.

Thrombosis. Unacceptable levels of thrombosis confounded early stenting procedures. These problems were greatly reduced by advances in procedure, i.e. high-pressure balloon expansion, and enhanced antiplatelet therapy. Recent studies have shown thrombosis rates of less than 2% for elective implantation and 5% for abrupt closure.[66-68] Even though these results are a great improvement over initial rates, thrombosis is a serious complication leading to myocardial infarction (61%) and death (12%).[69] Therefore, the reduction of stent thrombosis is still a key research objective.

There are two types of thrombosis: acute and subacute thrombosis. Acute thrombosis occurs within hours of stenting and is usually the result of incomplete stent

expansion and vessel dissection. Subacute thrombosis is more common and can occur up to 30 days after the stenting procedure.[61]

The factors that influence thrombosis can be broadly classified as surface interactions and rheological factors. Surface interactions are the result of the complex series of events that are initiated at the stent surface – blood interface. In animals, endothelialization of implanted stents occurs 2 to 3 months after implantation. The maximum risk of thrombotic occlusion is within the first two weeks post-implantation.[61] Plasma proteins start to adsorb to the stent surface immediately after deployment. These proteins form a monolayer on the stent surface whose composition depends on the concentration and surface affinity of the blood proteins.

Albumin is the blood protein in greatest abundance and usually coats the surface first. Other proteins with a lower blood concentration, but higher affinity, then slowly replace the albumin on the stent surface. This phenomenon is known as the Vroman effect.[70] Blood proteins with a high affinity to metal surfaces include fibrinogen, compliment factors, fibronectin, and high molecular weight kininogen.

Circulating platelets can adsorb to these proteins and exposed collagen from the underlying damaged vessel wall. Platelet activation leads to the release of chemo-attractant molecules and the subsequent formation of platelet aggregates.[61] This initiates the coagulation cascade which results in the formation of fibrin clots by the cleavage of fibrinogen by thrombin.

There are two pathways to initiation of the coagulation cascade: The intrinsic pathway is initiated by the adsorption of factor XII to the foreign surface and its subsequent conversion to factor XIIa. The extrinsic pathway occurs when factor VII

contacts thromboplastin released by the injured vessel. Circulating platelets can adsorb to these proteins and exposed collagen from the underlying damaged vessel wall. Platelet activation leads to the release of chemo-attractant molecules and the subsequent formation of platelet aggregates.[61] This initiates the coagulation cascade which results in the formation fibrin clots by the cleavage of fibrinogen by thrombin.

Rheological factors involve the flow dynamics of the blood through the stented area. The presence of a stent creates substantial differences in the hemodynamic and wall rheological characteristics of the vessel. Fluid dynamic studies in a stent model have revealed regions of low velocity before and after the stent and high turbulence is seen in the stented region.[61] Fibrin and platelet aggregation occurs preferentially in regions of low flow. Stent design should include flow analysis to reduce negative hemodynamic effects.

Restenosis. Neointimal hyperplasia is the predominant mechanism for stent restenosis. The neointima is formed from proliferating smooth muscle cells. Stent implantation can lead to significant injury to the internal elastic lamina, media, and adventitia. This damage causes inflammation and proliferation of smooth muscle cells that leads to restenosis. The stent struts provide a scaffold for the formation of thrombi. Reactive inflammatory cells migrate into and infiltrate these regions as early as 15 minutes to as late as 56 days in animal models. The local concentration of monocytes also increases after stent implantation reaching a maximum at around seven days. Reduction in adherent and tissue monocytes has been shown to correlate with a reduction in neointimal hyperplasia.[61] Smooth muscle cells (SMCs) migrate form the media to the neointimal layer where the thrombi provide a scaffold for SCM proliferation. The degree

of SMC proliferation and neointimal hyperplasia is proportional to the degree of early inflammatory cell involvement.[61]

Table 2.2. Summary of major coronary stent manufacturers and designs as of 1998.[71,72]

Manufacturer	*Stent Name*	*Materials/Design*	*Key Features*
Johnson & Johnson	Palmaz-Schatz	Uncoated stainless steel, slotted mesh	15 & 30 mm lengths, 3.0, 3.5 & 4.0 mm dia. FDA approved
Johnson & Johnson	Crown	Uncoated stainless steel, slotted mesh	More flexible than Palmaz-Schatz. Mounted and unmounted versions.
Johnson & Johnson	Cordis Stent	Tantalum, single sinusoidal helical coil	
Johnson & Johnson	Isostent	J&J stent coated with radioactive isotope	Coated with radioactive isotope
Medtronic	Wiktor	Tantalum, single wire sinusoidal helix coil	High radiopacity, flexible, 16mm, 3.0-4.5 mm dia. FDA approved
Medtronic	Wiktor I Wiktor 1 Plus	Tantalum, single wire sinusoidal helix coil	Tighter pattern than Wiktor, available in more lengths, "Plus" is heparin-coated.
Medtronic	beStent	Stainless steel, slotted tube.	
	InStent Cardio-Coil	Single wire, simple coil	Self expanding
Guidant/ACS	ACS MultiLink	Stainless steel, slotted tube, zig-zag rings joined by multiple links.	Elastic membrane btw. Balloon and stent distributes expansion force evenly. Retractable sheath which covers stent prior to deployment. FDA approved.
Arterial Vascular Engineering	Micro Stent	Stainless steel, welded, sinusoidal shaped rings (3mm segments, 4 crowns)	Moderately radiopaque. 6 – 24 mm length, 3, 3.5 & 4 mm dia.
Arterial Vascular Engineering	AVE GFX Stent	Stainless steel, welded, sinusoidal shaped rings (2mm segments, 6 crowns)	
Boston Scientific	NIR Stent	Stainless steel, continuous multicellular uniform design, tubular slotted.	Low profile, excellent flexibility.
Boston Scientific	Radius	Nitinol, tubular slotted mesh	Self expanding
Cook	GR Flex Stent	Stainless steel, flexible coil	
Cook	GRII	GR with wire spine.	
Global Therapeutics	Freedom and Freedom Force	Stainless steel, Zig-zag fishscale.	
Pfizer/ Schineider Progressive Angioplasty Systems	Wallstent ACT-one	Eligiloy, multiple wire braid. Nitinol, slotted tube.	Self expanding

Current Research Efforts. The most popular coating for stents currently is heparin. In March 1998, Medtronic introduced its heparin-coated stent, the Wiltor GX Hepamed to Europe and several international markets.[71] This stent has heparin covalently bonded to the surface of a tantalum wire stent. There is much debate on the efficacy of these coatings,[65,71] though this has not slowed the research efforts for development of heparin surface modification and controlled release for biomaterials.[73-75]

Non-biodegradable polymers and autologous veins have been used to cover stents. Though this technology is investigational, their potential is substantial. They cover diffuse atheromatous debris encountered in aged and degenerated vein grafts. The main problem with current designs is their high collapsed profiles. Materials are needed to provide a low-profile delivery while minimizing thrombosis and inflammation.[65]

One avenue to reduce the surface adsorption characteristics of stents is to use polymer coated or exclusively polymer stents. Both biodegradable and inert polymers have been investigated for use as stent materials, including:

- Polyethylene terephthalate (Dacron)[76,77]
- Polyhydroxybutyrate valerate[78]
- Poly-L-lactic acid (PLA)[79,80]
- Polyglycolic acid (PGA)[81,82]
- Co-polymers of PLA - PGA[83]

Results have shown that polymer stents can be balloon deployed and expanded, but suffer from problems such as distal migration and inflammatory response.[80]

The use of polymer coated metal stents is currently being investigated. The polymer component of these stents can be used to improve surface blood compatibility or for the local controlled release of drugs. Table 2.2. shows some of the many materials that have been used to coat metal stents in an effort to reduce thrombogenicity. Some of the most recent studies include: Polydimethylsiloxane (PDMS) applied to the metal surface by pulsed laser ablation deposition (PLAD) and dip-coating. [84, 5] The dip-coated PDMS system has been studied as a controlled release system for dexamethasone which inhibits the proliferation of smooth muscle cells.[5] Hyaluronic acid has been attached to stainless steel tubes with a subsequent reduction in platelet adhesion as determined by an A-V shunt model.[85] Lahann *et al.* used chemical vapor deposition to attach a functionalized [2.2]paracyclophanes to metal stent surfaces. These coatings were than pyrolyzed to functionalized poly(p-xylenes) and the thrombin inhibitor r-hiruden was immobilized to the film surface.[86] Biocompatibles Ltd. has developed the div Ysio stent that is coated with phosphorylcholine. These stents have been shown to minimize platelet adhesion in *in vitro* studies, which is hoped to lead to reduced thrombosis *in vivo.*[61] Commercially available coated stents are:

- InFlow, gold-coated
- NIR, gold-coated
- Tensum, silicon-carbide-coated
- Tenax, silicon-carbide-coated
- Diamond AS, diamond-like carbon coated
- Diamond Flex AS, diamond-like carbon coated
- Palmaz-Schatz, heparin coated

- Wiktor, heparin coated
- JOSATENT, heparin coated
- PRO-STENT, heparin coated
- DivYsio, phosphorylcholine coated

Table 2.3. Materials studied for use as stent surface modification.[61]

Synthetic Materials	*Natural Materials*
Polyurethane	Collagen
Segmented polyurethane/heparin	Heparin
Poly-L-lactic acid	Fibrin
Cellulose ester	Phosphorylcholine
Polyethylene Glycol	AZI adsorbed to cellulose
Polyphosphate ester	AZI/UK adsorbed to cellulose
Gold	
Silicon Carbide	
Diamond-like carbon	

AZI = monoclonal antibody directed against rabbit platelet integrin $\alpha_{IIb}\beta_{III}$.
AZI/UK = monoclonal antibody directed against rabbit platelet integrin $\alpha_{IIb}\beta_{III}$/urokinase conjugate.

Even though there are many new ideas and stent designs actively being pursued, there is also a vast need for improvement in surface compatibility. This is a problem that may eventually include polymeric surface coating and drug release in one design. This is why development of a silicone-phospholipid copolymer may prove to be advantageous.

The hydrophilic phospholipid component should migrate to the surface of the film when exposed to a hydrophilic environment and the silicone would provide the mechanical properties needed for retention of film coherence during stent expansion.

CHAPTER 3
MATERIALS AND METHODS

Gamma Radiation Surface Graft Modification of Silicone

Materials & Reagents

Substrates. The silicone substrates for the GRIP modification experiment consisted of poly(dimethylsiloxane) prepared from a two-part, non-silica filled, oligomer Shin-Etsu (KE-1935) system purchased from Shincor Silicones. The samples were cut as 1 cm diameter discs from sheets of cured silicone. These sheets were prepared by mixing in a plastic cup, 50 ml of each component. This mixture was then spread onto glass plate mold (16 cm x 24 cm) and degassed under vacuum (~ 76 cm Hg) at 40-50 °C for until no more bubbles formed and them cured at the same temperature with no vacuum. The 12" x 12" cast sample was then held under vacuum for 24 h. The final thickness ranged from 2-4 mm. Sample discs were cut from this plaque using a 1 cm cork borer. All samples were Soxhlet extracted in hexane to remove any residual oligomer and impurities then dried *in vacu* overnight.

Monomers & Reagents. The MPC monomer was supplied by Professor Y. Iwasaki, Institute for Medical and Dental Engineering, Tokyo Medical and Dental University, used without further purification and stored in a freezer and weighed-out in a glove box.

2-Hydroxyethylmethacrylate (HEMA), N-vinylpyrrolidone (NVP), methacrylic acid (MAA) and methylmethacrylate (MMA) (ARCOS chemical) were vacuum distilled

at 1mm Hg and in order to remove stabilizer. These monomers and oligomers were refrigerated until use. All water was ultra-purified to a resistance of 15 MΩ/cm. DMSO was purchased through Aldrich, 99.8%, anhydrous in a sure seal container and used without further purification. Methanol (Fisher Scientific, electronic grade) and chloroform (reagent grade) was used as received.

Sample Preparation & Substrate Extraction. Individual PDMS disc (1 cm diameter, 2 – 4 mm thick) samples were placed into 10 x 150 mm glass test tubes fitted with rubber septa. The presoak solution added and samples let stand for a pre-described time, after which the pre-soak solution was decanted off of the sample and the gamma solution added. These solutions were degassed by bubbling argon through the solution for two minutes. These sealed test tubes were place in a rotating sample turret and placed into a ^{60}Co source (as shown in Figure 3.1). These samples were irradiated for a time calculated to deliver a set radiation dosage. The sample were then removed and placed into fresh test tubes and extracted in a series of solvents dependent on monomer system. This was usually methanol, 1 day, water, 2 days. Contact angle measurements were then made, samples dried, FTIR and XPS spectra obtained.

Surface Modification Experiments

The following experiments were run in order to find a route to the surface grafting of MPC to PDMS via GRIP. Copolymer systems were used to increase the solubility of the MPC monomer into the PDMS system. This work was based on the success of Widenhouse in modification of PDMS surfaces with MMA.[34] Two-stage modification experiments were also tried in order to surface graft the MPC onto a PDMS surface that had already been modified with a hydrophilic monomer.

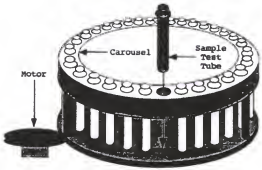

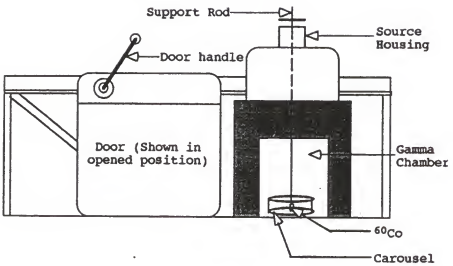

Figure 3.1. Sample turret and gamma ^{60}Co source configurations for gamma polymerization.[34]

Gamma Initiated MPC/HEMA and MPC/MAA Copolymer Modification of PDMS

Previous experiments had shown that HEMA and MAA could be used to surface modify PDMS using gamma initiated polymerization. These experiments showed a greater degree of modification was seen in the HEMA system. This lead to the use of

HEMA and MAA as co-monomers for the Hydrograft™ surface modification of PDMS with MPC. The following samples were made to delineate the effect of solvent system on the gamma radiation initiated modification of these monomers. Monomer ratios and concentrations were chosen with respect to previous experiments run in this research group for modification of other substrates.[87]

The first copolymer experiment was run with the pre-soak solutions of 20 w/w% monomer, 0.1 mole MPC and 0.9 mole HEMA or MAA. The pre-soak was three hours, the solution removed, and the gamma monomer solution added. The gamma solution for the HEMA/MPC system was 0.1 mole MPC, 0.9 mole HEMA, 7.5 w/w% monomer in 50:50 water/methanol. For the MAA/MPC system, the same molar ratio was used, but the total monomer concentration was 5 w/w% in water.

A third series of sample was run separately with repeated controls from the first two series. This series used the same monomer concentration but the pre-soak solutions were both in methanol and the gamma solutions were both in 50:50 water/methanol. The samples were exposed to a total gamma dosage of 0.05 Mrads at 270 rads/minute (4 " from the source). All samples were removed from the gamma solutions after irradiation and extracted in methanol for two days (changing the solvent twice per day) and then soaked in water at least one day prior to contact angle measurement. Samples for this experiment are listed in Table 3.1.

A second copolymer study was run for these systems and included modification with MPC alone. The monomer ratios were changed for this experiment. The HEMA/MPC soak solution was 6:1 moles HEMA : moles MPC at 18 w/w% in methanol. The HEMA/MPC gamma solution was 9:1 moles HEMA : moles MPC at 8w/w% in

50:50 water/methanol. For the MAA/MPC system, the soak solution was 8.5:1 moles MAA : moles MPC at 25 w/w% in methanol. The MAA/MPC gamma solution was 19:1 moles MAA : moles MPC at 10 w/w% in water. The MPC system was pre-soaked with 22 w/w% MPC in methanol at room temperature. The gamma polymerization solution was 11 w/w% MPC in methanol.

Table 3.1. Listing of samples for the first HEMA/MPC and MAA/MPC co-polymer study.

Sample	*Pre-Soak Solution*	*Gamma Solution*
1A, 1B, 1C	HEMA/MPC – Water	HEMA/MPC - Water/Methanol
2A, 2B, 2C	MAA/MPC – Water	MAA/MPC - Water
3A, 3B, 3C	HEMA/MPC – Methanol	HEMA/MPC – Water/Methanol
3D, 3E, 3F	MAA/MPC – Methanol	MAA/MPC – Water/Methanol
Control 1 & 1a	Water	Water
Control 2 & 2a	Water	Water/Methanol
Control 3	Methanol	Water/Methanol

Table 3.2. Listing of samples for the second HEMA/MPC and MAA/MPC co-polymer study.

Sample	*Pre-Soak Solution*	*Gamma Solution*
MH1, MH2, MH3	HEMA/MPC – Methanol	HEMA/MPC - Water/Methanol
MM1, MM2, MM3	MAA/MPC – Methanol	MAA/MPC - Water/Methanol
MPC1, MPC2, MPC3	MPC – Methanol	MPC – Methanol
Control 1	Methanol	Water/Methanol
Control 2	Methanol	Methanol
Control 3	Methanol	Water

The samples for this experiment are listed in Table 3.2. Gamma exposure was 0.05 Mrads at 270 rads/minute. All samples were removed from the gamma solutions

after irradiation and extracted in methanol for two days (changing the solvent twice per day) and then soaked in water at least one day prior to contact angle measurement.

Gamma MPC Modification of PDMS

In order to see if increasing the swelling of the MPC into the PDMS will increase the surface modification, chloroform was used as the pre-soak solvent in this experiment. The pre-soak solution for all samples was 20 w/v% MPC in chloroform. All the gamma solutions were at 10 w/v% MPC in water/methanol at the ratios shown in Table 3.3. Two different gamma dosages were used. Three samples were run at each condition listed in Table 3.3, plus three controls for each dosage, for a total of 25 samples. Controls were soaked in chloroform and irradiated in methanol/water without monomer. Three additional samples were included in the 0.025 Mrad condition (1.5 h at 278 rads/ min, 4 " from source) where the samples were irradiated in the pre-soak solution (condition 4).

All samples were removed from the gamma solutions after irradiation and extracted in methanol for two days (changing the solvent twice per day) and then soaked in water at least one day prior to contact angle measurement.

Table 3.3. Conditions for MPC surface modification of PDMS by gamma initiation.

Condition	*Gamma Solution MeOH: H_2O*	*Gamma Dosage (Mrad)*
1	25:75	0.025
2	50:50	0.025
3	75:25	0.025
4	Soak solution	0.025
5	25:75	0.050
6	50:50	0.050
7	75:25	0.050

Two-Stage Gamma Radiation Modification of PDMS

In order to get higher surface concentrations of the phospholipid on the surface the PDMS), a series of experiments were devised that consisted of first modifying the PDMS with HEMA, MAA, or NVP and then initiating a second modification with MPC. Both modifications were initiated via GRIP using the standard procedure stated above.

Eight samples were modified for each condition described below, plus six controls. The ^{60}Co source had been changed (recharged) during this time. Therefore two series of samples were run at two dose rates to determine any dependence on dose rate. The distance between the source and the samples adjusted the dose rate. The first series of samples were run at 8.3 inches (277 rads/min.) and the second series at a higher dose rate at 4 inches (1189 rads/min.). The sample holder on the rotating turret positions the test tubes at 4 " from the source center. An 8 " sample turret would not fit into the gamma chamber. Therefore adjusting the sample positions to obtain previously used dose rates eliminated the use of the rotating turret. Conditions for these experiments are listed in Table 3.4. All samples were pre-soaked for 3 hours, soak solutions decanted off and gamma polymerization solutions added. Standard protocol was used to wash and extract samples before CA, FTIR and XPS measurements.

The second stage of this experiment was to take some of the samples from the above experiment and modify them with the MPC monomer by pre-soaking and gamma initiation in 20 w/v% MPC in 50:50 $MeOH/H_2O$. Pre-soak was for 3 h. Gamma irradiation was at 8" for 1.5 h to give a dose of 0.025 Mrads (277 rads/min) without carousel rotation. After irradiation, samples were removed from the slightly gelled solutions and extracted in methanol for 1 day and then water for 2 days. Two previous

MPC-modified samples were included in this experiment. Table 3.5 lists the samples included for this experiment.

Table 3.4. Conditions for first stage modifications of PDMS by gamma initiation.

Sample(s)	*Pre-Soak Solution*	*Gamma Solution*	*Gamma Dose (Mrads)*	*Series 1 : Gamma Time (min.)*	*Series 2: Gamma Time (min)*
Control 1 & 1b	MeOH	50:50 MeOH/H_2O	0.05	240	38
Control 2 & 2b	MeOH	H_2O	0.05	240	38
Control 3 & 3b	MeOH	H_2O	0.10	480	77
SH1-8	0 v/v% HEMA MeOH	10 v/v% HEMA MeOH/H_2O	0.05	240	38
SM1-8	20 v/v% MAA MeOH	5 v/v% MAA H_2O	0.05	240	38
SP1-8	0 v/v% NVP MeOH	10 v/v% NVP H_2O	0.10	480	77

Table 3.5. Samples for the stage two MPC modifications of PDMS by gamma initiation..

Sample(s)	*Pre-Soak Solution*	*Gamma Solution*	*Gamma Dose(Mrads)*	*Series 1 : Gamma Time (min.)*	*Series 2: Gamma Time (min)*
Control 1b	MeOH	50:50 MeOH/H_2O	0.05	240	38
Control 3	MeOH	H_2O	0.10	480	77
SH2	20 v/v% HEMA MeOH	10 v/v% HEMA MeOH/H_2O	0.05	240	38
SM3 & SM5	20 v/v% MAA MeOH	5 v/v% MAA H_2O	0.05	240	38
SP2 & SP6	20 v/v% NVP MeOH	10 v/v% NVP H_2O	0.10	480	77
MPC 1 & MPC 4	20 w/v% MPC $CHCl_3$	10 v/v% MPC MeOH/H_2O	0.025	90	19

Gamma MPC Modification of PDMS

PDMS samples were modified with MPC by pre-soaking for three hours in a 20 w/v% MPC/$CHCl_3$ solution and then gamma irradiation in a 10 w/v% MPC in 50:50 water/methanol. The total dosage was 0.025 Mrads at 1189 rads/min(4", 19 min.) or 277 rads/min. (8", 90 min.). Three samples were run at each of the two conditions. Three controls were run: one at no gamma, and one at each of the two conditions. Samples were extracted with methanol for 1 day then for 2 days with water.

In order to investigate the use of DMSO as a solvent for the gama modification of PDMS with MPC, a series of samples were both pre-soaked and irradiated in the solutions outlined in Table 3.6. A second duplicate series of samples were run on PDMS discs which had been degassed by eight argon flush-vacuum cycles over 48 hours. This was to establish if trapped oxygen was leading to the variation in modifications often seen for these samples. All solutions were degassed for two minutes prior to irradiation. Irradiation was at a dose rate of 1178 rads/min. for 102 minutes, 0.12 Mrads total dosage. After irradiation, the samples were removed from the gamma solutions and placed in methanol for one day of extraction. This was followed by two days of extraction in water, with a change in the water each day.

Table 3.6. MPC modification of PDMS/DMSO.

Sample	***Pre-Soak/Gamma Solution***
C1-3, C7-9*	DMSO
C4-6, C10-12*	70:30 DMSO:MeOH
M1-3, M7-9*	0.034 M MPC in DMSO
M4-6, M10-12*	0.067 M MPC in 70:30 DMSO:MeOH

*Second series of samples.

Gamma MPC/MMA Copolymer Modification of PDMS

To determine if copolymerization with methyl methacrylate (MMA) would enhance the modification process, an experiment was devised based on the work of Widenhouse.[34] The soak and gamma solutions were the same and degassed with argon for 2 min. prior to irradiation. The samples were placed at 6.6" from the source to give a dose rate of 425 rads/min. for 235 min. and a total dose of 0.1 Mrad. Five controls were run in DMSO, five samples were run in 5 vol % MMA, and five samples were run in 0.2 M MPC and 0.5 M MMA in DMSO. These samples were extracted for one day each in water, methanol, and water.

Surface Modification by Electropolymerization

Substrates & Reagents

Substrates. Stainless steel electrodes (1 x 5 cm) were cut from 15 mil sheets by cutting on a metal shear. These electrodes were washed by fifteen minutes of sonification twice each in trichloroethane, acetone, and methanol. The electrodes were then dried *in vacu* and stored in plastic test tubes.

Preparation of Coupling Agent Coated Stainless Steel. Stainless steel electrodes with a coupling agent modified surface were prepared by a method developed by Widenhouse:[88]

Cleaning: Add each of the following solutions to the electrode container, sonicate for 15 minutes, and pour off solution prior to adding in the next solution:

1,1,1-trichloroethane
Chloroform
Acetone
Isopropanol
Ultrapure water
Ultrapure water (2^{nd} wash)

Place container in 60 °C, and let dry overnight.

B-2494 (bis(3-(triethoxysilyl)propyl)tetrasulfide) Modification: Make a 20 % (v/v) solution of B-2494 in chloroform. Add the solution to the container. Place into a 52 °C (between 50 and 55 °C) bath and allow to stand for 2 hours. Remove from bath, and remove solution by pipette. Rinse with chloroform (1-2 h), remove. Add fresh chloroform and rinse for 12-24 h.

Conversion to silanols: Remove chloroform with pipette. Rinse with 93% chloroform – 7% ethanol. Rinse with 100% ethanol. Add ethanol/water (95 v% / 5 v%) and let stand 3 hours.

SID-4612 (1,3-divinyltetramethyldisilazane) Modification: Make a 10 % (v/v) solution of SID-4612 in toluene. Remove ethanol/water solution. Rinse with 100% ethanol. Rinse with 93 % chloroform – 7 % ethanol. Rinse with chloroform. Rinse with toluene. Add the 10 % SID-4612/toluene solution to the container. Place in a water bath at 52 °C (between 52-55 °C) for 1 hour. Remove solution. Rinse with toluene. Let stand in second rinse of toluene for 12-24 hours. Dry samples at 60 °C (no vacuum).

Monomers & Reagents. MPC, methanol, water, and DMSO were as described above. The 1,3-divinyltetramethyldisiloxane (VMS), a low molecular weight oligomer was purchased from United Chemical Technologies (UTC) and used as received (specific gravity of 1.10, viscosity = 8 – 11 cs at 25 °C). The methacryloxypropyl terminated PDMS was also purchased from UCT and used as received (M_n = 33,000, viscosity = 1000 cs at 25 °C). The methacryloxy-terminated-polydimethylsiloxane (MAOP) oligomer (United Chemical Technologies) and vinylmethoxysiloxane (VMS) oligomer

(Gelest, VMM-010) were refrigerated and used as received. Tetraethylammonium bromide (TEAB) and ammonium persulfate was purchased from ACROS chemical. The TEAB was dried and stored in a glove box. The ammonium persulfate was stored in a refrigerator.

Electropolymerization Equipment & Cell Design

A simple electrochemistry cell was used as depicted in Figure 2.7. The working electrode (cathode) was the stainless steel to be coated. The cell was designed in collaboration with Drew Amery. The counter electrode was a coiled platinum electrode (Bioanalytical Systems, MW-1033) and the reference electrode was a SCE electrode (Fisher Scientific, 13-620-57). Argon was bubbled into the solution via a stainless steel syringe needle. A magnetic stir bar at a constant setting for all experiments stirred the solution. The potentiostat (Pine, AFRDE4 bi-potentiostat) was used on conjunction with a chart recorder to obtain cyclic voltamograms (CVs).

Feasibility Study

An initial feasibility study was conducted by running several hydrophilic monomers and the MAOP monomer. These experiments were run in scanning mode between 0 and –2 V versus either SCE or Ag/AgCl in order to establish the potential of the monomer or initiator reduction peak Several solvents and electrolyte systems were

Table 3.7 Preliminary experiments for the polymeric electrochemical surface modification of stainless steel.

Expt. #	*Sweeps*	*Sweep rate (mV/s)*	*Electrode*	*Filename*	*Comments*
Experiment: 2-vinylpyridine (2VP), pH 4.5, 0.4685g, NH_4ClO_4, 9:1 MeOH:H_2O					
1	1	1	New	71299A	
2	1	10	Same	71299A	
3	1	30	Same	71299B	
4	10	10	Same	71299C	
5	20	30	Same	71299D	Total = 35 sweeps
6	1	30	New	71299E	
7	100	30	Same	71299F	Total = 101 sweeps
8	1	10	New	71299G	
9	1	80	Same	71299H	
10	1	80	Same	71299I	
11	7	80	Same	71299J	Total = 10 sweeps
Experiment: 7.5 % HEMA in H_2O, 0.4780g NH_4ClO_4					
1	1	80	New		
2	1	80	Same		
3	1	80	New	71299K	
4	10	80	Same	71299L	Total = 13 sweeps
5	10	80	Same	71299M	
Experiment: 5 % MAA in H_2O, 0.4780g NH_4ClO_4					
1	1	80	New	71299N	Gas bubbles on both electrodes
2	2	80	Same	71299O	Gas bubbles on both electrodes
3	10	80	Same	71299P	Gas bubbles on both electrodes
4	1	80	New	71299Q	Gas bubbles on both electrodes
5	10	80	Same	71299R	Cleaned Pt electrode
Experiment: 10 % NVP in H_2O, 0.4713g NH_4ClO_4, NVP slightly yellow.					
1	1	10	New	71499A	
2	10	10	Same	71499D-F	
Experiment: 20 % MAOP in CH_2Cl_2, 0.4097g TEAB.					
Experiment: 2.5% MPC in 1:1 MeOH:H_2O, 0.4750g NH_4ClO_4.					
1	1	10	New	71299S	No gas evolution
2	10	10	Same	71299T-U	No gas evolution
1	1	10	New	71499G	
2	10	10	Same	71499H-I	

tried to establish the best system for each monomer. After this initial work, the study was involved silicone and MPC monomers.

Electrochemical Experimental Design & Surface Modification Experiments

The scan rate for the cyclic voltamograms (CVs) and any sweep experiments was 30 V/s. CVs were recorded between 0 and –2 volts to SCE (standard calomel electrode). The coating potentials for each experiment were chosen with respect to the reduction peak of the monomer as shown on the CV. Coating experiments were ran for between 6 and 24 hours.

After coating, the stainless steel electrodes were removed, placed into a glass test tube and dried under vacuum overnight. These samples were then extracted in a series of solvents. MAOP samples were extracted in chloroform, 1 day, methanol, 1 day, water, 2 days. MPC and VMS samples were extracted in methanol for 1 day and water for 2 days. The contact angles were then measured and samples dried and contact angle, FTIR, XPS, and SEM characterization performed.

Electrolyte and solvent systems were chosen from the preliminary studies and with consideration of relative monomer solubilities and potential biological toxicity. With this in mind, MeOH and DMSO were considered to be the best candidates for solvents and TEAB and ammonium persulfate the best electrolytes. An electrolyte concentration, which provided a saturated solution, was chosen to reduce variability and provide the maximum current flow. Monomer concentration, coating time and solvent/electrolyte system were chosen as variables for study. A screening study determined the practical systems for polymerizations with each monomer and copolymer studies. Experiments were also designed to conserve the limited supply of MPC monomer kindly supplied by

the Ishihara and Nakabayashi research groups in Tokyo. These experiments are outlined in Tables 3.8-3.13.

Experimental Designs

Methacryoloxy-Terminated-Polydimethylsiloxane (MAOP) Oligomer

Table 3.8. MAOP experimental design.

Expt.	MAOP (Vol %)	Time (h)	Solvent/Electrolyte
P1b	1	6	DMSO/TEAB
P2b	1	6	DMSO/NH_4HSO_4/ coupling agent
P3b	1	6	DMSO/TEAB coupling agent
P4b	1	24	DMSO/NH_4HSO_4
P5b	5	6	DMSO/TEAB coupling agent
P6b	5	6	DMSO/NH_4HSO_4
P7	20	24	DMSO/TEAB
P7b	5	24	DMSO/TEAB
P8b	5	24	DMSO/NH_4HSO_4 coupling agent
P7	20	24	DMSO/TEAB

Vinylmethoxysiloxane (VMS) Oligomer

Table 3.9.VMS Experimental Design.

Expt.	Monomer Vol %	Time (h)	Solvent/ Electrolyte
VMS 1	5	6	DMSO/TEAB
VMS 2	5	6	MeOH/NH_4HSO_4
VMS 3	5	24	MeOH/TEAB
VMS 4	5	24	DMSO/NH_4HSO_4
VMS 5	20	6	MeOH/TEAB
VMS 6	20	6	DMSO/NH_4HSO_4
VMS 7	20	24	DMSO/TEAB
VMS 7B	20	24	DMSO/TEAB
VMS 8	20	24	MeOH/NH_4HSO_4
VMS 9	20	24	MeOH(95%)/NH_4HSO_4
VMS 10	5	24	DMSO/TEAB

Table 3.10. Coupling agent coated electrodes & VMS, experimental design.

Expt.	Monomer Vol %	Time (h)	Solvent/Electrolyte
CV1	VMS 5	6	DMSO/TEAB
CV2	VMS 5	6	MeOH/NH_4HSO_4
CV5	VMS 20	24	MeOH/TEAB
CV7	VMS 20	24	DMSO/TEAB
CV8	VMS 20	24	DMSO/NH_4HSO_4
CV9	VMS 5	24	DMSO/TEAB
CV10	VMS 5	24	MeOH/NH_4HSO_4

Methacroylphosphorylcholine (MPC) Monomer

Table 3.11. MPC experimental design.

Expt.	MPC g/50ml	Time (h)	Solvent/Electrolyte
M1	1	6	DMSO/TEAB
M2	1	6	MeOH/NH_4HSO_4
M3	1	24	MeOH/TEAB
M4	1	24	DMSO/NH_4HSO_4
M5b	2	24	MeOH/TEAB
M5c	2	24	MeOH/TEAB
M6	2	6	DMSO/NH_4HSO_4
M7	2	24	DMSO/TEAB
M8	2	24	MeOH/NH_4HSO_4
	Non-	**Dried**	**Samples:**
M2b	1	24	MeOH/NH_4HSO_4
M2c	1	6	MeOH/NH_4HSO_4
M3b	1	24	MeOH/TEAB
M3b Sweep	1	24	MeOH/TEAB
M5b	2	24	MeOH/TEAB
M5b Sweep	2	24	MeOH/TEAB
M8b	2	24	MeOH/NH_4HSO_4
M8b Sweep	2	24	MeOH/

Copolymerization Studies

VMS – MPC Copolymer

The copolymerization study of VMS and MPC was conducted by choosing conditions that had been found to be optimum for MPC coating. Coupling agent modified substrates were used except in a couple experiments. The coupling agent seems to improve the VMS film adhesion to the stainless steel substrate. Two concentration ranges were used to determine if this effected the MPC surface concentration. Samples for the same monomer concentration and solvent/electrolyte were run in the same solutions, just switching to a new electrode and cleaning the platinum electrode. This was done out of the necessity to conserve MPC monomer.

Table 3.12. Copolymerization coating experiments with MPC and VMS.

Expt.	MPC/VMS	Time (h)	Solvent/Electrolyte/Potential
VM1	2g/2.5ml	6	MeOH/NH_4HSO_4/ CA/-1.3V
VM1b	2g/2.5ml	14	MeOH/NH_4HSO_4/ CA/-1.3V
VM2	2g/2.5ml	6	MeOH/TEAB/CA/-1.2V
VM2b	2g/2.5ml	14	MeOH/TEAB /CA/-1.2V
VM2c	2g/2.5ml	16	MeOH/TEAB/ -1.3V
VM3	2g/0.5ml	24	MeOH/NH_4HSO_4/-1.2V
VM3b	2g/0.5ml	24	MeOH/NH_4HSO_4/ CA/-1.2V
VM4	2g/0.5ml	24	MeOH/TEAB/-1.2V
VM4b	2g/0.5ml	24	MeOH/TEAB/CA/-1.2V

MAOP – MPC Copolymer

Table 3.13. Co-polymerization coating experiments with MPC and MAOP.

Expt.	*MAOP/MPC*	*Time (h)*	*Solvent/Electrolyte/Potential*
MM1	2g/2.5ml	6	MeOH/NH_4HSO_4/CA/-1.3V
MM1b	2g/2.5ml	24	MeOH/NH_4HSO_4/CA/-1.3V
MM2	2g/2.5ml	6	MeOH/TEAB /CA/-1.2V
MM2b	2g/2.5ml	24	MeOH/TEAB /CA/-1.2V
MM2c	2g/2.5ml	24	MeOH/TEAB/-1.2V
MM3	2g/0.5ml	24	MeOH/NH_4HSO_4/CA/-1.2V
MM3b	2g/0.5ml	6	MeOH/NH_4HSO_4/CA/-1.3V
MM4	2g/0.5ml	6	MeOH/TEAB /CA/-1.2V
MM4b	2g/0.5ml	24	MeOH/TEAB /CA/-1.2V

Electropolymerization Control Experiments

Two sets of controls were made in order to establish the effect of adsorption of monomers to the stainless steel and of coating of the stainless steel by the electrolyte/solvent system.

Controls were obtained by placing stainless steel electrodes into the same monomer/solvent/electrolyte systems under the same conditions for 24 hours. Solutions for these controls were chosen at the highest factor levels of the monomer concentration and time. These samples (Table 2.14) were extracted and analyzed in the same manner as the electrocoated samples.

Table 3.14. Absorption study experiments.

Expt	*Monomer/ Conc.*	*Solvent/Electrolyte*	*Electrode Type*	*Time (h)*
P3b	MAOP / 2.5 ml	DMSO/TEAB	CASS*	6
P8b	MAOP / 2.5 ml	DMSO / NH_4HSO_4	CASS*	24
M5	MPC / 2g	MeOH / TEAB	Plain	24
M8	MPC / 2g	MeOH / NH_4HSO_4	Plain	24
CV7	VMS / 20 %	DMSO/TEAB	CASS*	24
CV8	VMS / 20 %	MeOH / NH_4HSO_4	CASS*	24

*CASS = coupling agent coated stainless steel

The electrolyte/solvent controls were also selected from conditions used in the coating experiments. These experiments were run under the same conditions as the coating experiments but with the absence of monomer. Table 2.15 outlines these experiments.

Table 3.15. Electrolyte/solvent control experiments.

Expt.	*Solvent/Electrolyte*	*Time (h)*	*Potential (V)*	*Type of Electrode*
1	DMSO/TEAB	6	-0.8	CASS
2	DMSO/TEAB	6	-1.3	Plain
3	DMSO/TEAB	24	-0.65	CASS
4	DMSO / NH_4HSO_4	6	-1.6	Plain
5	DMSO / NH_4HSO_4	24	-0.8	Plain
6	MeOH / TEAB	24	-1.3	Plain
7	MeOH / NH_4HSO_4	6	-1.2	CASS
8	MeOH / NH_4HSO_4	6	-1.3	Plain
9	MeOH / NH_4HSO_4	24	-1.1	Plain
10	MeOH / NH_4HSO_4	24	-1.2	CASS

Electropolymer Characterization Techniques

Contact Angle

A simple, non-destructive technique for determining the relative hydrophilicity of solid substrates is contact angle goniometry. This study used a Rame-Hart contact angle goniometer to evaluate modified and non-modified surfaces. A captive-bubble technique was used, which involves placing air bubbles (*ca.* 0.2 µl) onto the water-submerged surface of the substrate. The bubbles are placed on the surface by using a microliter syringe. The angle between the surface and the bubble is measured and is dependent on the solid-vapor (γ_{sv}), solid-liquid (γ_{sl}) and liquid-vapor (γ_{lv}) interfacial free energies. The relationship between these values is Young's equation:

$$\text{Cos}(\theta) = (\gamma_{sv} - \gamma_{sl}) / \gamma_{lv}. \quad (2.1)$$

The samples were measured to minimum of five sets of angles (five bubbles, ten measurements). Contact angles $\leq 20°$ are considered hydrophilic, between 50-60° are intermediate and over 100° are hydrophobic. This technique is depicted in Figure 3.2.

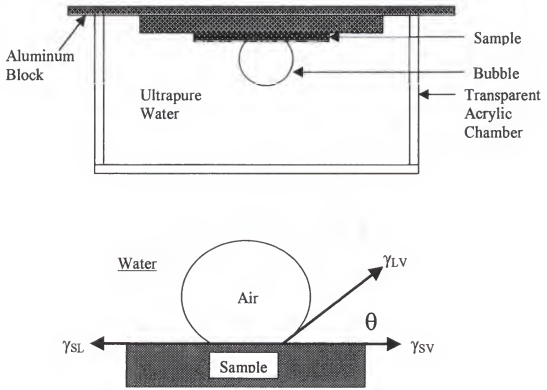

Figure 3.2. Depiction of captive bubble contact angle measurement technique showing (a) sample analysis chamber and (b) bubble at interface.

X-Ray Photoelectric Spectroscopy

X-ray photoelectric spectroscopy (XPS) provides both a quantitative and qualitative atomic chemical compositional analysis of surfaces. This technique is based on the photoelectric effect where core atomic electrons are ejected as the result of X-ray bombardment. The energy emitted by this electron is discrete and related to the binding energy of the electron and the excitation radiation, as shown in equation 2.2.

$$E_b = h\nu - E_k - \Phi \qquad (2.2)$$

E_b is the binding energy, hν is the photon energy (h = Plank's constant, ν = X-ray frequency), E_k is the kinetic energy of the electron, and Φ is the instrumental work function. The chemical bonding environment of the atom also effects the binding energy, and therefore some functional group information can be implied from this data. A Kratos model XSAM-800 spectrometer with a Mg K_α X-ray source was used to obtain surface analyses for both PDMS and coated stainless steel substrates. The X-ray gun was operated at 12 to 12.6 KeV and 9 to 10 mA. The analysis chamber was maintained at 10^{-7} to 10^{-8} torr during analysis. Spectra were quantified using Kratos DS800 software. The C 1s peak (285 eV) was used for calibration on all spectra. The depth of analysis is substrate dependent, but can be assumed to be *ca.* 50 angstroms.

Scanning Electron Microscopy

A Jeol 6400 scanning electron microscope (SEM) was used to determine the surface texture and relative quality of the coated electrode surfaces. SEM micrographs of the un-coated and coupling agent-modified stainless steel were also obtained as controls. The surfaces were analyzed at 5 eV and at magnifications of 100 to 5000x. Samples were mounted onto metal studs, spotted with carbon paint to prevent charging and coated by Paul Martin with a thin layer (50 – 100 angstroms) of gold palladium for 3 minutes using a Hummer V sputter-coating system (Technics, Alexandria, VA).

Fourier Transform Infrared Spectroscopy

Fourier-transform infrared (FTIR) spectroscopy is a well-known technique for acquisition of functional group information in polymers. This technique measures the vibrational modes of the bonds in a molecule by use of a laser beam that emits energy in

the infrared region (4000 to 400 cm^{-1}). The relative absorbence of the functional groups in the molecule relates to the type of group and the concentration of that group.

Attenuated total reflectance FTIR (ATR-FTIR) is a technique which is extremely useful for the non-destructive evaluation of polymer surfaces. In this technique, the sample is placed onto a crystal through which the laser light is propagated. This light is reflected at an angle so that the beam is reflected at the surface of the air-crystal interface.

When the sample is placed in intimate contact with the crystal surface, the beam enters into the sample to a certain depth at each reflection. The depth of penetration (d_p) of the beam into the surface is dependent on the refractive index of the sample and the wavelength of the beam. This relationship is shown in equation 3.3:

$$d_p = \lambda/(2\pi n_1(\sin^2\theta - n_2/n_1)^{1/2}) \qquad (3.3)$$

Where λ is the wavelength of the incident IR radiation, n_1 is the refractive index of the ATR crystal, n_2 is the refractive index of the sample, θ is the incident and exit angle of the IR beam. A diagram of the ATR crystal, beam reflection, and sample placement is shown as Figure 2.3.

An ATR-FTIR microscope was used to obtain IR spectra on the coated stainless steel samples, which were incompatible with the regular ATR-FTIR technique due to the high reflectivity of the stainless steel. The ATR-FTIR microscope allows information to be obtained from a specific area on the sample. The disadvantage of this technique proved to be the limit in sensitivity due to the small sample area.

The instrument used in this study was a Nicolet Magna 706 with microscope attachment. Omnic software was used to process and analyze the spectra.

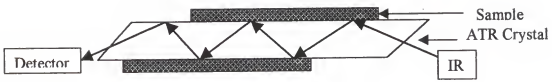

Figure 3.3. Schematic of ATR-FTIR crystal, sample and propagation path of laser light.

CHAPTER 4
RESULTS AND DISCUSSION

Gamma Radiation Surface Graft Polymerization Modification of Silicone

Results for these experiments (Table 4.1.) showed some (14 °- 18 °) variation in contact angle for PDMS controls within the same sample set. Otherwise, the modified samples did show reduced contact angles compared to the control samples (30 ° to 50 °), the most significant of which were the HEMA/MPC modification series 3A-3C with average contact angles of 31-33 °($p => 0.01$, n = 3 samples with 10 averaged measurements/sample). This was also the only modification that showed FTIR evidence of modification (Figure 4.1). The HEMA/MPC series 1A-1C and the MAA/MPC series 2A-2C and 3D-3F also showed exhibited significance ($p => 0.05$, n = 3 samples with 10 averaged measurements/sample). in average contact angle reduction with respect to their controls.

XPS analysis did not afford evidence of modification compared to control samples. This may be due to re-organization of the mobile silicone surface molecular structure.

For the second series of gamma modifications (Table 4.2), the HEMA/MPC system again produced a significant decrease ($p => 0.01$, n = 3 samples with 10 averaged measurements/sample)(reduction of 35 ° to 42 °) in contact angle versus its control. The MPC samples also showed a significant ($p => 0.05$, n = 3 samples with 10 averaged

measurements/sample) reduction in average contact angle. The contact angles for the MAA/MPC (28° to 32°) lowered in comparison to unmodified PDMS (78 °), but did not show significant reduction with respect to the control (37 °). XPS and FTIR spectra were negative for evidence of modification. Surprisingly, the MMA/MPC and MPC PDMS controls showed a great increase in wettability (37 ° and 48°, respectively) with respect to unmodified PDMS

(78 °). The combined contact angle results of these two series of experiments are depicted in Figure 4.2. This chart indicates that the surface hydrophilicity of the silicone is increased with modification in all these systems.

Table 4.1. Listing of samples and contact angle results for the first HEMA/MPC and MAA/MPC copolymer study.

Sample	*Soak Solution*	*Gamma Solution*	*Avg. Contact Angle*
1A	HEMA/MPC Water	HEMA/MPC - Water/Methanol	44 ± 6
1B			40 ± 6
1C			38 ± 6
Control 1	Water	Water/Methanol	56 ± 9
Control 1a			74 ± 8
2A	MAA/MPC Water	MAA/MPC - Water	38 ± 12
2B			39 ± 7
2C			39 ± 7
Control 2	Water	Water	66 ± 5
Control 2a			80 ± 9
3A	HEMA/MPC Methanol	HEMA/MPC – Water/Methanol	33 ± 5
3B			31 ± 6
3C			32 ± 5
3D	MAA/MPC Methanol	MAA/MPC – Water/Methanol	50 ± 5
3E			35 ± 5
3F			40 ± 8
Control 3	Methanol	Water/Methanol	68 ± 8

Table 4.2. Samples and contact angle results for the second HEMA/MPC and MAA/MPC copolymer study.

Sample	*Soak Solution*	*Gamma Solution*	*Avg. Contact Angle*
MH1	HEMA/MPC - Methanol	HEMA/MPC - Water/Methanol	28 ± 5
MH2			35 ± 4
MH3			30 ± 4
Control MH	Methanol	Water/Methanol	70 ± 7
MM1	MAA/MPC - Methanol	MAA/MPC - Water	28 ± 4
MM2			29 ± 6
MM3			32 ± 4
Control MM	Methanol	Water	37 ± 7
MPC1	MPC - Methanol	MPC – Methanol	29 ± 3
MPC2			31 ± 5
MPC3			36 ± 4
Control MPC	Methanol	Methanol	48 ± 3

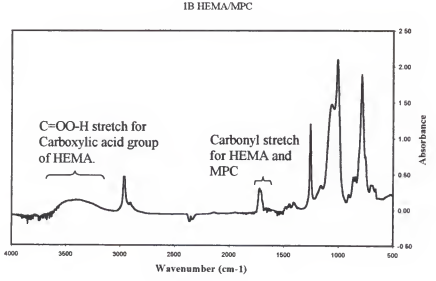

Figure 4.1. FTIR spectrum of sample 1B: HEMA/MPC gamma radiation modified PDMS.

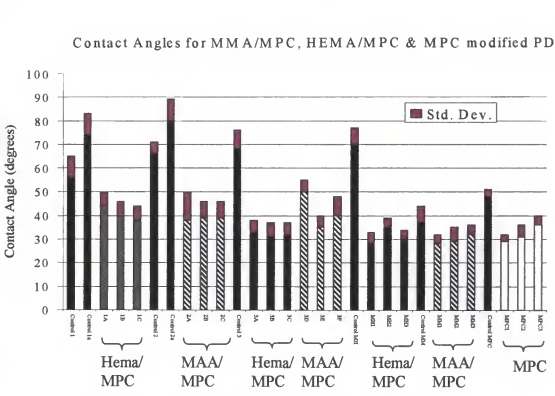

Figure 4.2. Combined contact angle results for silicone modifications.

Gamma MPC Modification of PDMS

Contact angle results for the gamma radiation surface graft modification of PDMS with MPC for the conditions presented in Table 4.3, Table 4.4 and Figure 4.3. These results show some variability within the sample sets and no strong evidence of reduced contact angle compared to the controls. The exception was the 025-4 (P= >0.01, wrt control 3, n = 3 samples with 10 averaged measurements/sample) (27° to 29 °) and the 05-7 series (p=> 0.01, n = 3 samples with 10 averaged measurements/sample) (37° to 55 °) and the 025-3 series (p=> 0.05, n = 3 samples with 10 averaged measurements/sample) (30° to 48 °).The 025-4 series did not have a control, but gave the lowest contact angles and lowest standard deviations. This was the sample set where the

pre-soak solution was used for the gamma radiation polymerization solution. No evidence of modification was however found for the XPS and FTIR data for these samples.

Table 4.3. Conditions and contact angle results for MPC surface modification of PDMS by gamma radiation surface graft polymerization.

Sample	*Condition*	*Gamma Solution MeOH: H_2O*	*Contact Angle (degrees)*
Control 1	1	25:75	69 ± 14
025-1a			47 ± 8
025-1b			36 ± 4
025-1c			86 ± 3
Control 2	2	50:50	37 ± 6
025-2a			28 ± 7
025-2b			60 ± 11
025-2c			66 ± 5
Control 3	3	75:25	55 ± 7
025-3a			41 ± 6
025-3b			30 ± 3
025-3c			48 ± 6
025-4a	4	Pre-soak solution	29 ± 3
025-4b			24 ± 4
025-4c			27 ± 7
Control 5	5	25:75	49 ± 6
05-5a			33 ± 5
05-5b			52 ± 4
05-5c			61 ± 8
Control 6	6	50:50	46 ± 4
05-6a			40 ± 9
05-6b			44 ± 7
05-6c			40 ± 5
Control 7	7	75:25	74 ± 3
05-7a			47 ± 5
05-7b			37 ± 5
05-7c			55 ± 5

For the MPC gamma radiation surface graft modification of PDMS in DMSO solvent, no significant reduction in contact angle was seen compared to the controls. No difference was noted between degassed PDMS and non-degassed PDMS samples XPS analysis again did not yield data for surface MPC.

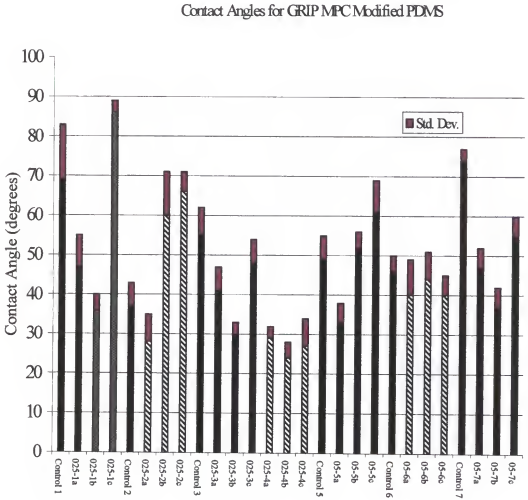

Figure 4.3. Contact angle results for MPC gamma radiation modification of PDMS with MeOH/water solvent.

Table 4.4 MPC modification of PDMS in DMSO.

Sample	*Soak/Gamma Solution*	*Contact Angle (degrees)**
C1	DMSO / degassed PDMS	73 ± 3
C2		66 ±11, 74 ± 11
C3		65 ± 5, 62 ± 3
C4	70:30 DMSO:MeOH /	66 ± 4, 62 ± 5
C5	degassed PDMS	91 ± 5, 86 ± 6
C6		81 ± 2, 63 ± 3
C7	DMSO	59 ± 4, 63 ± 9
C8		60 ± 5, 75 ± 4
C9		57 ± 4, 48 ± 3
C10	70:30 DMSO:MeOH	71 ± 10, 62 ± 6
C11		57 ± 13, 62 ± 9
C12		65 ± 3, 61 ± 5
M1	0.034 M MPC in DMSO/	80 ± 5, 74 ± 4
M2	degassed PDMS	63 ± 3, 68 ± 5
M3		59 ± 10, 60 ± 8
M4	0.067 M MPC in 70:30	62 ± 4, 70 ± 7
M5	DMSO:MeOH /	62 ± 6, 61 ± 4
M6	degassed PDMS	73 ± 9
M7	0.034 M MPC in DMSO	75 ± 3, 56 ± 8
M8		74 ± 8, 48 ± 7
M9		71 ± 4
M10	0.067 M MPC in 70:30	72 ± 8, 59 ± 6
M11	DMSO:MeOH	58 ± 5
M12		67 ± 3, 84 ± 5

*Two measurements represent two sides of sample, 5 drops (10 measurements) each side.

Two-Stage Gamma Graft Modification of PDMS

For the first stage modification of the two-stage experiment, the two systems that showed a significant reduction in contact angle over the control sample were: The MAA modification ($P=<0.001$, with SM6 removed by Q-test, n = 7 samples with 10 averaged measurements/sample) (31° to 39° reduction) and the HEMA modification ($P=<0.05$, with SH5 and SH7 removed by Q-test, n = 7 samples with 10 averaged measurements/sample) (3° to 18° reduction). These results are listed in Table 4.5.

FTIR spectra were taken for the samples that were used in the second stage modification.

These results are summarized in Table 4.6.

Table 4.5. Samples and contact angle results for first stage modifications of PDMS by gamma radiation surface graft polymerization.

Sample(s)	*Soak Solution*	*Gamma Solution*	*Gamma Dose (Mrads)*	*Contact Angle (degrees)*
Control 1	MeOH	50:50 MeOH/H_2O	0.05	31 ± 5
Control 1b				27 ± 6
SH1	20 v/v% HEMA/ MeOH	10 v/v% HEMA-MeOH/H_2O	0.05	23 ± 4
SH2				20 ± 5
SH3				19 ± 5
SH4				22 ± 4
SH5				32 ± 7
SH6				24 ± 5
SH7				46 ± 16
SH8				24 ± 3
Control 2	MeOH	H_2O	0.05	57 ± 12
Control 2b				61 ± 9
SM1	20 v/v% MAA/ MeOH	5 v/v% MAA / H_2O	0.05	25 ± 6
SM2				18 ± 4
SM3				20 ± 3
SM4				24 ± 3
SM5				26 ± 6
SM6				34 ± 8
SM7				24 ± 5
SM8				31 ± 10
Control 3	MeOH	H_2O	0.10	27 ± 4
Control 3b				49 ± 12
SP1	20 v/v% NVP /MeOH	10 v/v% NVP /H_2O	0.10	30 ± 7
SP2				44 ± 6
SP3				48 ± 10
SP4				35 ± 9
SP5				38 ± 8
SP6				30 ± 6
SP7				28 ± 5
SP8				36 ± 5
Control 4b	$CHCl_3$	MeOH/ H_2O	0.025	63 ± 5
Control 4c				70 ± 5
MPC1	20 w/v % MPC in $CHCl_3$	10 w/v % MPC in MeOH/ H_2O	0.025	71 ± 7
MPC2				73 ± 4
MPC3				72 ± 7
MPC4				60 ± 6
MPC5				71 ± 4
MPC6				72 ± 4

Table 4.6. Samples and contact angle results for the stage two MPC modifications of PDMS by gamma radiation surface graft polymerization.

	Stage 1:				*Stage 2:*
Sample(s)	***Soak Solution***	***Gamma Solution***	***Gamma Dose (Mrads)***	***FTIR Results***	***Contact Angle (degrees)***
Control 1b	MeOH	50:50 MeOH/H_2O	0.05	No evidence of mod.	38 ± 7
Control 3	MeOH	H_2O	0.10	No evidence of mod.	35 ± 8
SH2	20 v/v% HEMA MeOH	10 v/v% HEMA MeOH/H_2O	0.05	Strong hydroxyl & carbonyl	20 ± 2
SM3	20 v/v% MAA	5 v/v% MAA	0.05	Weak carbonyl	24 ± 8
SM5	MeOH	H_2O		No evidence of mod.	22 ± 7
SP2	20 v/v% NVP	10 v/v% NVP	0.10	Strong carbonyl & 1425 cm^{-1}	24 ± 5 (44 ± 6)*
SP6	MeOH	H_2O		Weak carbonyl	33 ± 3 (33 ± 6)*
MPC 1	20 w/v% MPC	10 w/v% MPC	0.025	No evidence of mod.	42 ± 12 (71 ± 7)*
MPC 4	$CHCl_3$	MeOH/H_2O		No evidence of mod.	46 ± 10 (60 ± 6)*

*Stage 1 contact angle results.

The HEMA, MAA and NVP modified samples showed evidence of modification by FTIR, but no significant change over the controls was seen in the XPS.

For the second stage modification in this experiment, the systems which showed reduction in average contact angle over the stage one measurements were SP2 (24 °) and SP6 (33 °) (NVP modified); MPC1 (42 °) and MPC4 (46 °). No statistical comparisons could be made since the sample size was one. FTIR and XPS spectra of these systems showed no change from the stage one samples.

MPC/MMA Copolymer Modification of PDMS

The gamma radiation surface graft copolymer modification of PDMS with MMA and MMA/MPC did show significant reductions in the average contact angles (34 ° and 32°, respectively) of the modified samples compared to the controls ($P=<0.05$ and $P=<0.01$, respectively, n = 5 samples with 10 averaged measurements/sample). As seen in Table 4.7, the average reduction in contact angle was the same for the MAA and the MAA/MPC (average of 34 °) systems. There was no evidence of modification in the XPS spectra of these samples.

Table 4.7. Samples and contact angle results for MPC/MMA copolymer modification of PDMS.

Sample(s)	*Gamma Solution*	*Contact Angle (degrees)*
Control 1	DMSO	87 ± 11
Control 2		102 ± 15
Control 3		63 ± 7
Control 4		67 ± 15
Average	Contact Angle:	70 ± 28
MMA1	0.5 M MMA in DMSO	32 ± 12
MMA2		30 ± 7
MMA3		40 ± 15
MMA4		29 ± 11
MMA5		43 ± 10
Average	Contact Angle:	34 ± 12
MPC/MMA1	0.5 M MMA & 0.2 M MPC in DMSO	21 ± 6
MPC/MMA1		37 ± 10
MPC/MMA1		29 ± 9
MPC/MMA1		39 ± 9
MPC/MMA1		33 ± 9
Average	Contact Angle:	32 ± 10

Discussion of Gamma Polymerization of Hydrogel Monomers on PDMS

These experiments for gamma radiation modification of PDMS have shown that the gamma radiation graft surface polymerization process is inherently highly variable for PDMS. This may be due to inhomogeneities in the PDMS polymer discs introduced in the mixing and curing stages of the samples preparation or floating and sample alignment in the test tube during irradiation. However, this study did demonstrate that:

1. PDMS was surface modified with HEMA by gamma radiation surface graft polymerization with some variability in contact angle.
2. PDMS was surface modified by MAA and MPC, but characterization of these samples by XPS and FTIR was problematic. This may be due to the strong IR absorbance of PDMS, the low XPS sensitivity for nitrogen and phosphorous, and the tendency of silicone surfaces to reorganize in different environments (*ie.* water for contact angle measurements versus high vacuum for XPS analysis).
3. PDMS was made more hydrophilic by gamma irradiation alone in methanolic solvents.

An interesting aspect of gamma initiated polymerization is that it provides a continuous source of initiation as compared to chemical initiation, *i.e.* AIBN radical polymerization. Gamma initiation will therefore uniquely affect the molecular weight and molecular weight distribution of the resultant polymer. Grumski[89] reported gamma initiated molecular weights much higher than the maximum for his PEO standards (850,000) upon GPC analysis of bulk gamma polymerized MPC. Ishihara's AIBN initiated MPC-BMA copolymers gave M_w = 1.29 to 2.85 x 10^4, PDI = 1.40 to 1.68.[19] But Ishihara does not report molecular weight data for AIBN initiated polyMPC.

One explanation for high molecular weights for polyMPC could be the alignment of the MPC monomers in solution due to molecular association. This type of behavior has been reported in other polymerizable phospholipid systems due to their amphiphilic and amphiprotic structure. These monomers are reported to form vesicles in solution and align on solid substrates to enhance their polymerization kinetics in both solution and in the solid state. [90-93] If the MPC monomers are aligning in solution prior to initiation, the kinetics of polymerization will be accelerated due to the reduction of diffusion control. The rate of termination reactions should also be reduced by this phenomenon. Also, the pendent phosphoryl choline groups on the poly(MPC) chain can associate and influence the alignment of approaching monomers to the growing chain ends.

Recent work in the Goldberg research group has shown that pH of aqueous systems affects the rate of gamma polymerization and surface grafting. It is suggested that future studies include the determination of pH effects on these polymerizations.

Electropolymerization of MPC and Silicone Oligomers on Stainless Steel

Electropolymerization of Methacryloxy-Terminated-Polydimethylsiloxane (MAOP) Oligomer

Contact angle and XPS results. Table 4.8 shows the contact angle and XPS results for the MAOP modification of stainless steel. These results indicate that MAOP electropolymerizes onto the metal surface. A wide range of contact angles (20° to 112 °) was observed apparently related to the combination of specific solvent and reduction potential. For the DMSO/TEAB systems, the contact angle seemed to decrease with increased potential. This can be seen when comparing samples P1b (112 °) with the rest

of the DMSO/TEAB samples (20 ° to 66 °). This may be due to hydrolysis of the silicone by reaction with the solvent at higher potentials. Otherwise, no clear dependence on time, monomer concentration or electrode type was indicated.

The DMSO/NH_4HSO_4 system showed a tendency toward lower contact angles with an increase in reaction time. Monomer concentration and potential did not seem to have an effect, though no low potential samples were run.

SEM Results. The SEM results (Figures 4.4 - 4.12), indicate that the DMSO/NH_4HSO_4 samples, in gerneral, gave thicker and more uniform coatings than the DMSO/TEAB samples. Scratches seen in these micrographs are inflicted upon SEM sample mounting and are shown to give a perspective as to the coating thickness. This is especially evident in P4b (Figure 4.7) were a very thick coating is seen compared to P5b (Figure 4.8), P7 and P7b (Figures 4.10, 4.11) where thin or speckled (non-uniform) coatings were seen. This speckled appearance could also be associated with corrosive pitting as seen in P5b (Figure 4.8).

P1b (Figure 4.4) shows a very uniform surface with some surface roughness. Smooth, uniform coatings are seen in P2b, P3b, P4b (Figures 4.5 to 4.7), P6b (Figure 4.9), and P8b (Figure 4.12). The 5000x micrographs for samples P3b and P4b give further support to quality of this coating. In Figure 4.7, an indention caused by forceps is shown to demonstrate the thickness of this coating.

Table 4.8. MAOP Experimental Design/Results.

Expt.	MAOP Vol %	Time (h)	Solvent/Electrolyt/ Electrode (potential)	Contact Angle (°)*	XPS Atomic % Si	Observation
P1b	1	6	DMSO/TEAB (-0.65 V)	112 ± 6	29	Clear, thin film.
P2b	1	6	DMSO/NH_4HSO_4/ CASS (-1.6 V)	73 ± 14 89 ± 17	24	Thin, clear coating on both sides.
P3b	1	6	DMSO/TEAB/CASS (-1.3 V)	53 ± 10 42 ± 3	24	Thin, clear coating on both sides
P4b	1	24	DMSO/NH_4HSO_4 (-1.5 V)	44 ± 13 44 ± 11	27	Clear, thin film.
P5b	5	6	DMSO/TEAB/CASS (-1.0 V)	21 ± 4 20 ± 2	5	Thin, clear coating with brown tinge.
P6b	5	6	DMSO/NH_4HSO_4 (-1.65 V)	70 ± 11 84 ± 10	27	Clear, thin film.
P7	20	24	DMSO/TEAB (-0.7 V)	66 ± 13	29	Clear, thin film.
P7b	5	24	DMSO/TEAB (-0.6 V)	36 ± 7	19	Clear, thin film.
P8b	5	24	DMSO/NH_4HSO_4/ CASS (-1.0 V)	35 ± 2 29 ± 6	23	Thin, clear coating on both sides

*Two measurements represent two sides of sample.

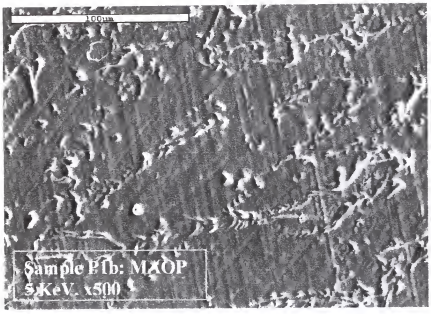

Figure 4.4. SEM micrographs of sample P1b at magnification of 500x. MAOP coated stainless steel (1 vol % MAOP, DMSO/TEAB, plain electrode, -0.65 V, 6 h).

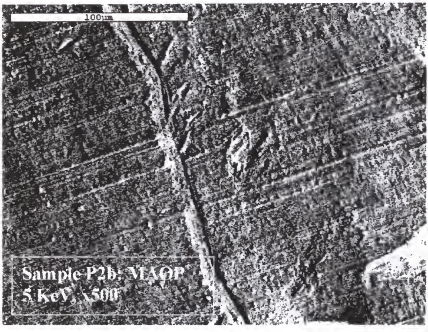

Figure 4.5. SEM micrographs of sample P2b at magnification of 500x. MAOP coated stainless steel (1 vol % MAOP, DMSO/NH_4HSO_4, CASS electrode, -1.6 V, 6 h).

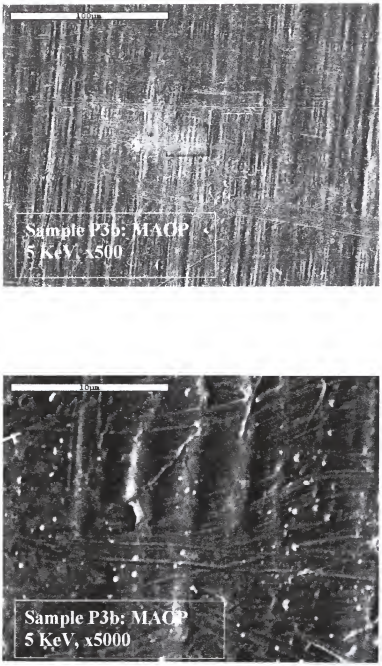

Figure 4.6. SEM micrographs of sample P3b at magnifications of 500x and 5000x. MAOP coated stainless steel (1 vol % MAOP, DMSO/TEAB, CASS electrode, -1.3 V, 6 h).

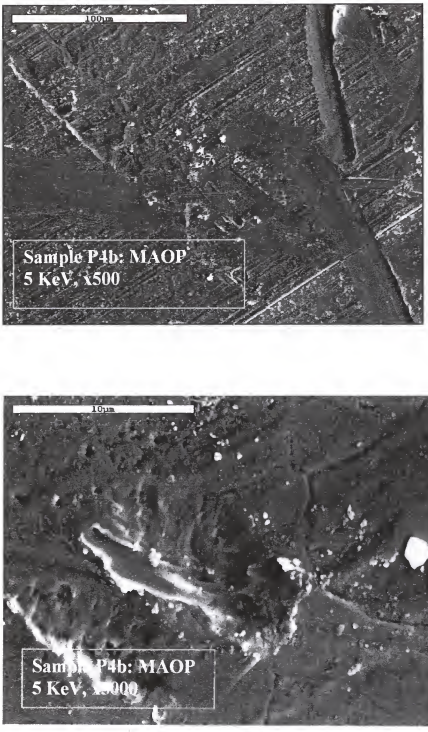

Figure 4.7. SEM micrographs of sample P4b at magnifications of 500x and 5000x. MAOP coated stainless steel (1 vol % MAOP, DMSO/NH_4HSO_4, plain electrode, -1.5 V, 24 h).

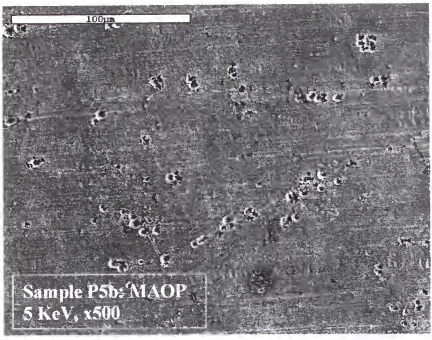

Figure 4.8. SEM micrographs of sample P5b at magnification of 500x. MAOP coated stainless steel (5 vol % MAOP, DMSO/TEAB, CASS electrode, -1.0 V, 6 h).

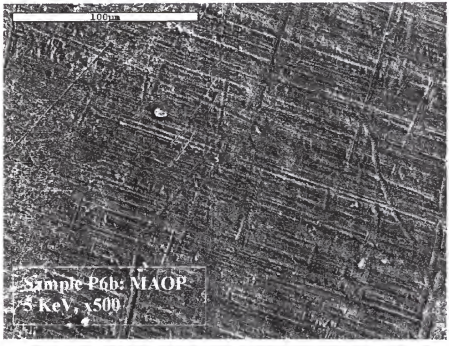

Figure 4.9. SEM micrographs of sample P6b at magnification of 500x. MAOP coated stainless steel (5 vol % MAOP, DMSO/NH_4HSO_4, plain electrode, -1.65 V, 6 h).

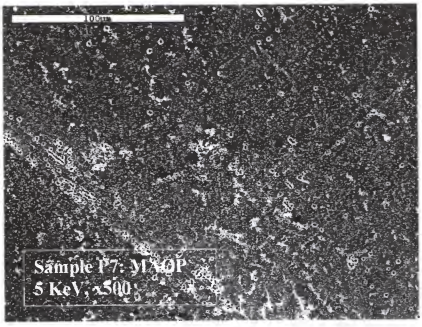

Figure 4.10. SEM micrographs of sample P7 at magnification of 500x. MAOP coated stainless steel (20 vol % MAOP, DMSO/TEAB, plain electrode, -0.7 V, 24 h).

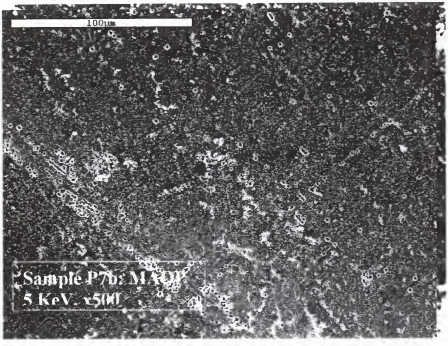

Figure 4.11. SEM micrographs of sample P7b at magnification of 500x. MAOP coated stainless steel (5 vol % MAOP, DMSO/TEAB, plain electrode, -0.6 V, 24 h).

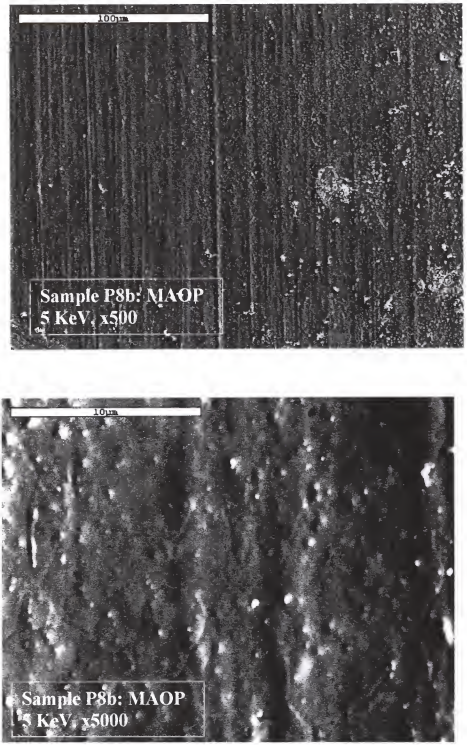

Figure 4.12. SEM micrographs of sample P8b at magnifications of 500x and 5000x. MAOP coated stainless steel (5 vol % MAOP, DMSO/NH_4HSO_4, CASS electrode, -1.0 V, 24 h).

Electropolymerization of Vinylmethoxysiloxane (VMS) Oligomer

Contact angle and XPS results. The results of this study, as shown in Table 4.9 and 4.10, indicate that the main problem with the electropolymerization of VMS was lack of good adhesion of the films to the substrate.

The MeOH/TEAB (VMS 3, VMS 5) and MeOH/NH_4HSO_4 (VMS 2, VMS 8) systems provided the best results with respect to film coating observations and contact angles. The VMS 9 sample was run in 95 % MeOH/H_2O to see if an increase in the solvent polarity would improve coating with respect to sample VMS 8 (run in 100% MeOH). However this change in solvent polarity did not show improve the uniformity of the coating. Sample VMS 3 exhibited a lack of throwing power by only showing coating on one side of the electrode

For DMSO/ NH_4HSO_4, (VMS 4, VMS 6) gave a patchy coating at 5 vol % monomer and bulk polymerized with an increase in monomer concentration.

The DMSO/TEAB system (VMS 1, VMS 7, VMS 7b and VMS 10) showed thick coatings that had a tendency to peel when the solvent was changed from MeOH to water or chloroform. The reduction in potential between samples VMS 7 and VMS 7b showed a decrease in film thickness. Comparison of VMS 1 and VMS 10 shows that an increase in time translates into film which are thick, patchy and flake more easily. This may be due to uneven film growth.

XPS results show that several of the samples show low atomic % Si. This may be due to the loss of film due to extraction. This reiterates the problem of adhesion in this system.

SEM results. The SEM micrographs for the electropolymerized VMS samples are shown in Figures 4.13 to 4.22. The morphology shown in these figures supports the

observations made above. Some interesting additions are that the film portion of VMS 4 (Figure 4.16, x500) appears to be very uniform, though rough textured. This system may show some promise with better adhesion.

By far the most interesting morphology was seen in Figure 4.19 for VMS 7b (20 vol % monomer in DMSO/TEAB for 24h at –0.55 V). These micrographs show a spherical growth morphology. This is very different than the growth morphology shown in the other samples including the ones for the same solvent/electrolyte system (VMS1 and VMS 7). The main difference between this sample and the others is that it was run at a potential of ~ 50 % of that of VMS 1 and VMS 7. This unique morphology maybe the results of a relatively slow initiation rate. The initial amperage was significantly lower for VMS 7b than for VMS 7 (0.0022 mA versus 1.1 mA, respectively).

Rough surface textures for many of these coatings, some of which have thick, flaky layers over an underlying smooth layer. This may be best seen for VMS 2 (Figure 4.14), VMS 9 and VMS 10 (Figures 4.21 and 4.22). This could indicate a different growth mechanism after the first layer is deposited onto the electrode surface, at which time the current density drops and the rate of initiation becomes much slower. VMS 3 (Figure 4.15), VMS 5, VMS 7 and VMS 8 (Figures 4.17 - 4.19) all show smooth uniform coatings, though the VMS 7 sample has a lot of debris (artifact?) visible.

Table 4.9. VMS Experimental Design/Results:

Expt.	*Monomer Vol %*	*Time (h)*	*Solvent/ Electrolyte (potential)*	*Contact Angle (°)*	*Observation*
VMS 1	5	6	DMSO/TEAB (-1.0 V)	Not measurable	Thick, uniform film. Not adhesive.
VMS 2	5	6	MeOH/NH_4HSO_4 (-1.6 V)	25 ± 10	Thick, but flaky.
VMS 3	5	24	MeOH/TEAB (-1.0 V)	28 ± 7	Light opaque white film on one side. Uniform, yet patchy.
VMS 4	5	24	DMSO/NH_4HSO_4 (-1.4 V)	Film 30 ± 8 Metal 24 ±	Both sides coated with patchy, opaque, white film.
VMS 5	20	6	MeOH/TEAB (-1.0 V)	37 ± 13	Light clear film
VMS 6	20	6	DMSO/NH_4HSO_4 (-1.4 V)	--	Bulk Polymerization
VMS 7	20	24	DMSO/TEAB (-1.2 V)	Not measurable	Very thick white coating on both sides which came off when sample was put into chloroform.
VMS 7b	20	24	DMSO/TEAB (-0.55 V)	29 ± 4	Thick, patchy, SEM shows spherical microstructure.
VMS 8	20	24	MeOH/NH_4HSO_4 (-1.25 V)	24 ± 4	Great film, thin white, yet visible. Stable to MeOH, but came off in water.
VMS 9	20	24	MeOH (95%)/ NH_4HSO_4 (-1.6 V)	19 ± 3	Thick, patchy, flaky
VMS 10	5	24	DMSO/TEAB (-1.2 V)	Not measurable	Thick, patchy, flaky

Table 4.10. XPS results for VMS on stainless steel.

	Atomic Percent				
Expt.	*Si 2p*	*C 1s*	*O 1S*	*Cr 2p3*	*Fe 2p3*
VMS 1	26	32	32	0	0
VMS 2	7	47	41	5	0
VMS 3	20	47	33	0	0
VMS 4	17	50	33	0	0
VMS 5	21	48	32	0	0
VMS 7	18	47	35	0	0
VMS 7b	23	47	30	0	0
VMS 8	6	58	36	0	0
VMS 9	14	46	37	3	0

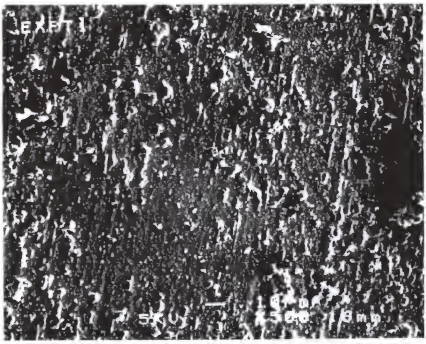

Figure 4.13. SEM micrographs of sample VMS 1 at magnification of 500x. VMS coated stainless steel (5 vol % VMS, DMSO/TEAB, plain electrode, -1.0 V, 6 h).

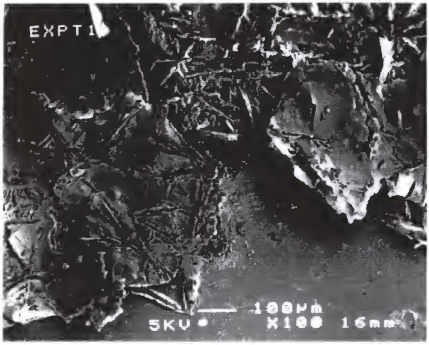

Figure 4.14. SEM micrographs of sample VMS 2 at magnification of 100x. VMS coated stainless steel (5 vol % VMS, DMSO/NH_4HSO_4, plain electrode, -1.0 V, 6 h).

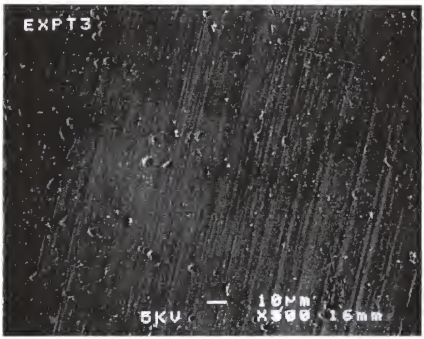

Figure 4.15. SEM micrographs of sample VMS 3 at magnification of 500x. VMS coated stainless steel (5 vol % VMS, MeOH/TEAB, plain electrode, -1.6 V, 24 h).

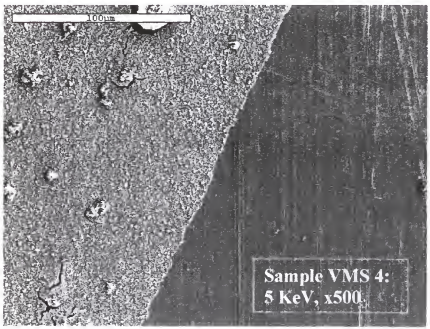

Figure 4.16. SEM micrographs of sample VMS 4 at magnifications of 500x and 5000x. VMS coated stainless steel (5 vol % VMS, MeOH/NH_4HSO_4, plain electrode, -1.4 V, 24 h).

Figure 4.17. SEM micrographs of sample VMS 5 at magnification of 500x. VMS coated stainless steel (20 vol % VMS, MeOH/TEAB, plain electrode, -1.0 V, 6 h).

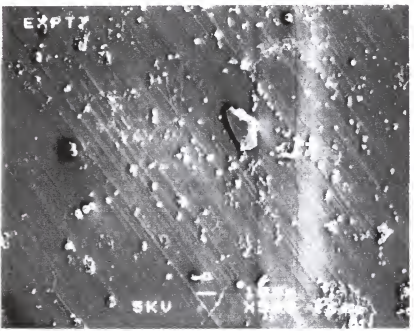

Figure 4.18 SEM micrographs of sample VMS 7 at magnification of 500x. VMS coated stainless steel (20 vol % VMS, DMSO/NH_4HSO_4, plain electrode, -1.4 V, 24 h).

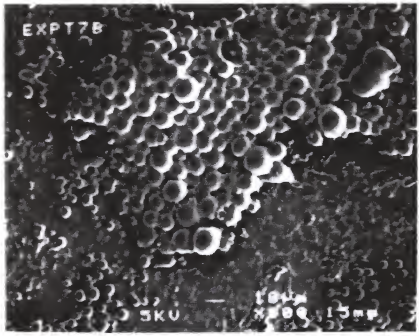

Figure 4.19. SEM micrographs of sample VMS 7b at magnification of 500x. VMS coated stainless steel (20 vol % VMS, DMSO/TEAB, plain electrode, -0.55 V, 24 h).

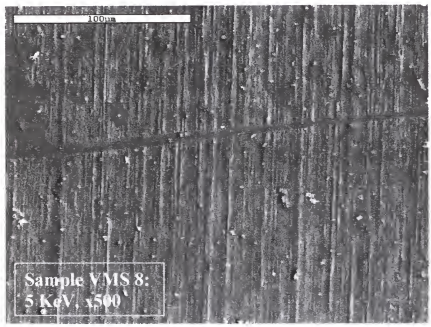

Figure 4.20. SEM micrographs of sample VMS 8 at a magnification of 500x. VMS coated stainless steel (20 vol % VMS, MeOH/NH_4HSO_4, plain electrode, -1.5 V, 24 h).

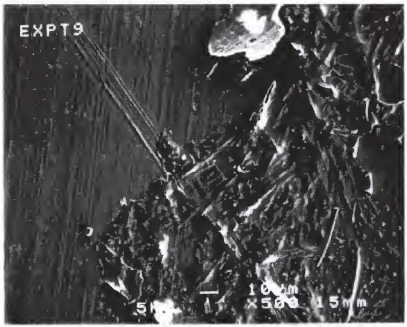

Figure 4.21. SEM micrographs of sample VMS 9 at magnification of 500x. VMS coated stainless steel (20 vol % VMS, MeOH (95 %)/NH_4HSO_4, plain electrode, -1.6 V, 24 h).

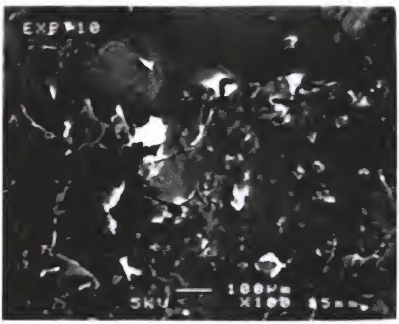

Figure 4.22. SEM micrographs of sample VMS 10 at magnification of 100x. VMS coated stainless steel (5 vol % VMS, MeOH/TEAB, plain electrode, -1.2 V, 24 h).

Electropolymerization of VMS on Electrodes Coated with Coupling Agent

Contact angle and XPS results. Table 4.11 shows the results of the VMS electropolymerization experiments using the coupling agent modified stainless steel (CASS) electrodes. These results show a general improvement in film adhesion. The contact angles for these films were low (17° to 46°) and show the hydrophilicity of this oligomer is generally greater than that of the MAOP oligomer (contact angles of 21° to 112°).

The DMSO/NH_4HSO_4 system resulted previously in bulk polymerization of VMS and therefore this system was not considered viable for an industrially applicable coating system. Though bulk polymerization does prove that this monomer is polymerizing under these conditions.

The DMSO/TEAB system provided coatings at both monomer concentrations. CV1 (5 vol % VMS) and CV7 (20 vol % VMS) did not indicate an increase in film thickness with an increase in monomer concentration. CV7 (-0.65 V) andCV9 (-0.65 V) indicated a better film formation occurred with a decrease in potential compared to CV1 (-1.0 V). Though these samples had about the same atomic % Si (22 and 23 %, respectively) by XPS, their SEMs showed very different morphologies. CV9 (Figure 4.28) resembles the start of the same spherical-type growth pattern exhibited by VMS 7b (Figure 4.19). CV9 and VMS 7b were run under the same conditions of solvent/ electrolyte, time and oligomer concentration, but the potential for CV9 was 0.1V more negative and this translated into an initial amperage ten times higher (0.023 mA). The spherical "bubbly" morphology could also be related to increased hydrophilicity of the growing polymer chain with respect to the DMSO solvent or the presence of vesicles or

droplets of monomer in the solvent that adsorb and then initiate on the metal surface. The presence of the coupling agent could also have influenced the growth pattern. These samples give an insight into the subtle complexity of electropolymerization, especially as it applies to a coating process.

The $MeOH/NH_4HSO_4$ solvent/electrolyte indicated an increase in coating thickness is related to an increase in oligomer concentration and time. CV2 (5 vol % VMS and 6 h) had a much lighter coating than CV8 (20 vol % VMS and 24 h) and CV10 (5 vol % and 24h), CV10 showing oxidation.

MeOH/TEAB was only used for one condition, CV5, which provided a thick, patchy coating.

SEM results. Figure 4.23 (CV 1) shows a smooth, yet thin surface coating. The rest of the coatings provided varied surface morphologies. CV2 (Figure 4.24) shows what may have been a smooth coating that became wrinkled upon drying. CV 5 (Figure 4.25) also depicts a smooth, thick coating that is exhibiting cracking which may also be due to drying. Samples CV 7 and CV 8 (Figures 4.26 and 4.27) show thick flaky coatings over thin uniform coatings. Figure 4.28 shows that the conditions for CV 9 produced a rough surface that under high magnification (5000x) shows an interesting droplet-type structure.

Table 4.11. Coupling agent coated electrodes & VMS, experimental design and results:

Expt.	Monomer Vol %	Time (h)	Solvent/ Electrolyte (potentials)	Contact Angle (°)**	XPS Atomic % Si	Observation
CV1	5	6	DMSO/TEAB (-1.0 V)	*	28	Thick, patchy film.
CV2	5	6	MeOH/NH_4HSO_4 (-1.2 V)	17 ± 3 21 ± 5	27	Uniform coverage, non-uniform thickness. "speckled"
CV5	20	24	MeOH/TEAB (-1.0 V)	34 ± 16 46 ± 9	29	Clear, patchy coating.
CV7	20	24	DMSO/TEAB (-0.65 V)	27 ± 3 28 ± 6	23	Coating white and fairly heavy. Uniform with few small patches.
CV8	20	24	MeOH/NH_4HSO_4 (-1.25 V)	25 ± 10 32 ± 16	23	Fairly uniform white coating, some clumps.
CV9	5	24	DMSO/TEAB (-0.65 V)	20 ± 2 23 ± 4	22	Excellent film. White, uniform on both sides. No clumps or patches.
CV10	5	24	MeOH/NH_4HSO_4 (-1.2 V)	Not measured	Not measured	Thick film, clumpy and brown (oxidized).

*Film too thick to measure. **Two measurements represent two sides of sample.

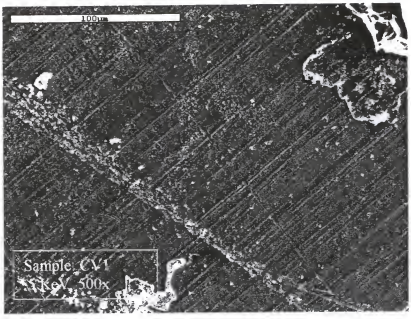

Figure 4.23. SEM micrographs of sample CV1, VMS on CASS electrode, at magnification of 500x (5 vol % VMS, DMSO/TEAB, -1.0 V, 6 h).

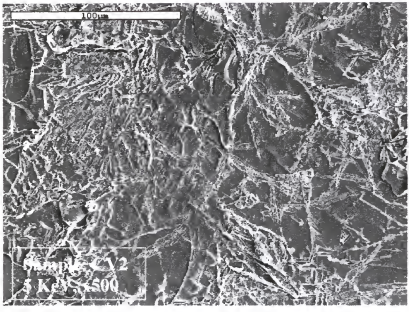

Figure 4.24. SEM micrographs of sample CV2, VMS on CASS electrode, at magnification of 500x (5 vol % VMS, MeOH/NH_4HSO_4, -1.2 V, 6 h).

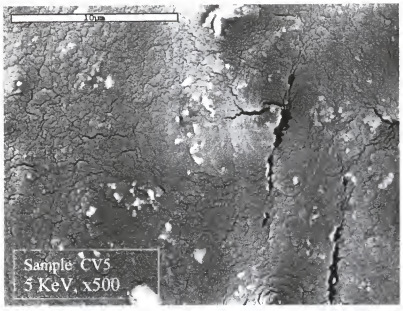

Figure 4.25. SEM micrographs of sample CV5, VMS on CASS electrode, at magnification of 500 (20 vol % VMS, MeOH/TEAB, -1.0 V, 24 h).

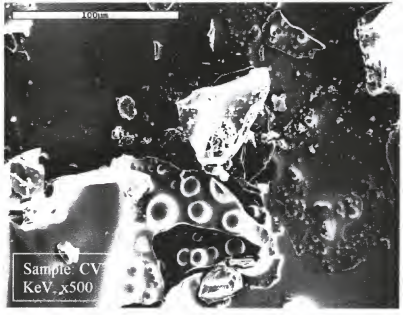

Figure 4.26. SEM micrographs of sample CV7, VMS on CASS electrode, at magnification of 500x (20 vol % VMS, DMSO/TEAB, -0.65 V, 24 h).

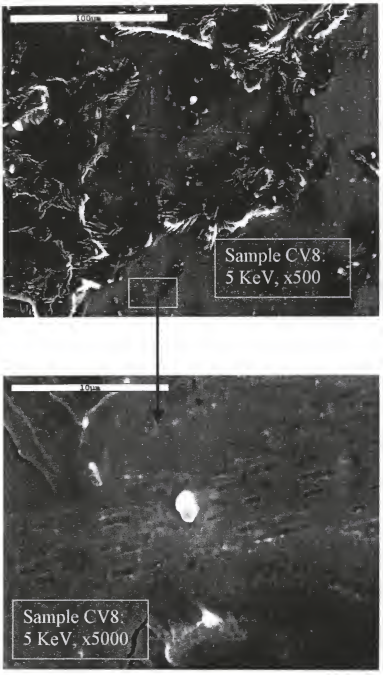

Figure 4.27. SEM micrographs of sample CV8, VMS on CASS electrode, at magnifications of 500x and 5000x (20 vol % VMS, MeOH/NH_4HSO_4, -1.25 V, 24 h).

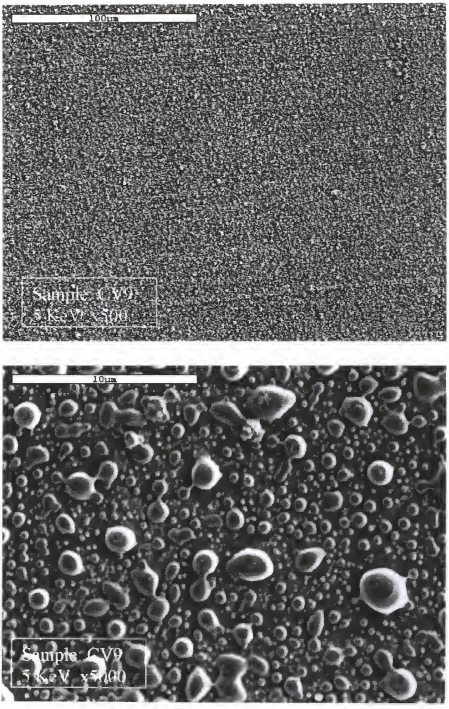

Figure 4.28. SEM micrographs of sample CV9, VMS on CASS electrode, at magnifications of 500x and 5000x (5 vol % VMS, DMSO/TEAB, -0.65 V, 24 h).

Electropolymerization of Methacroylphosphorylcholine (MPC) Monomer

Contact angle and XPS results. The results of the MPC modification of stainless steel were very promising. As seen in Table 4.12, most of the samples exhibited relatively high atomic percentage of phosphorus. A pure control MPC film run on the same instrument gave an atomic % P = 4.56 (theoretical is 5.55 %) at a binding energy of 131.85 eV. In general, the contact angles for these samples are all very low (15 ° to 26 °), even when no phosphorus is detected by XPS. It may be that these films are too thin to have a bulk concentration within the sensitivity of the XPS for phosphorous.

The DMSO/TEAB system (M1 and M7) showed no phosphorous by XPS, but did exhibit extremely low contact angles (24 °). It is interesting that the contact angle was the same for both of these samples, though the M7 system was run at twice the MPC concentration (2g / 50 ml) and time (24 h). Samples M4 and M6 exhibited bulk polymerization, which has been shown to be a problem with the DMSO/NH_4HSO_4 system.

The samples run in MeOH/TEAB showed good atomic % P at all conditions except M5b (0 atomic % P). All these samples showed very low contact angles (16 ° to 32 °). These films were translucent but uniform. This is supported by the low standard deviations in the contact angle measurements. No significant improvement in results with increased MPC concentration was seen as demonstrated by M3b (1g / 50 ml, 24 h, 2.2 atomic % P) compared to M5 and M5c (2 g / 50 ml, 24 h, 2.7 and 1.2 atomic % P, respectively). The samples of M5b and M5c show that there is large variability in atomic % P (0 and 2.1 %, respectively) between duplicate samples.

M2 and M2c (6h) versus M2b (24 h) showed a dependence on time of polymerization between 6 and 24 hours in $MeOH/NH_4HSO_4$. The increase in atomic % P between M2 (1 g / 50 ml, 6 h, 1.8 % P) and M8 (2 g / 50 ml, 24 h, 3.5 % P) could be due to increased time or monomer concentration, but M2b (1 g / 50 ml, 24 h, 1.3 % P) versus M2c (1 g / 50 ml, 6 h, 0 % P) in comparison to M8b (2 g / 50 ml, 24 h, 1.3 % P) seems to indicate a time dependence instead of a monomer concentration dependence on the atomic % P in the resulting polymer film.

The difference between the samples that were dried prior to extraction and those that were not dried is non-conclusive. Some systems showed a decrease in atomic % P and some systems showed an increase.

Sweep experiments were conducted by sweeping the applied voltage from 0 to –2 V at 30 mV/sec and back. This study showed improvement in atomic % P for M5b versus M5b sweep (0 % vs. 2.1 %), but no difference for M3b versus M3b sweep (2.2 % and 2.7 %) and the M8b versus M8b sweep (1.3 % each) samples.

SEM results. Figures 4.29 to 4.43 show the SEM micrographs for the MPC coating experiments. The most striking result is shown in Figure 4.29 for M1 (DMSO/TEAB, where corrosion pits are evident on this sample. Sample M7 (Figure 4.40) does not show signs of corrosion for the same solvent/electrolyte system. M1 was run at a higher potential (-1.4 V) than M7 (-1.0 V), though both had an initial current of 0.015 mA. M7 had twice the monomer concentration than M1, which could have provided a protective mechanism for the substrate. Though none of the electrolyte/solvent controls showed signs of corrosion for this solvent system.

There does seem to be a difference in morphology between some of the dried samples and there non-dried analogues. Samples M2, M3, M4, M5 and M6 all show a linear striation in their surface morphology (Figures 4.30, 4.32, 4.35, 4.36 and 4.39) This striated morphology is not evident for samples M2b, M3b or M5b (Figures 4.31, 4.33 and 4.37).

Table. 4.12. MPC Experimental Design/Results:

Expt.	*MPC g/50ml*	*Time (h)*	*Solvent/ Electrolyte (potential)*	*Contact Angle (°)*	*XPS: Atomic % P*	*Observation*
M1	1	6	DMSO/TEAB (-1.4 V)	24 ± 4	0	No visible film.
M2	1	6	MeOH/NH_4HSO_4 (-1.3 V)	15 ± 2	1.8	Uniform film on both sides.
M3	1	24	MeOH/TEAB (-1.4 V)	17 ± 3	1.4	No visible film.
M4	1	24	DMSO/NH_4HSO_4 (-1.4 V)	15 ± 2	1.6	Bulk Polymerization
M5	2	24	MeOH/TEAB (-1.2 V)	16 ± 4	2.7	No visible film.
M5c	2	24	MeOH/TEAB (-1.2 V)	19 ± 3	1.2	No visible film.
M6	2	6	DMSO/NH_4HSO_4 (-1.8 V)	17 ± 3	1.2	Bulk Polymerization
M7	2	24	DMSO/TEAB (-1.0 V)	24 ± 7	0	Light, patchy, clear film
M8	2	24	MeOH/NH_4HSO_4 (-1.1 V)	15 ± 3	3.5	No visible film.
Non-		**Dried**	**Samples:**			
M2b	1	24	MeOH/NH_4HSO_4 (-1.3 V)	16 ± 2 15 ± 2	1.3	Visible white film, uniform coating
M2c	1	6	MeOH/NH_4HSO_4 (-1.3 V)	16 ± 2 15 ± 2	0	No visible film.
M3b	1	24	MeOH/TEAB (-1.3 V)	19 ± 6 19 ± 5	2.2	No visible film.
M3b Sweep	1	24	MeOH/TEAB (0 to –1.7 V)	22 ± 5 17 ± 4	2.7	No visible film.
M5b	2	24	MeOH/TEAB (-1.2 V)	20 ± 5 17 ± 5	0	No visible film.
M5b Sweep	2	24	MeOH/TEAB (0 to –1.6 V)	32 ± 3 26 ± 4	2.1	No visible film.
M8b	2	24	MeOH/NH_4HSO_4 (-1.3 V)	20 ± 2 18 ± 1	1.3	No visible film.
M8b Sweep	2	24	MeOH/NH_4HSO_4 (0 to -1.3 V)	20 ± 2 17 ± 3	1.3	No visible film.

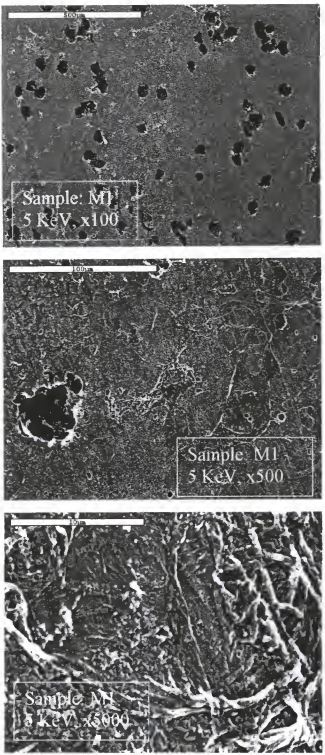

Figure 4.29. SEM micrographs of sample M1, MPC on SS electrode at magnifications of 100x, 500x and 5000x (1g MPC / 50 ml., DMSO/TEAB, -1.4 V, 6h).

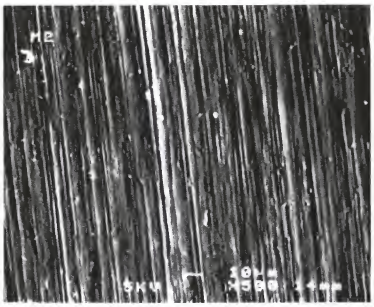

Figure 4.30. SEM micrographs of sample M2, MPC on SS electrode at magnification of 500x (1g MPC / 50 ml., $MeOH/NH_4HSO_4$, -1.3 V, 6h).

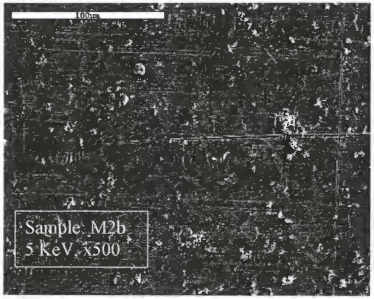

Figure 4.31. SEM micrographs of sample M2b, MPC on SS electrode at magnification of 500x (1g MPC / 50 ml., $MeOH/NH_4HSO_4$, -1.3 V, 24h).

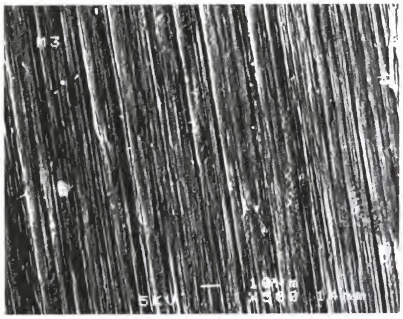

Figure 4.32. SEM micrographs of sample M3, MPC on SS electrode at magnification of 500x (1g MPC / 50 ml., MeOH/TEAB, -1.4 V, 24h).

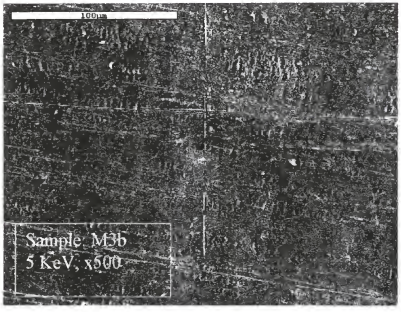

Figure 4.33. SEM micrographs of sample M3b, MPC on SS electrode at magnification of 500x (1g MPC / 50 ml., MeOH/TEAB, -1.3 V, 24h).

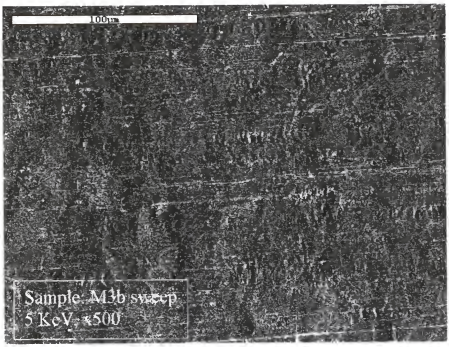

Figure 4.34. SEM micrographs of sample M3b sweep, MPC on SS electrode at magnification of 500x (1g MPC / 50 ml., MeOH/TEAB, 0 to -1.7 V, 24h).

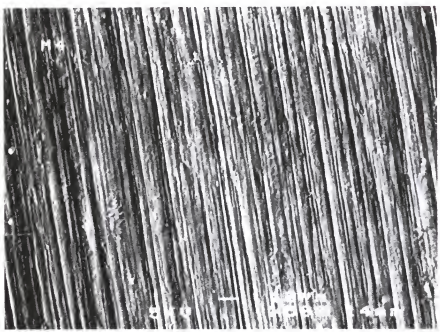

Figure 4.35. SEM micrographs of sample M4, MPC on SS electrode at magnification of 500x (1g MPC / 50 ml., DMSO/NH_4HSO_4, -1.4 V, 24h).

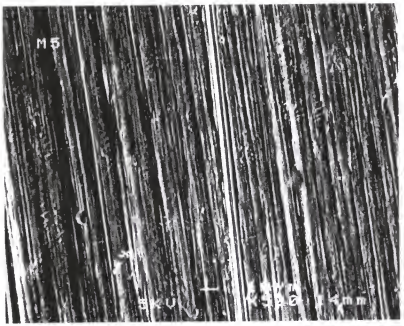

Figure 4.36. SEM micrographs of sample M5, MPC on SS electrode at magnification of 500x (2g MPC / 50 ml., MeOH/TEAB, -1.2 V, 24h).

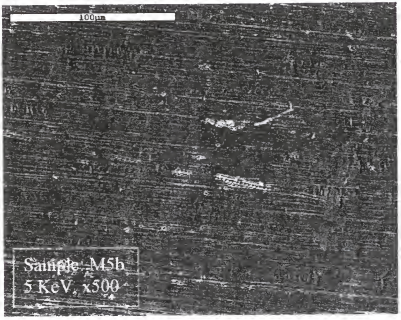

Figure 4.37. SEM micrographs of sample M5b, MPC on SS electrode at magnification of 500x (2g MPC / 50 ml., MeOH/TEAB, -1.2 V, 24h).

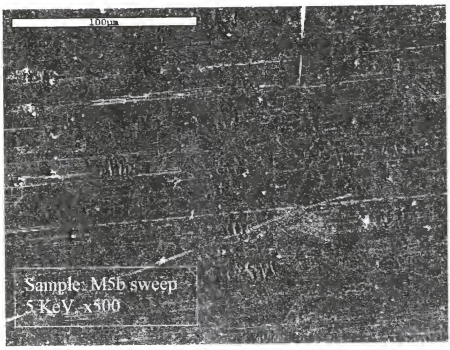

Figure 4.38. SEM micrographs of sample M5b sweep, MPC on SS electrode at magnification of 500x (2g MPC / 50 ml., MeOH/TEAB, 0 to -1.6 V, 24h).

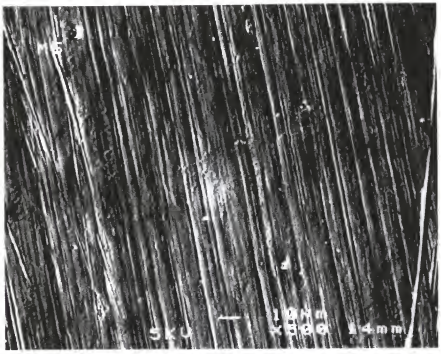

Figure 4.39. SEM micrographs of sample M6, MPC on SS electrode at magnification of 500x (2g MPC / 50 ml., DMSO/NH_4HSO_4, -1.8 V, 6h).

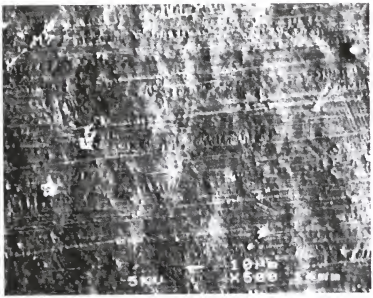

Figure 4.40. SEM micrographs of sample M7, MPC on SS electrode at magnification of 500x (2g MPC / 50 ml., DMSO/TEAB, -1.0 V, 24h).

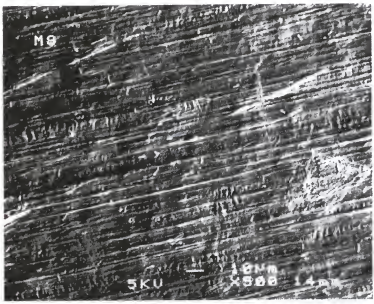

Figure 4.41. SEM micrographs of sample M8, MPC on SS electrode at magnification of 500x (2g MPC / 50 ml., MeOH/NH_4HSO_4, -1.1 V, 24h).

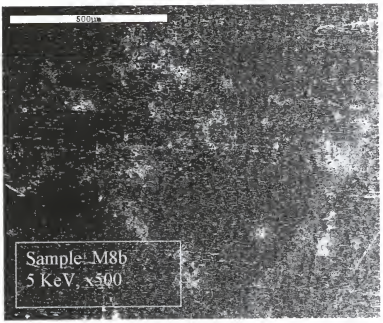

Figure 4.42. SEM micrographs of sample M8b, MPC on SS electrode at magnification of 500x (2g MPC / 50 ml., MeOH/NH_4HSO_4, -1.1 V, 24h).

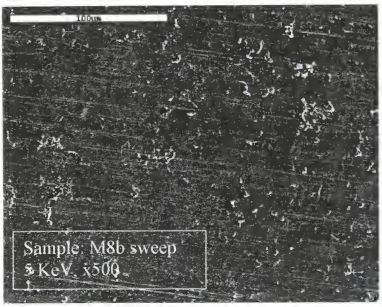

Figure 4.43. SEM micrographs of sample M8b sweep, MPC on SS electrode at magnification of 500x (2g MPC / 50 ml., MeOH/NH_4HSO_4, 0 to -1.3 V, 24h).

Electrochemical Copolymerization of Silicone Oligomers with MPC

Conditions for the copolymer experiments were chosen to optimize for the MPC monomer. This was to increase the MPC concentration in the coating. MPC concentration was held constant while the silicone oligomer concentration was varied between two levels.

VMS – MPC copolymer

Contact angle and XPS results. These films showed the expected results with respect to contact angle, ranging between 15 ° and 33 ° (Table 4.13), with the contact angles falling in the range of the VMS and MPC coated samples. Two sets of samples (VM1, VM1b & VM2, VM2b) exhibited oxidation with an increased reaction time (6 to 14 h. This was surprising in that neither VMS nor MPC showed a tendency towards oxidation in previous experiments.

There was not clear difference between using a plain versus a coupling agent coated (CASS) electrode, with respect to contact angle or atomic % P. VM2 and VM2b (CASS) versus VM2c (plain) showed a decrease in atomic % P (0.5, 0, and 1.4 % P, respectively). VM3 (plain) and VM3b (CASS) demonstrated the opposite behavior (0.4 and 1.3 % P, respectively).

The MeOH/NH_4HSO_4 system showed an expected decrease in film atomic % Si content with a decrease in solution VMS oligomer concentration (4 to 15 % Si at 2.5 ml VMS and 2 to 6 % Si at 0.5 ml VMS). Though the MPC content of the films did not increase significantly with decrease in VMS concentration. This may indicate a much higher reactivity rate for the VMS over MPC. This correlates with the results seen in the

oligomer/monomer studies, where VMS produced much thicker coatings for all conditions in comparison to MPC.

SEM results: Figures 4.44 to 4.51 shows the SEM micrographs from the VMS/MPC copolymer study. The micrographs of VM1 (6 h) and VM1b (14 h) (Figures 4.44 and 4.45) show an interesting growth pattern that would be expected to further converge growth regions and form coherent films with increased reaction time. The presence of oxidation in VM1b with increased time may indicate that a step-down in voltage with time may be needed to optimize film growth. This would significantly increase coating time. This same growth pattern is seen in Figures 4.45 and 4.46 for VM2 and VM2b. Here, an increase in film coverage with reaction time (6 to 14 h) is obvious. VM2c (Figure 4.47) shows a different morphology on its surface that may be influence by the plain electrode (VM2 and VM2b used CASS electrodes). This sample showed a significant increase in atomic % P (1.4 %). The VM3 series (Figure 4.48 to 4.49) and the VM4 sereis (Figure 4.50 to 4.51) show a similar surface morphology to VM2c. This seems to correlate with a decrease in the atomic % Si content of the film, indicating that the film growth seen in VM1, VM2 & VM2b is dominated by the VMS polymerization.

Table 4.13: Results of VMS – MPC copolymer experiments.

Expt.	*MPC/VMS*	*Time (h)*	*Solvent/Electrolyte/ electrode type (potential)*	*XPS: At % C/O/Si/P*	*Contact Angle (°)**	*Observation*
VM1	2g/2.5ml	6	MeOH/NH_4HSO_4/ CASS (-1.3V)	55/34/8/**1**	18 ± 4 16 ± 2	Thin, opaque white coating on both sides.
VM1b	2g/2.5ml	14	MeOH/NH_4HSO_4/ CASS (-1.3V)	51/34/15/**0**	19 ± 3 19 ± 4	Clumpy and golden brown.
VM2	2g/2.5ml	6	MeOH/TEAB/ CASS (-1.2V)	51/39/8/**0.5**	18 ± 2 19 ± 3	Light coating on both sides
VM2b	2g/2.5ml	14	MeOH/TEAB/ CASS (-1.2V)	53/32/15/**0**	18 ± 2 33 ± 7	Light white film with dark edges on both sides.
VM2c	2g/2.5ml	16	MeOH/TEAB/ Plain (-1.3V)	48/41/4/**1.4**	15 ± 2 19 ± 3	Thin, opaque white coating on both sides.
VM3	2g/0.5ml	24	MeOH/NH_4HSO_4/ Plain (-1.2V)	50/42/4/**0.4**	22 ± 3 22 ± 2	Good uniform coating on both sides.
VM3b	2g/0.5ml	24	MeOH/NH_4HSO_4/ CASS (-1.2V)	46/43/3/**1.3**	21 ± 2 27 ± 5	Good uniform coating on both sides.
VM4	2g/0.5ml	24	MeOH/TEAB/ Plain (-1.2V)	32/47/6/**1.5**	28 ± 4 22 ± 5	No visible film.
VM4b	2g/0.5ml	24	MeOH/TEAB/ CASS (-1.2V)	59/32/2/**1**	23 ± 4 23 ± 3	No visible film.

*Two measurements represent two sides of sample.

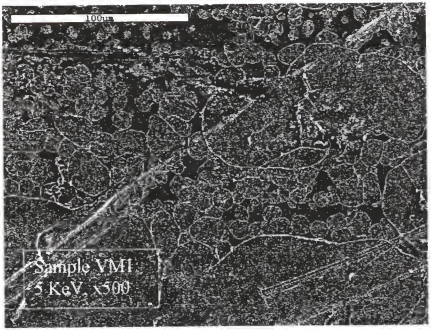

Figure 4.44. SEM micrographs of sample VM1, VMS-co-MPC on CASS electrode at magnification of 500x (2g / 2.5 ml MPC/VMS, MeOH/NH_4HSO_4, -1.3 V, 6h).

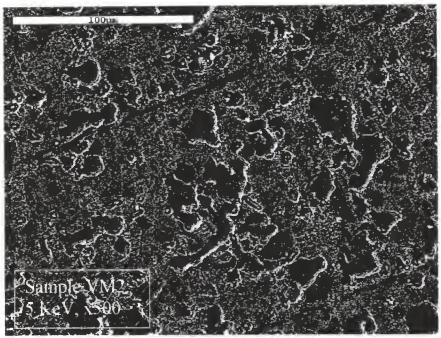

Figure 4.45. SEM micrographs of sample VM2, VMS-co-MPC on CASS electrode at magnification of 500 (2g / 2.5 ml MPC/VMS, MeOH/TEAB, -1.2 V, 6h).

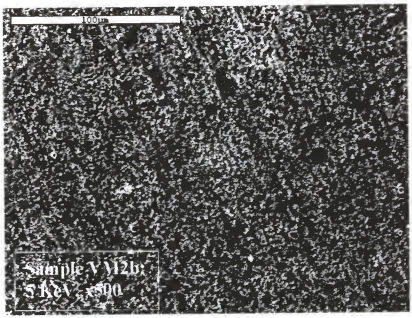

Figure 4.46. SEM micrographs of sample VM2b, VMS-co-MPC on CASS electrode at magnification of 500x (2g / 2.5 ml MPC/VMS, MeOH/TEAB, -1.2 V, 14h).

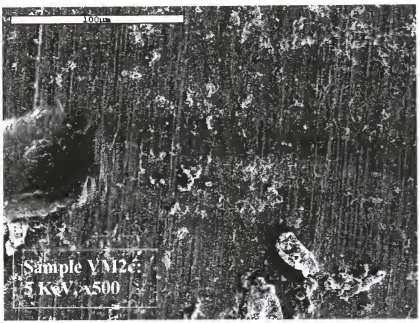

Figure 4.47. SEM micrographs of sample VM2c, VMS-co-MPC on a plain electrode at magnification of 500x (2g / 2.5 ml MPC/VMS, MeOH/TEAB, -1.3 V, 16h).

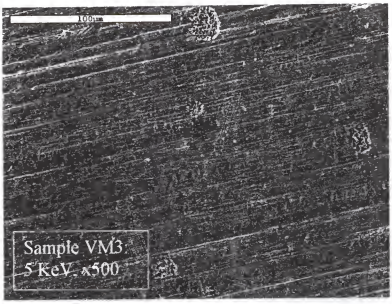

Figure 4.48. SEM micrographs of sample VM3, VMS-co-MPC on SS electrode at magnification of 500 (2g / 0.5 ml MPC/VMS, MeOH/NH_4HSO_4, -1.3 V, 24h).

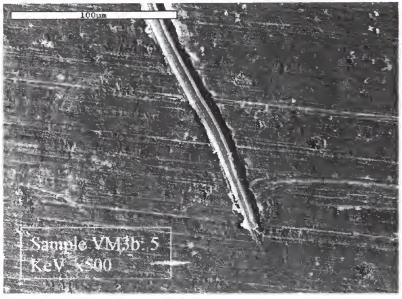

Figure 4.49. SEM micrographs of sample VM3b, VMS-co-MPC on CASS electrode at magnification of 500x (2g / 0.5 ml MPC/VMS, MeOH/NH_4HSO_4, -1.2 V, 24h).

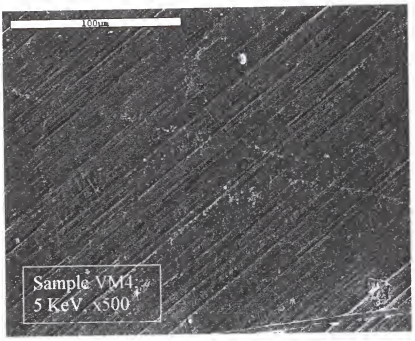

Figure 4.50. SEM micrographs of sample VM4, VMS-co-MPC on SS electrode at magnification of 500x (2g / 0.5 ml MPC/VMS, MeOH/TEAB, -1.2 V, 24h).

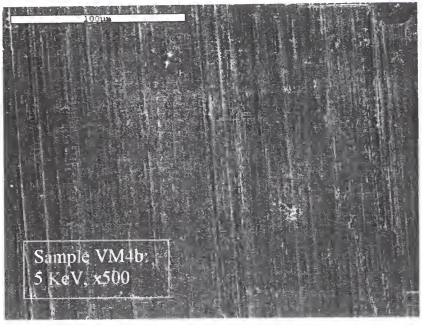

Figure 4.51. SEM micrographs of sample VM4b, VMS-co-MPC on CASS electrode at magnification of 500x (2g / 0.5 ml MPC/VMS, MeOH/TEAB, -1.2 V, 24h).

MAOP – MPC Copolymer

Contact angle and XPS results. Results for these experiments showed small concentrations of polyMPC in the copolymer (0-2 atomic % P by XPS), have a large influence on contact angle (16 ° to 35 ° for copolymer versus 20 ° to 112 ° for MAOP). The overall average contact angle for these samples (23 ± 5) is not significantly greater than that for the polyMPC films (18 ± 5). These films were all clear, translucent and not visible to the naked eye.

SEM results. Comparison of the SEMs for MM1 (6 h) and MM1b (24 h) (Figures 4.52 & 4.53) shows that an increase in time for this system increases the uniformity of the film. The MM1 coating is thick with what seems to be chunks of polymer coming off the surface. The MM1b sample also has a thick coating, but does not exhibit the same loss of polymer from the surface. The same trend is seen for MM2 (6 h) and MM2b (24 h) (Figures 4.54 & 4.55). This difference in coating thickness is especially apparent in the 5000x micrographs. MM2c (Figure 4.56) shows signs of corrosive pitting. Once again in a TEAB system with MPC (refer to sample M1). The fact that MM2a and MM2b both used a CASS electrode could indicate a protective mechanism associated with the coupling agent.

MM3 (24 h) and MM3b (6 h) do not exhibit any notable increase in film thickness with increase in reaction time (Figures 4.57 & 4.58). The SEMs of MM4 and MM4b (Figures 4.59 & 4.60) are very interesting and seem to indicate two phase deposition. This pattern is similar to some of the micrographs seen in the Electrolyte/Solvent Control section. The XPS data for these samples does show an increase in the chromium content

of the surface (6 and 5 atomic %, respectively). This may indicate a competitive surface oxidation reaction occurring in these samples.

Table 4.14. Copolymerization coating experiments with MPC and MAOP.

Expt.	*MAOP/MPC*	*Time (h)*	*Solvent/ Electrolyte/ Electrode type (Potential)*	*XPS: Atomic % C/O Si/P*	*Contact Angle (°)**
MM1	2g/2.5ml	6	MeOH/NH_4HSO_4/ CASS (-1.3V)	62/28 **7/1**	23 ± 4 21 ± 3
MM1b	2g/2.5ml	24	MeOH/NH_4HSO_4/ CASS (-1.3V)	44/43 **4/1**	24 ± 2 22 ± 3
MM2	2g/2.5ml	6	MeOH/TEAB/ CASS (-1.2V)	44/46 **5/1**	25 ± 5 24 ± 2
MM2b	2g/2.5ml	24	MeOH/TEAB/ CASS (-1.2V)	50/34 **11/1**	32 ± 3 35 ± 6
MM2c	2g/2.5ml	24	MeOH/TEAB/ Plain (-1.2V)	44/44 **5/2**	20 ± 5 20 ± 3
MM3	2g/0.5ml	24	MeOH/NH_4HSO_4/ CASS (-1.2V)	57/32 **4/1**	23 ± 2 21 ± 1
MM3b	2g/0.5ml	6	MeOH/NH_4HSO_4/ CASS (-1.3V)	56/35 **4/0**	22 ± 1 20 ± 2
MM4	2g/0.5ml	6	MeOH/TEAB/ CASS (-1.2V)	46/41 **7/0**	23 ± 5 29 ± 10
MM4b	2g/0.5ml	24	MeOH/TEAB/ CASS (-1.2V)	46/37 **9/2**	16 ± 1 22 ± 3

*Two measurements indicate two sides of sample.

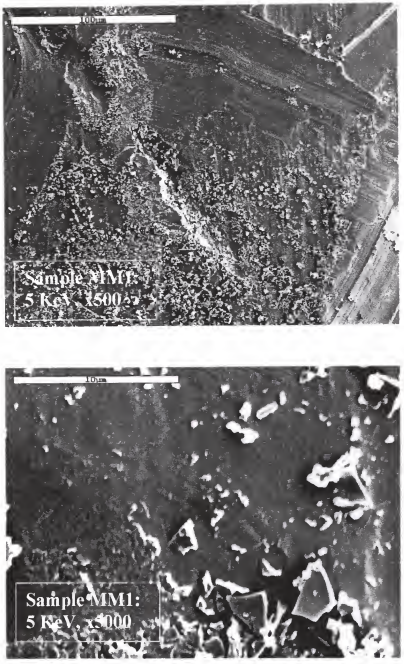

Figure 4.52. SEM micrographs of sample MM1, MAOP-co-MPC on CASS electrode at magnifications of 500x and 5000x (2g / 2.5 ml MAOP/VMS, MeOH/NH_4HSO_4, -1.3 V, 6h).

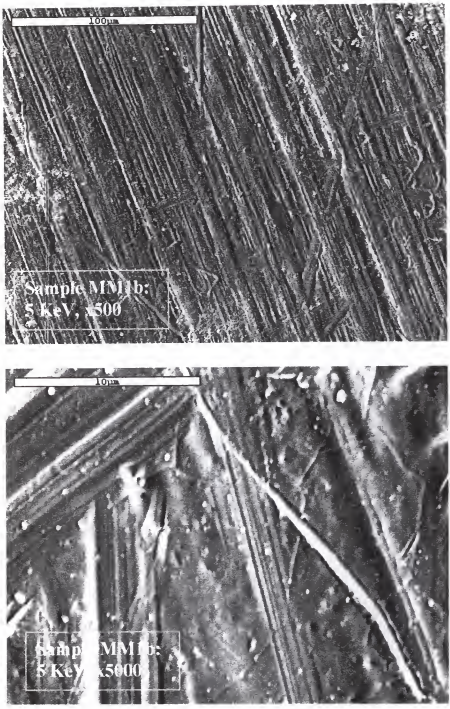

Figure 4.53. SEM micrographs of sample MM1b, MAOP-co-MPC on CASS electrode at magnifications of 500x and 5000x (2g / 2.5 ml MAOP/VMS, MeOH/NH_4HSO_4, -1.3 V, 24h).

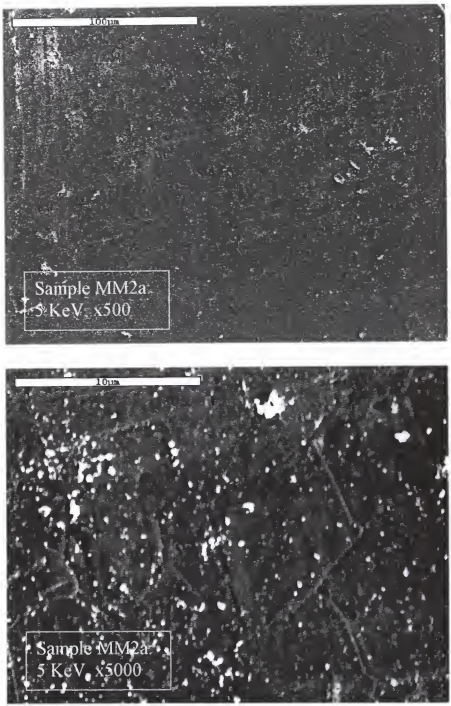

Figure 4.54. SEM micrographs of sample MM2a, MAOP-co-MPC on CASS electrode at magnifications of 500x and 5000x (2g / 2.5 ml MAOP/VMS, MeOH/TEAB, -1.2 V, 6h).

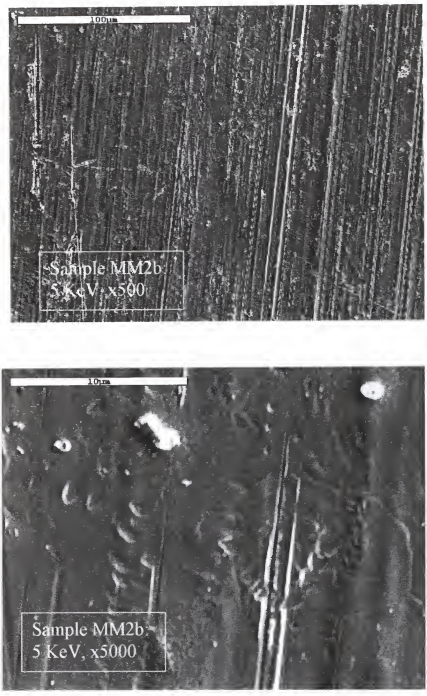

Figure 4.55. SEM micrographs of sample MM2b, MAOP-co-MPC on CASS electrode at magnifications of 500x and 5000x (2g / 2.5 ml MAOP/VMS, MeOH/TEAB, -1.2 V, 24h).

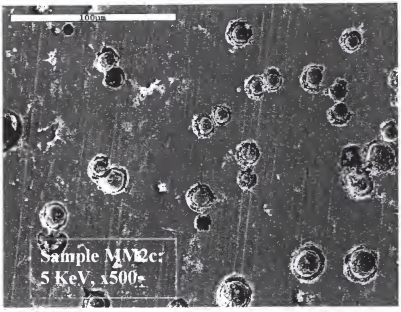

Figure 4.56. SEM micrographs of sample MM2c, MAOP-co-MPC on plain electrode at magnification of 500x (2g / 2.5 ml MAOP/VMS, MeOH/TEAB, -1.2 V, 24h).

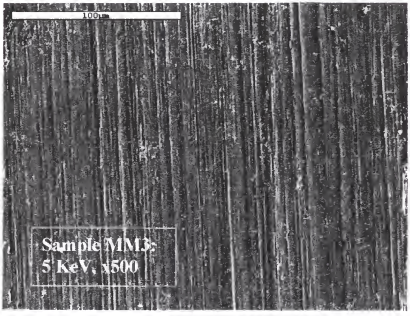

Figure 4.57. SEM micrographs of sample MM3, MAOP-co-MPC on CASS electrode at magnification of 500x (2g / 0.5 ml MAOP/VMS, MeOH/NH_4HSO_4, -1.2 V, 24h).

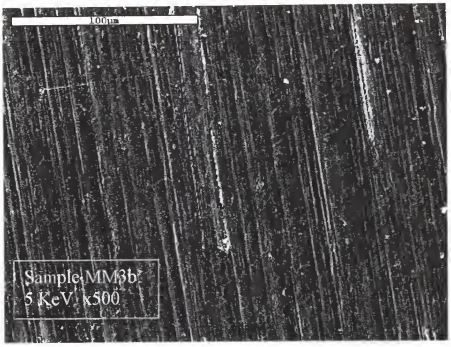

Figure 4.58. SEM micrographs of sample MM3b, MAOP-co-MPC on CASS electrode at magnification of 500x (2g / 0.5 ml MAOP/VMS, MeOH/NH_4HSO_4, -1.3 V, 6h).

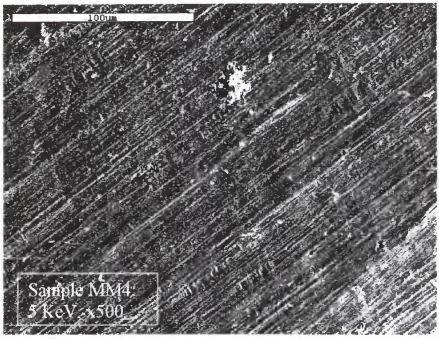

Figure 4.59. SEM micrographs of sample MM4, MAOP-co-MPC on CASS electrode at magnification of 500x (2g / 0.5 ml MAOP/VMS, MeOH/TEAB, -1.2 V, 6h).

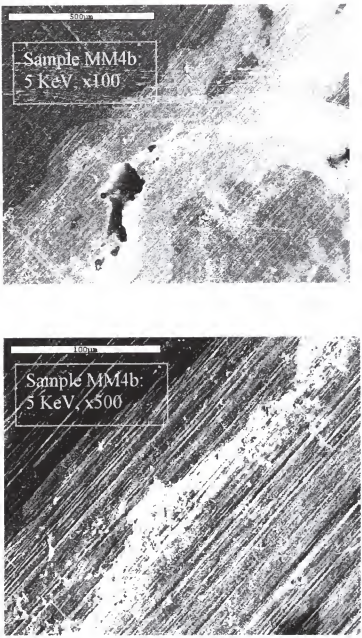

Figure 4.60. SEM micrographs of sample MM4b, MAOP-co-MPC on CASS electrode at magnifications of 100x and 500x (2g / 0.5 ml MAOP/VMS, MeOH/TEAB, -1.2 V, 24h).

Electropolymerization Control Experiments

Monomer adsorption study experiments

Contact angle and XPS results. Table 4.15 shows the results for the monomer adsorption control study. Significant adsorption was seen in all systems, indicating that monomer/oligomer adsorption may be an important phenomenon in the electropolymerization mechanism.

The large amount of adsorption seen in the MPC samples (0.6 to 4 atomic % P) indicates that a pre-polymerization MPC solution soak may increase the MPC surface concentration in the homopolymer and copolymer coatings. The presence of silicon in the XPS spectra of the MPC monomer series of samples is probably due to background silicone contamination seen in the XPS system. This contamination my come directly from the XPS chamber or from the vacuum oven where these samples were dried prior to analysis.

SEM results. Figures 4.61 to 4.67 show the SEM micrographs of the adsorption study controls. The most apparent evidence of coating is seen in Figure 4.64 for AM5 (MPC). This sample shows a roughened texture similar to that seen in CV9 (Figure 4.28) and could indicate the MPC adsorbing onto the metal surface as droplets. The rest of these micrographs show relatively smooth surfaces.

Table 4.15. Adsorption study experiments.

Expt	*Monomer/ Conc.*	*Solvent/Electrolyte*	*Electrode Type*	*Time (h)*	*XPS: At % C/O/Si/P*	*Contact Angle (°)*
AP2b	MAOP / 2.5 ml	DMSO / NH_4HSO_4	Plain	6	NA	41 ± 2
AP3b	MAOP / 2.5 ml	DMSO/TEAB	CASS*	6	48/38/**13**/0	98 ± 8
AP8b	MAOP / 2.5 ml	DMSO / NH_4HSO_4	CASS*	24	48/31/**27**/0	39 ± 3
AM2	MPC / 1g	MeOH / NH_4HSO_4	Plain	6	57/37/1/**2** 58/34/2/4***	20 ± 7
AM5	MPC / 2g	MeOH / TEAB	Plain	24	47/44/6/**0.6**	24 ± 2
AM8	MPC / 2g	MeOH / NH_4HSO_4	Plain	24	63/27/3/**3**	24 ± 4
ACV7	VMS / 20 %	DMSO/TEAB	CASS*	24	51/40/7/0.9	21 ± 3
ACV8	VMS / 20 %	MeOH / NH_4HSO_4	CASS*	24	52/37/**8**/0	35 ± 12
SS**	none	None	Plain	-	45/47/1.6/0	71 ± 8
CASS	none	None	CASS*	-	53/25/15/0	70 ± 7

*CASS = coupling agent coated stainless steel. **XPS results for stainless steel controls, average of nine samples. *** Second analysis for the same sample.

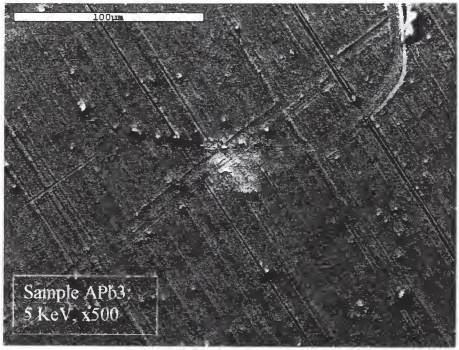

Figure 4.61. SEM micrographs of sample AP3b. Adsorption control of MAOP on CASS electrode at magnification of 500x (2.5 ml MAOP / 50 ml, DMSO/TEAB, 6 h).

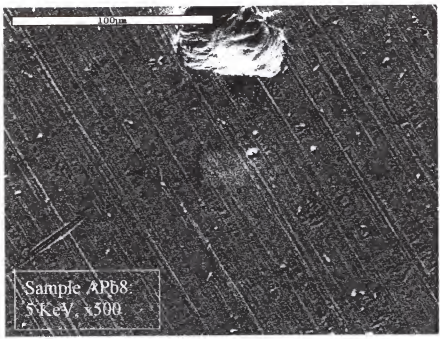

Figure 4.62. SEM micrographs of sample AP8b. Adsorption control of MAOP on a CASS electrode at magnification of 500x (2.5 ml MAOP / 50 ml, DMSO/NH_4HSO_4, 24 h).

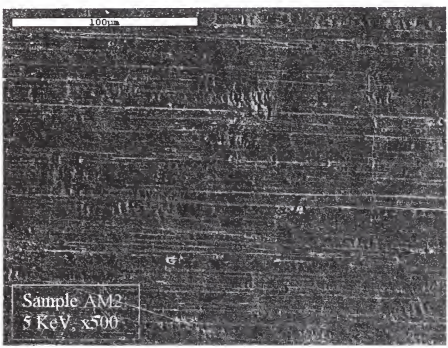

Figure 4.63. SEM micrographs of sample AM2. Adsorption control of MPC on a plain electrode at magnification of 500x (1 g MPC / 50 ml, MeOH/NH_4HSO_4, 6 h).

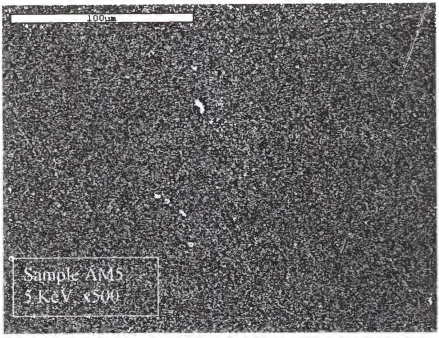

Figure 4.64. SEM micrographs of sample AM5. Adsorption control of MPC on a plain electrode at magnification of 500x (2 g MPC / 50 ml, MeOH/TEAB, 24 h).

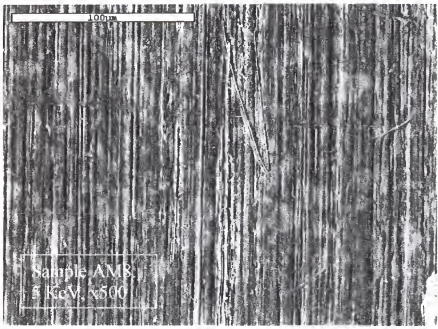

Figure 4.65. SEM micrographs of sample AM8. Adsorption control of MPC on a plain electrode at magnification of 500x (2 g MPC / 50 ml, MeOH/NH_4HSO_4, 24 h).

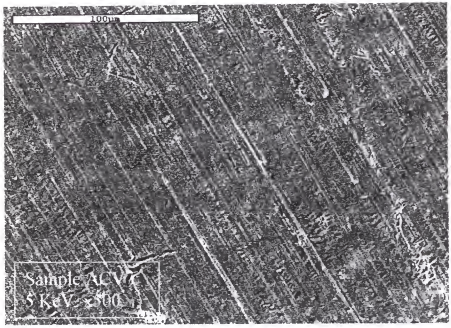

Figure 4.66. SEM micrographs of sample ACV7. Adsorption control of VMS on a CASS electrode at magnifications of 500x (20 vol % VMS, DMSO/TEAB, 24 h).

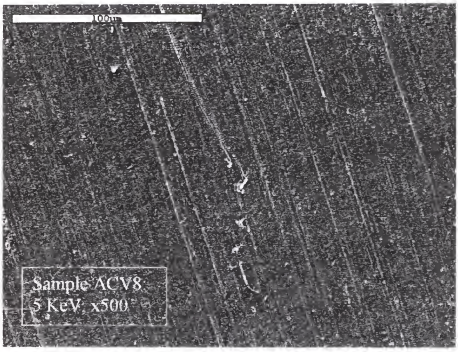

Figure 4.67. SEM micrographs of sample ACV8. Adsorption control of VMS on a CASS electrode at magnification of 500x (20 vol % VMS, MeOH/NH_4HSO_4, 24 h).

Electrolyte/solvent control experiments with no monomer present

Contact angle and XPS results. Tables 4.17 and 4.18 list the results for the electrolyte/solvent controls. The most striking result is the large reduction in contact angle seen in these samples (14 ° to 50 ° reduction).

XPS results show a slight lowering of the atomic % O for the plain electrodes (average 34 $\pm$ 6 %) compared to stainless steel at 48 atomic % O. A slight increase is seen for the CASS (coupling agent modified) electrodes (average 34 $\pm$ 5 %) compared to the CASS control (26 %).

The only major trend is the increase in the atomic % Cr (3 to 5 %) and N (1 to 2 %) seen in the samples ran in MeOH solvent (E6 through E10) compared to the controls. Both the stainless steel and the CASS controls showed 0 atomic % N, 1 and 0 atomic % Cr, respectively. This could suggest am ammonium chromate coordination complex forming on the surface. The silicone contamination seems to be much greater in the samples ran in DMSO. This may suggest that the DMSO solvent had become contaminated with silicone.

SEM results. The SEM micrographs for these samples (Figures 4.68 to 4.76) show a significant change in surface morphology. For comparison, SEM micrographs of stainless steel and CASS controls are shown as Figures 4.77 and 4.78, respectively. This is most apparent for samples E1, E2, E5, E7, and E10.

Figures 4.68, 4.73, and 4.76 show samples E1, E7 and E10. There is an obvious deposit on these metal surfaces that could represent oxidation or salt deposition. All three of these samples were run in NH_4HSO_4 solutions. Chromium – amine complexes are known to form readily and this could be deposition of the NH_4HSO_4 onto the metal

surface.[94] E2 also shows some signs of a deposit or oxidation (Figure 4.69), though this was a TEAB system.

Sample E5 showed evidence of either a coating or a change in surface morphology as seen in Figure 4.71.

It is important to remember that the absence of monomer completely changes the chemical potential of the solution and thus the electrochemistry. The initiating species could be entirely different in these systems than in the monomer containing systems. Therefore, evidence of surface oxidation in this study does not directly correlate to surface oxidation in the electropolymerization experiments. In fact, the only sample to show a SEM that indicated possible surface oxidation was MM4 and MM4b (Figures 4.59 and 4.60). These samples were run in MeOH/TEAB. The MeOH/TEAB electrolyte/solvent control for this system was E6, which did not show evidence of oxidation or salt deposition. This point is also supported by the lack of corrosive pits in these control samples, whereas several of the electropolymerization samples showed evidence of corrosion.

Table 4.17. Electrolyte/solvent control experiments.

Expt.	*Solvent/Electrolyte*	*Time (h)*	*Potential (V)*	*Type of Electrode*	*Contact Angle (°)*
E1	DMSO/TEAB	6	-0.8	CASS	33 ± 3 44 ± 3
E2	DMSO/TEAB	6	-1.3	Plain	35 ± 3 56 ± 11
E3	DMSO/TEAB	24	-0.65	CASS	24 ± 5 35 ± 5
E4	DMSO / NH_4HSO_4	6	-1.6	Plain	24 ± 5 35 ± 5
E5	DMSO / NH_4HSO_4	24	-0.8	Plain	37 ± 5 42 ± 3
E6	MeOH / TEAB	24	-1.3	Plain	34 ± 8
E7	MeOH / NH_4HSO_4	6	-1.2	CASS	22 ± 5 20 ± 3
E8	MeOH / NH_4HSO_4	6	-1.3	Plain	30 ± 6 29 ± 5
E9	MeOH / NH_4HSO_4	24	-1.1	Plain	22 ± 2 27 ± 4
E10	MeOH / NH_4HSO_4	24	-1.2	CASS	22 ± 4 24 ± 3
	SS Control	-	-	Plain	71 ± 8
	CASS Control	-	-	CASS	70 ± 7

Table 4.18. XPS results for the electrolyte/solvent control experiments.

XPS Atomic Percent:

Expt.	*C 1s*	*O 1s*	*Si 2p*	*N 1s*	*Br 2p*	*Cr 2p3*	*Fe 2p3*
E1*	60	30	10	0	0	1	0
E2	54	33	13	0	0	0	0
E3*	44	41	13	0	0	1	1
E4	64	27	8	1	0	1	1
E5	53	28	18	0	0	1	0
E6	46	3943	3	2	0.6	4	1
E7*	55	34	5	2	1	3	0
E8	54	36	5	2	1	3	0
E9	51	41	1	2	1	5	0
E10*	62	30	2	1	1	3	0
SS Control	48	48	2	0	0	1	0
CASS Control	59	26	15	0	0	0	0

*CASS electrode

Figure 4.68. SEM micrographs of sample E1, DMSO/TEAB at –0.8 V for 6h on a CASS electrode. Magnifications of 100x, 500x and 5000x.

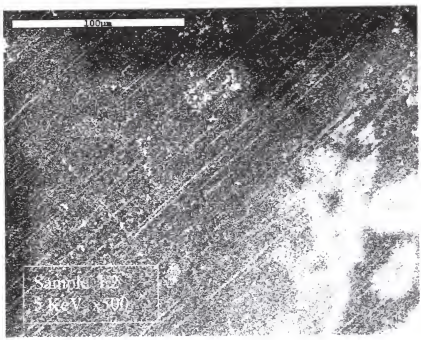

Figure 4.69. SEM micrographs of sample E2, DMSO/TEAB at –1.3 V for 6h on a plain electrode. Magnifications of 500x and 5000x.

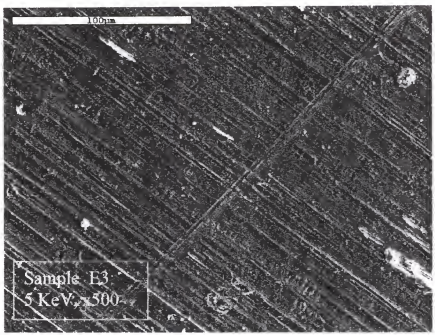

Figure 4.70. SEM micrographs of sample E3, DMSO/TEAB at –0.65 V for 24h on a CASS electrode. Magnifications of 500x and 5000x.

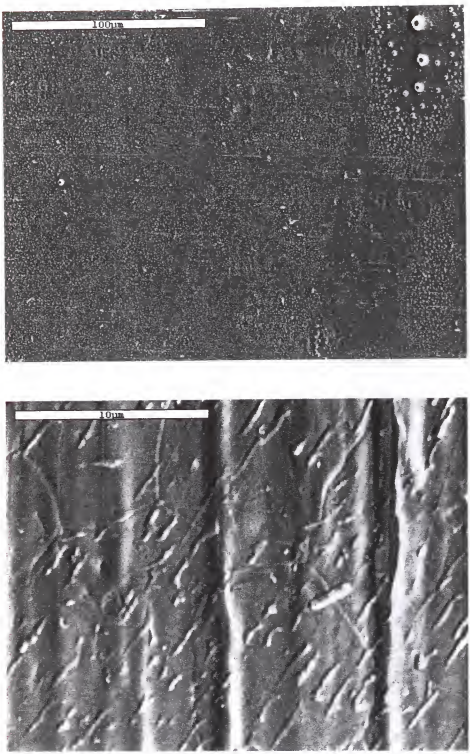

Figure 4.71. SEM micrographs of sample E5, DMSO/NH_4HSO_4 at –0.8V for 24h on a plain electrode. Magnifications of 500x and 5000x.

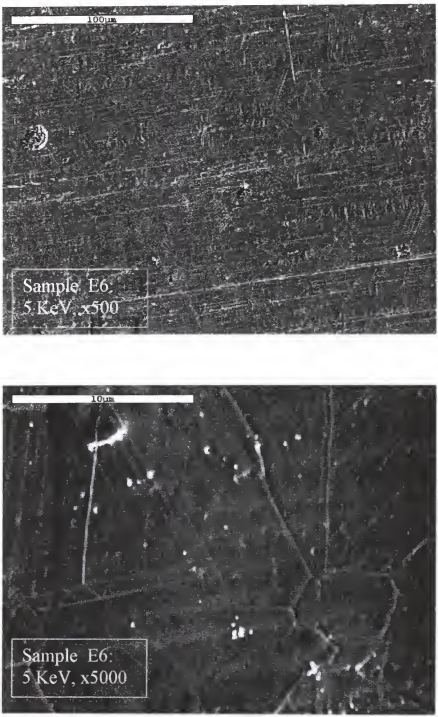

Figure 4.72. SEM micrographs of sample E6, MeOH/TEAB at –1.3 V for 24h on a plain electrode. Magnifications of 500x and 5000x.

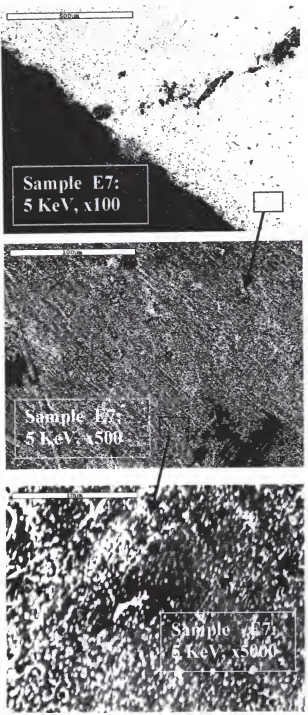

Figure 4.73. SEM micrographs of sample E7, MeOH/NH_4HSO_4 at –1.2 V for 6h on a CASS electrode. Magnifications of 100x, 500x and 5000x.

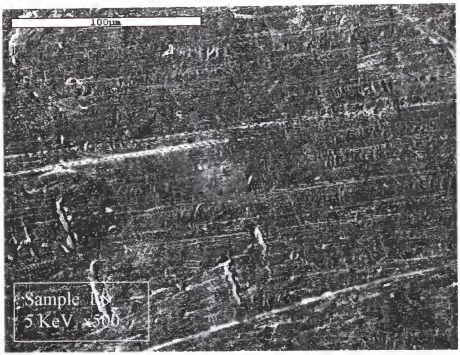

Figure 4.74. SEM micrographs of sample E8, $MeOH/NH_4HSO_4$ at –1.3 V for 6h on a plain electrode. Magnifications of 500x.

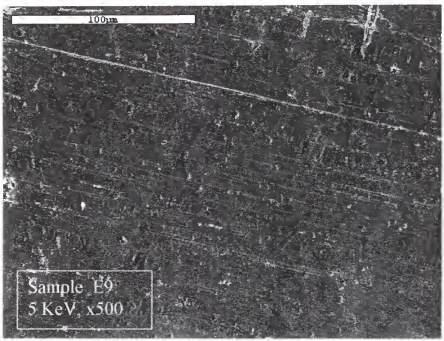

Figure 4.75. SEM micrographs of sample E9, $MeOH/NH_4HSO_4$ at –1.1 V for 24h on a plain electrode. Magnifications of 500x.

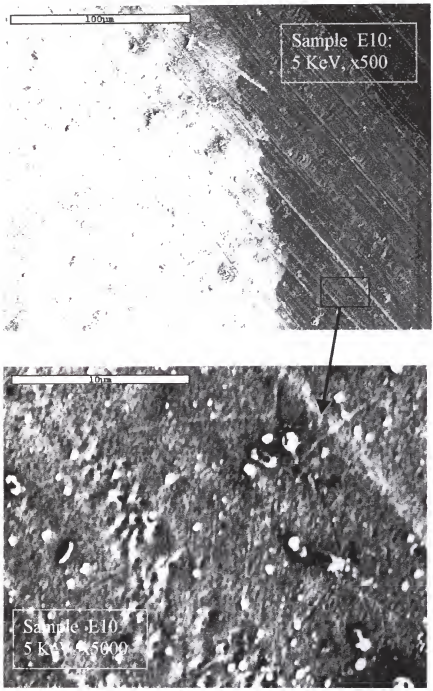

Figure 4.76. SEM micrographs of sample E10, MeOH/NH_4HSO_4 at –1.2 V for 24h on a CASS electrode. Magnifications of 500x and 5000x.

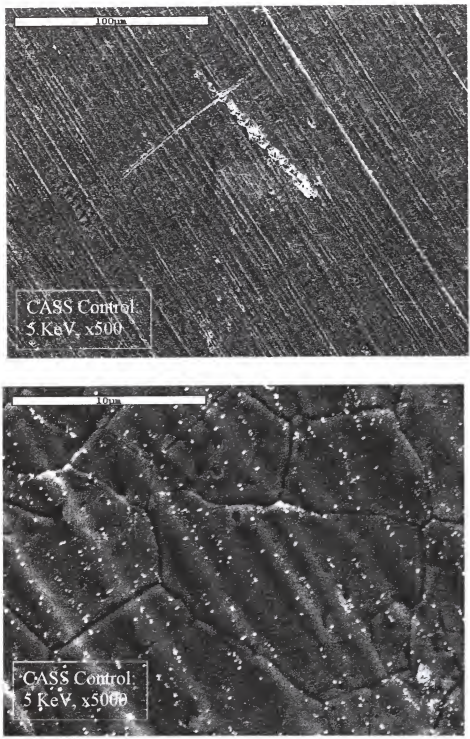

Figure 4.77. SEM micrograph of CASS control. Magnifications of 500x and 5000x.

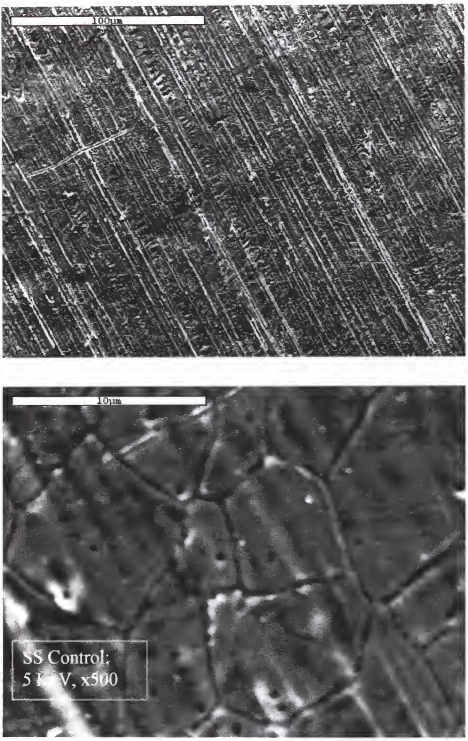

Figure 4.78. SEM micrograph of SS control. Magnifications of 500x and 5000x.

Discussion of Electropolymerization Results

This study was initiated to determine the feasibility of using electropolymerization to coat stainless steel with silicone polymers, polyMPC and MPC copolymers.

The results are very promising with all systems showing good coatings with one or more of the reaction conditions used. Figure 4.79 shows contact angle averages calculated from all the samples obtained from each oligomer/monomer system. The standard deviations presented represent the sensitivity of the system to changes in experimental factors and levels (experimental conditions) rather than the consistency of samples within a set condition. This graph shows the expected trend for coating a substrate with these polymer systems. The highest contact angle was produced using the non-modified stainless steel control (71 °).

The MAOP silicone polymer exhibits the next highest contact angles (50 °) with the largest sensitivity to conditions. This sensitivity to conditions could be related to this oligomer's limited solubility in polar solvents. Phase separation was seen in some of the high oligomer concentration solutions.

The VMS silicone coating showed a much greater reduction in contact angles (27°, ca. 40 ° reduction). This is to be expected considering the structure of this oligomer. This oligomer was chosen for its high degree of vinyl functionality for grafting, polymerization and crosslinking, and for its large number of hydrophilic methoxy groups. These methoxy groups can be easily hydrolyzed in protic solvents, thus further increasing the hydrophilic nature of the resultant polymer. This polymer was thought to not only provide a very highly functionalized and hydrophilic silicone surface, but to be more

compatible with the MPC monomer for copolymerization than the less hydrophilic MAOP oligomer. This polymer coating also provides functionality that could be used to couple drugs or proteins to the stent surface.

The electrochemically produced MPC polymer gave the lowest average contact angles for all systems (18°). This is expected due to the highly hydrophilic phosphorylcholine head group. The copolymers of MPC and VMS and MAOP were not significantly different in average contact angles (18 ± 5 and 23 ± 5, respectively). These results show that a small concentration of MPC in the copolymers can significantly decrease the contact angle of copolymer surface coatings. This supports by similar findings by Ishihara.[7] Such MPC coatings show promise for development of improved stents.

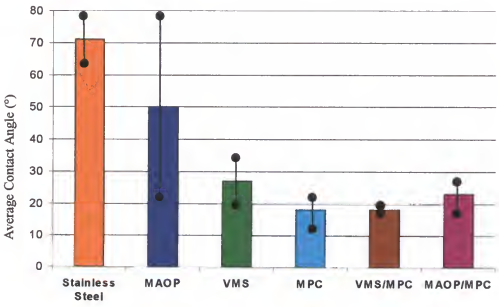

Figure 4.79. Graph showing the overall average contact angles for the oligomer/monmer and copolymer electropolymerization samples compared to non-coated stainless steel.

XPS control results indicate a background silicon contamination of 2 – 6 %. Sources of this contamination are likely from the XPS chamber itself, the vacuum oven in which the samples were dried and the plastic syringes used to measure the DMSO solvent.

Another interesting result of these experiments is the spherical "bubbly" morphology seen for some of the VMS coatings onto both plain and CASS electrodes. This surface structure occured only in DMSO solvent and can be best seen in Figures 4.16 (VMS 4), 4.19 (VMS 7b), 4.26 (CV7) and 4.28 (CV9). This may be due to the growing polymer being more hydrophilic than the solvent. This would induce a more spherical morphology to reduce the surface area of interaction. Another possibility is that the under these solvent/electrolyte conditions, the polymer is emulsified and polymerization is initiated when these droplets come in contact with the electrode surface.

The solutions for these polymerizations were not analyzed for molecular weight. Conditions were optimized to avoid bulk polymerization, not to encourage it. The molecular weight of bulk polymerized polymer would prove that polymer is being formed in these systems though would not be directly related to the molecular weight of the surface coatings or grafts. However, bulk polymerization did occur and was observed for all these systems for at least one condition; indicating that these monomers were subject to electropolymerization.

The flakey, rough morphologies seen in some of these samples could be from three sources. One being an artifact of the differential swelling effects experienced by these coatings when changed between solvent systems during extraction. The thicker

coating may result in stress cracking upon swelling. This could cause spalling of these films. The second source could be from the stresses induced during drying. These polymers are formed in the swollen state and upon drying the free volume of the system is reduced, which imparts stress on the film.

Thirdly, after the initial layer of polymer is formed on the stainless steel cathode, the amperage of the system decreases rapidly. This can be seen in consecutive sweeps in the cyclic voltamogram. Each consecutive sweep decreases in amperage (this is considered evidence that coating is occuring). Most of the coating occurs at very low amperages. In these experiments amperages varied depending on the solvent system but a ten-fold reduction in amperage between start and finish was typical. This translates to a different initiation rate between initial layers and subsequent layers. This could lead to the non-uniformity seen in some of the thicker coatings.

The ionic nature of the solvent/electrolyte of these systems could greatly effect the polymerization as well as competing corrosive and passivation reactions. These conditions may also be changing during the course of electropolymerization. It would be desirable in future studies to monitor the pH or conductivity of the solution before, during and after the reaction.

Grumski's work[89] has shown that MPC polymerizes to exceptionally high molecular weights under the influence of gamma initiation. These results point to a possible mechanism involving the alignment of the MPC monomer in solution where the methacrylic head groups are brought into close proximity. This would enhance the kinetics of polymerization by reducing the diffusion influence on rate and lower the probability of termination. In comparison, electrochemistry also provides a continuous

form of initiation at least for the first few layers until the surface resistivity becomes too high. This may indicate that pre-adsorption of the MPC to the electrode surface, as seen in sample AM5 (adsorption control, plain electrode, 1g MPC / 50 ml, $MeOH/NH_4HSO_4$, Figure 4.64), would be beneficial, especially if the monomer exhibits alignment on the stainless steel surface.

Another study that would further the understanding of the electrochemical coating of these substrates would be to conduct metal etching and metallurgical analysis of the stainless steel (SS) substrates. This would establish the presence and size of chemical and physical non-uniformities in the metal surface such as grain boundaries. SEM micrographs should be taken of the SS substrates to establish any effect that the coating procedure may have had on the surface.

CHAPTER 5
SUMMARY AND CONCLUSIONS

Two new types of polymerization methods for the surface modification of metals and polymers of interest for medical devices such as cardiovascular stents and grafts were explored in this work. These were gamma radiation graft surface polymerization and electropolymerization. Gamma radiation graft surface polymerization was used to surface modify a pre-cured silicone for dip-coated applications and electropolymerization to directly modify a metal surface. For the gamma radiation graft surface polymerization experiments, pre-cured PDMS discs were modified with several hydrophilic monomers and copolymers thereof. Two silicone oligomers (MAOP and VMS) and a novel phospholipid monomer system (MPC) were used in the electropolymerization experiments to produce coatings on stainless steel.

This work furthers the science of surface modification by grafting a hydrophilic PL monomer and PL copolymers onto the surface of the silicone (gamma radiation graft surface polymerization) and stainless steel (electropolymerization). This may not only improve the lubricity and blood compatibility of the cardiovascular implant surface, but also provide functional groups that can be further used for the incorporation of locally targeted drugs and beneficial proteins. The use of gamma surface graft and electrochemical polymerization provides two new routes to PL modified silicone and metal surfaces, furthering the technology of surface modification.

For the gamma radiation graft surface modification, HEMA, MAA, NVP and MPC monomers were grafted onto the surface of silicone. The effects of solvent system, dose rate, total dose, and monomer concentration were studied. Conditions were found for each of the monomers that resulted in the decrease the contact angle of the PDMS surface. XPS and FTIR analysis of these samples proved to be inadequate to conclusively prove modification. Further evaluation of these surfaces to determine improved biocompatibility over PDMS is suggested.

The goal of the electropolymerization experiments was to produce highly adherent coatings with the elastic properties of silicone, and the improved blood compatibility due to the MPC copolymer structures; also to provide surface functionality for attachment of drugs and proteins.

These coatings showed an interesting relationship between contact angle and polymer composition and surprisingly indicated that incorporation of even small concentrations of polyMPC into the MAOP silicone resulted in a remarkable increase in hydrophilicity. These findings were supported by SEM and XPS analysis.

Further development of these promising surface modification techniques and polymers should include the coating of stents and animal A-V shunt and implant studies.

CHAPTER 6

SUGGESTED FUTURE RESEARCH

Gamma Radiation Graft Surface Polymerization Modification of PDMS

The following is suggested for continuation of the gamma radiation graft surface modification of silicone:

1. Hydrolyzation of the PDMS surface by exposure to an acid or base to improve adsorption of the MPC monomer to the polymer surface prior to gamma exposure. This procedure is currently being explored in this lab for grafting of HEMA and NVP on to PDMS.
2. Modifications of thin film PDMS dip-coated metal substrates to increase surface concentrations. This would more closely mimic the modification of cardiovascular grafts.
3. Drug coupling on HEMA and MAA modified substrates.
4. Determination of influence of pH on the gamma polymerization of these monomers both in solution and in surface grafting.
5. Study the gamma polymerization of the MAOP and the VMS oligomers. It would be especially interesting to surface graft the VMS to the surface of the Shin Etsu PDMS to provide functionalization for further coupling.

Electropolymerization

The preliminary results for the electropolymerization of silicones and MPC onto stainless steel were promising. Further work may be of importance in the following areas:

1. Optimization of conditions for coating of actual stent surfaces. Changing the surface area of the working electrode will change the potentials and times of reaction for these systems. The cyclic voltamogram will give insight into where the reduction peak(s) are for the system, but once again the conditions will have to be screened to find optimized conditions for coating. This study should include the monitoring of solution conductivity (non-aqueous) or pH (aqueous/ methanolic).
2. Electropolymerized surfaces should be made for the best candidate systems. At least five samples should be produced for each system. These samples should be quantified by contact angle, SEM, XPS, and additionally by nanoscratch to determine adhesion.
3. Drug loading of coated stent materials should be evaluated by a method similar to that used by Widenhouse to evaluated dexamethasone in PDMS.[5]
4. Coated stents should be evaluated by ex-vivo canine shunt and implant studies.

LIST OF REFERENCES

1) Ishihara, K.; Oshida, H.; Endo, Y.; Watanabe, A.; Ueda, T.; Nakabayashi, N. *J Biomed Mater Res* **1993**, *27*, 1309-14.

2) Ishihara, K.; Takayama, R.; Nakabayashi, N.; Fukumoto, K.; Aoki, J. *Biomaterials* **1992**, *13*, 235-9.

3) Ishihara, K.; Tsuji, T.; Kurosaki, T.; Nakabayashi, N. *J Biomed Mater Res* **1994**, *28*, 225-32.

4) Ishihara, K.; Fukumoto, K.; Iwasaki, Y.; Nakabayashi, N. *Biomaterials* **1999**, *20*, 1553-9.

5) Widenhouse, C. W.; Seegar, J. M.; Klingman, N.; Martin, P. J.; Goldberg, E. P. *Kinetics of Dexamethasone Release from Silicone Coatings on Vascular Devices*: Providence, R.I., 1999, pp 395.

6) Ishihara, K.; Shibata, N.; Tanaka, S.; Iwasaki, Y.; Kurosaki, T.; Nakabayashi, N. *J Biomed Mater Res* **1996**, *32*, 401-8.

7) Arkles, B. *Chemtech* **1983**, *13*, 542-555.

8) Nakaya, T.; Li, Y. J. *Prog. Polym. Sci.* **1999**, *24*, 143-181.

9) Toth, W. J.; Tobolsky, A. V. *J. Polym. Sci. Part B* **1970**, *8*, 289.

10) Minezaki, S.; Nakaya, T.; Imoto, M. *Makromol. Chem.* **1974**, *175*, 3017.

11) Nishio, K.; Nakaya, T.; Imoto, M. *Makromol. Chem.* **1974**, *175*, 3319.

12) Nisho, K.; Nakaya, T.; Imoto, M. *Makromol. Chem.* **1978**, *179*, 1117.

13) Nakaya, T.; Nishio, K.; Memita, M.; Imoto, M. *Makromol. Chem. Rapid Commun.* **1993**, *14*, 77.

14) Nakaya, T.; Memita, M.; Kang, M. *Makromol. Reports* **1993**, *A30*, 349.

15) Paustian, T. *www.bact.wisc.edu/microtextbook*; Univ. of Wisconsin-Madison, 1999.

16) Kuo, J.-H. S. *Synthesis and Characterization of Polymerizable Phospholipids and Related Polymers*; University of Florida: Gainesville, 1992, pp 153.

17) Thanh, T. N.; Chabrier, P. *Bull. Soc. Chem. Fr.* **1974**, *3-4*, 667.

18) Nakaya, T.; Nakai, S. *Kagaku* **1987**, *42*, 725.

19) Ishihara, K.; Ueda, T.; Nakabayashi, N. *Polymer Journal* **1990**, *22*, 355-360.

20) Yianni, Y. P.; Wiles, M. C. *Polymeric Coating*; Biocompatibles Limited: USA, 1996.

21) Ueda T; Oshida H; Kurita K; Ishihara K; N., N. *Polymer Journal* **1992**, *24*, 1259-1269.

22) Kojima, M.; Ishihara, K.; Watanabe, A.; Nakabayashi, N. *Biomaterials* **1991**, *12*, 121-4.

23) Ishihara, K.; Oshida, H.; Endo, Y.; Ueda, T.; Watanabe, A.; Nakabayashi, N. *J Biomed Mater Res* **1992**, *26*, 1543-52.

24) Ueda, T.; Ishihara, K.; Nakabayashi, N. *J Biomed Mater Res* **1995**, *29*, 381-7.

25) Ishihara, K.; Ziats, N. P.; Tierney, B. P.; Nakabayashi, N.; Anderson, J. M. *J Biomed Mater Res* **1991**, *25*, 1397-407.

26) Ishihara, K.; Fujiike, A.; Iwasaki, Y.; Kurita, K. *ournal of Polymer Science: Part A: Polymer Chemistry* **1996**, *34*, 199-205.

27) DeFife, K. M.; Yun, J. K.; Azeez, A.; al., e. *J Biomed Mater Res* **1995**, *29*.

28) Yu, J.; Lamba, N. M. K.; Courtney, J. M.; al., e. *Biomaterials* **1994**, *17*, 499-504.

29) Nakabayashi, N. *Concept and History of Phopholipid Polymer Biomaterials*; Nakabayashi, N., Ed.; Society for Biomaterials: Kamuela, Hawaii, 2000.

30) Yoneyama, T.; Ishihara, K.; Nakabayashi, N.; Ito, M.; Mishima, Y. *J Biomed Mater Res* **1998**, *43*, 15-20.

31) Furuzono, T.; Ishihara, K.; Nakabyashi, N.; Tamada, Y. *Biomaterials* **2000**, *21*, 327-333.

32) Chang, P. C.-T.; Lee, S.-D.; Hsiue, G.-H. *J. Biomed. Mater. Res.* **1998**, *39*, 380-389.

33) Hsiue, G.-H., Personal conversation regarding the analysis of MPC modified PDMS.

34) Widenhouse, C. W. *Surface Modification of Vascular Prosthesis and Intracorneal Lens Polymers*; University of Florida: Gainesville, 1996, pp 208.

35) Cooper, S. L.; Fabrizius-Homan, D. J. *J. Biomater. Sci. Polymer Edn.* **1991**, *3*, 27-47.

36) Ip, W. F.; Sefton, M. V. *Journal of Biomedical Materials Research* **1991**, *25*, 1321-1324.

37) Lin, H. B.; Hergenrother, R. W. *J. Mater. Sci.: Materials in Medicine* **1994**, *5*, 207-213.

38) Silver, J. H.; R.W., H.; Lin, J.-C.; Lim, F.; Lin, H.-B.; Okada, T.; Chaudhury, M. K.; Cooper, S. L. *J. Biomed. Mater. Res.* **1995**, *29*, 535-548.

39) Goldberg, E. P.; Seeger, J. M., Unpublished Data from the Goldberg (Dept. of Materials Sci. & Eng., Univ. of Florida) and Seeger (Dept. of Cardiovascular Surgery, Univ. of Florida) Research groups.

40) Granke, K.; Ochsner, J. L.; McClugage, S. G.; Zdrahal, P. *Cardiovascular Surgery* **1993**, *1*, 254-261.

41) Norgren, L.; Hallberg, E.; Jawien, A.; Krantz, P.; Parsson, H.; Ribbe, E.; Thorne, J. *Annals of Cardiovascular Surgery* **1990**, *4*, 575-579.

42) Walen, R. L.; Cardona, R. R.; Kantrowitz, A. *ASAIO Journal* **1992**, *38*, M207-M212.

43) Morel, N. M. L.; Dodge, A. B.; Patton, W. F.; Herman, I. M.; Hechtman, H. B.; Shepro, D. *J. Cell. Phys.* **1989**, *14 1*, 653.

44) Chapiro, A. *Radiation chemistry of polymeic systems*; Wiley-Interscience: New York, 1962.

45) Lee, C. S.; Bell, J. P. *J. Appl. Poly. Sci.* **1995**, *57*, 931-938.

46) Mengoli, G.; Tidswell, B. M. *Polymer* **1975**, *16*, 881-888.

47) Funt, B. L.; Williams, F. D. *Journal of Polymer Science, Part A* **1964**, *2*, 862-880.

48) Ling, X.; Byerley, J. J.; Pritzker, M. D.; Burns, C. M. *J. Applied Electrochem.* **1997**, *27*, 1343-1348.

49) Fox, S. I. *Human Physiology*; Wm. C. Brown: Dubuque, 1987.

50) Gloor, B.; Wehrli, E.; Rotzer, A.; Brunner, D.; Wilms, C.; Largiader, J. *Swiss Surg. Suppl.* **1996**, *1*, 13-8.

51) Whittmore, R. L.; Clowes, A. W.; Couch, N. P.; Mannick, J. A. *Ann. Surg.* **1981**, *193*, 35-42.

52) Brothers, T. E.; Stanley, J. C.; Burkel, W. E.; Graham, L. M. *J. Biomed. Mater. Res.* **1990**, *24*, 761-771.

53) Leake, D. L.; Cenni, E.; Cavedagna, D.; Stea, S.; Ciapetti, G.; Pizzoferrato, A. *Biomaterials* **1989**, *10*, 441-444.

54) Vermette, P.; Thibault, J.; Levesque, S.; Laroche, G. *J. Biomed. Mater. Res.* **1999**, *48*, 660-8.

55) Jankowski, R. J.; Wagner, W. R. *Clinics in Plastic Surgery* **1999**, *26*, 605-614.

56) Jeschke, M. G.; Hermanutz, V.; Wolf, S. E.; Koveker, G. B. *J. Vasc. Surg.* **1999**, *29*, 168-76.

57) Guidoin, R.; Chakfe, N.; Maurel, S.; How, T.; Batt, M.; Marois, M.; Gosselin, C. *Biomaterials* **1993**, *14*, 678-693.

58) Pevec, W. C.; Darling, R. C.; L'Italien, G. J.; Abbott, W. M. *J. Vasc. Surg.* **1992**, *16*, 60-5.

59) Lim, F.; Yang, C. Z.; Cooper, S. L. *Biomaterials* **1994**, *15*, 408-416.

60) Nojiri, C.; Senshu, K.; Okano, T. *Artif. Organs* **1995**, *19*, 32-8.

61) Kutryk, M.; Serruys, P. W. *Coronary Stenting: Current Prospectives*; Martin Dunitz: London, 1999.

62) Holmes, J., D.R.; Camrud, A. R.; Jorgenson, M. A.; Edwards, W. D.; Schwartz, R. S. *Journal of the American College of Cardiology* **1994**, *24*, 525-31.

63) Zheng, H.; Barragan, P.; Corcos, T.; Simeoni, J.-B.; Favereau, X.; Roquebert, P.-O.; Guerin, Y.; Sainsous, J. *Clinical Experience With a New Biocompatible Phosphorylcholine-Coated Coronary Stent*; Medscape, Inc., 1999; Vol. 1999.

64) Kruft, M.-A. B.; Benzina, A.; Blezer, R.; Koole, L. H. *Biomaterials* **1996**, *17*, 1803-1812.

65) Osterle, S. N.; Whitbourn, R.; Fitzgerald, P. J.; Yeung, A. C.; Stertzer, S. H.; M.D., D.; Yock, P. G.; Virmani, R. *American Heart Journal* **1998**, *136*, 578-599.

66) Lablanche, J.-M.; McFadden, E. P.; Bonnet, J.-L. *European Heart Journal* **1996**, *17*, 1373-80.

67) Keane, D.; Haase, J.; Slager, C.; al., e. *Circulation* **1995**, *91*, 2402-12.

68) Goods, C. M.; Al-Shaibi, K. F.; Yadav, S. S.; al., e. *Circulation* **1996**, *93*, 1803-08.

69) Mak, K.-H.; Belli, G.; Ellis, S. G.; Moliterno, D. J. *J. Am. Coll. Cardiol.* **1996**, *27*, 494-503.

70) Andrade, J. D.; Hlady, V. *Plasma protein adsorption. The big twelve.*; Leonard, E. F., Turitto, V. T. and Vroman, L., Ed.; New York Academy of Science: New York, 1987, pp 158-72.

71) www.medicaldata.com *Coronary Stents: Near the Top of the Market?*; Medical Data International, Inc., 1998; Vol. 1998.

72) Smith, A. C.; Migliori, F. *Cardiovascular Quarterly* **1997**, *December*, 1-19.

73) Srinivasan, G.; Rosebrough, S.; Zhang, X.; Whitbourne, R. *Antithrombogenic Coatings for Medical Devices*: Providence, R.I., 1999, pp 105.

74) Chan, A. K. C.; Berry, L.; Mitchell, L.; Andrew, M.; Klement, P. *Evaluation of Antithrombin-Heparin Covalent Complex Coated Endoluminal Grafts in Rabbits*: Providence, R.I., 1999, pp 102.

75) Weber, N.; Wendel, H. P.; Ziemer, G. *Different Heparin-Coated Surfaces and Their Binding Capacities of Coagulation and Complement Enzymes: Influence on Thrombogenicity*: Providence, R.I., 1999, pp 101.

76) Murphy, J. G.; Schwartz, R. S.; Edwards, W. D.; Camrud, A. R.; Vlietstra, R. E.; Holmes, D. *Circulation* **1992**, *86*, 1596-604.

77) Van Beusekom, H. M. M.; Van der Giessen, W. J.; Van Ingen Schenau, D.; Slager, C. J. *Circulation* **1992**, *86*, I-731.

78) Lincoff, A. M.; Schwartz, R. S.; Van der Giessen, W. J.; al., e. *Circulation* **1992**, *86*, I-801.

79) Zidar, J. P.; Gammon, R. S.; Chapman, G. D.; al., e. *J. Am. Coll. Cardiol.* **1993**, *21*, 439A.

80) Su, S. H.; Wu, J.; Landau, C.; Chao, R. Y. N.; Timmons, R. B.; Meidell, R. S.; K., N.; Eberhart, R. C. *Progress in Bioresorbable Polymer Stent Development*: Providence, R.I., 1999, pp 143.

81) Tamai, H.; Doi, T.; Hsu, Y. S.; al., e. *J. Invas. Cardiol.* **1995**, *7*, 9A.

82) Susawa, T.; Shiraki, K.; Shimizu, Y. *J. Am. Coll. Cardiol.* **1993**, *21*, 483A.

83) Chapman, G. D.; Gammon, R. S.; Baumann, R. P.; al., e. *Circulation* **1990**, *82*, 483A.

84) Rau, K.; Ollinger, M.; Singh, R. K.; Goldberg, E. P. *Medical Device Surface Modification by Pulsed Laser Ablation Deposition (PLAD) of Silicone onto Stainless Steel*: Providence, R.I., 1999, pp 573.

85) Wan, B.; MacGregor, H.; Clavin, M.; Chang, G.; Shiedlin, A.; Nickerson, C.; Miller, B.; Skinner, K. *Evaluation of Immobilized Hyaluronic Acid: Stability and Platelet Deposition Studies*: Providence, R.I., 1999, pp 228.

86) Lahann, J.; Klee, D.; Hocker, H. *An one-step coating and functionalization procedure as a general tool for drug immobilization*: Providence, R.I., 1999, pp 227.

87) Grumski, M., Personal communication regarding experimental results.

88) Widenhouse, C. W., Preparation Method for Coupling Agent Surface Modification of Stainless Steel.

89) Grumski, M. G. *Surface Modification of Biomedical Polymers by Gamma Polymerization with 2-Methacryloyloxyethyl Phosphorylcholine*; University of Florida: Gainesville, 2000, pp 100.

90) Rhodes, D. G.; Blechner, S. L.; Yager, P.; Schoen, P. E. *Chemistry and Physics of Lipids* **1988**, *49*, 39-47.

91) Binder, H.; Anikin, A.; Kohlstrunk, B. *J. Phys. Chem. B* **1999**, *103*, 450-460.

92) Regen, S. L.; Singh, A.; Oehme, G.; Singh, M. *J. Am. Chem. Soc.* **1982**, *104*, 791-795.

93) Singh, A.; Schnur, J. M. *Polymers for Advanced Technologies* **1994**, *5*, 358-373s.

94) Douglas, B. E.; McDaniel, D. H.; Alexander, J. J. *Concepts and Models of Inorganic Chemistry*; 3rd ed.; John Wiley & Sons, Inc.: New York, 1994.

BIOGRAPHICAL SKETCH

Lauri L. Jenkins graduated from the University of Florida in 1983 with a Bachelor of Science degree in interdisciplinary studies. She entered the University of Central Florida's graduate program in industrial chemistry in 1986 and obtained her Master of Science degree in 1989. Her research at UCF involved the synthesis and characterization of interpenetrating polymer networks. While attending UCF, she also worked as a project chemist for Engineering Technology Inc. (ETI) where she was involved in the testing of air filtration systems on battlefield obscurants for the U.S. Army.

After graduation, Lauri worked for TRI-Tessco, Inc. as a chemist at the Naval Research Laboratory's Underwater Sound Reference Laboratory. Here she developed new composite materials for use in anachoic coatings and sonar domes. At this time, she also worked as a consultant for ETI on a project to develop conductive polymer coated fibers as battlefield obscurants. She left these positions in 1994 to take a position with MK Research, Inc. where she conducted research on conductive polymers and non-linear materials.

She returned to the University of Florida in 1995 to enter the graduate program in organic chemistry and joined the research group of Dr. Ken Wagener. Her work at the in the Wagener research group involved the acyclic diene metathesis reactivity of aromatic conjugated double bonds with the objective of designing soluble monomers to produce

σ - π conjugated polymers. In May of 1997, Lauri earned her Master of Science degree in Organic Chemistry with a specialization in Polymer Chemistry.

Lauri then transferred to the Department of Materials Science and Engineering at the University of Florida to pursue her Ph.D. Here she has engaged in research involving the phospholipid and silicone surface modification of polymeric and metallic biomaterials in the research group of Dr. E. P. Goldberg. This dissertation is the culmination of this research.

After graduation, Lauri hopes to find lucrative employment in the area of polymer chemistry and pay-off her student loans!

I certify that I have read this study and that in my opinion it conforms to acceptable standards of scholarly presentation and is fully adequate, in scope and quality, as a dissertation for the degree of Doctor of Philosophy.

Eugene P. Goldberg, Chairman
Genzyme Professor, Biomaterials,
Materials Science and Engineering

I certify that I have read this study and that in my opinion it conforms to acceptable standards of scholarly presentation and is fully adequate, in scope and quality, as a dissertation for the degree of Doctor of Philosophy.

Christopher D. Batich
Professor of Materials Science and
Engineering

I certify that I have read this study and that in my opinion it conforms to acceptable standards of scholarly presentation and is fully adequate, in scope and quality, as a dissertation for the degree of Doctor of Philosophy.

Anthony B. Brennan
Associate Professor of Materials Science
and Engineering

I certify that I have read this study and that in my opinion it conforms to acceptable standards of scholarly presentation and is fully adequate, in scope and quality, as a thesis for the degree of Doctor of Philosophy.

Cammy R. Abernathy
Professor of Materials Science and
Engineering

I certify that I have read this study and that in my opinion it conforms to acceptable standards of scholarly presentation and is fully adequate, in scope and quality, as a dissertation for the degree of Doctor of Philosophy.

Dr. James M. Seeger
Professor of Surgery, College of Medicine

This dissertation was submitted to the Graduate Faculty of the College of Engineering and to the Graduate School and was accepted as partial fulfillment of the requirements for the degree of Doctor of Philosophy.

August 2000

M. J. Ohanian
Dean, College of Engineering

Winfred M. Phillips
Dean, Graduate School